Comparison of probabilistic seismic hazard estimations with observations (accelerations and intensities)

Hilal Oksuz

UNIVERSITÉ DE GRENOBLE

THÈSE

Pour obtenir le grade de

DOCTEUR DE L'UNIVERSITÉ DE GRENOBLE

Spécialité : **Sciences de la Terre, l'Univers et l'Environnement**

Arrêté ministériel : 7 août 2006

Présentée par

HILAL OKSUZ

Thèse dirigée par **Céline BEAUVAL**, **Agnès HELMSTETTER** et **Philippe GUEGUEN**

préparée au sein de l'**Institut des Sciences de la Terre**
dans **l'École Doctorale Terre Univers Environnement**

Comparaison des estimations d'aléa sismique probabiliste avec les observations (accélérations et intensités)

Thèse soutenue publiquement le **23 Juin 2014**,
devant le jury composé de:

M. GUEGUEN Philippe
Directeur de recherche, ISTerre/IFSTTAR, Directeur de thèse
Mme. BEAUVAL Céline
Chargée de Recherche, ISTerre/IRD, CoDirecteur de thèse
Mme. HELMSTETTER Agnès
Chargée de Recherche, ISTerre/CNRS, CoDirecteur de thèse
Mme. PERUZZA Laura
Senior Researcher, OGS di Trieste, Rapporteur
M. SCHORLEMMER Danijel
Senior Researcher, GFZ Potsdam, Rapporteur
M. BARD Pierre-Yves
Ingénieur Général des Ponts des Chaussées, ISTerre/IFSTTAR, Examinateur
Mme. SENFAUTE Gloria
Ingénieur sismologue, EDF, Examinateur
M. AKKAR Sinan
Professeur, Bogazici University, Examinateur

Université Joseph Fourier / Université Pierre Mendès France /
Université Stendhal / Université de Savoie / Grenoble INP

Acknowledgements

First, I would like to express my gratitude to my thesis supervisors Céline Beauval, Agnès Helmstetter and Philippe Guéguen for their encouragement, motivation and guidance.

I would like to thank specifically to Pierre-Yves Bard for key discussions and immense knowledge.

Many thanks to Laura Peruzza, Instituto Nazionale di Oceanografia e di Geofisica Sperimentale, and David Schorlemmer, GFZ German Research Center for Geosciences, who agreed to be the rapporteurs of my thesis. I am also very grateful to Sinan Akkar, Kandilli Observatory and Earthquake Research Institute, who accepted to participate in the jury of my thesis as an examiner.

My sincere appreciation goes to Gloria Senfaute for her supports and guidance. I also would like to acknowledge to Jean Michel Thirry for following my work closely. I recognize that this research would not have been possible without the financial assistance of AREVA and EDF.

I have greatly appreciated discussions with Frank Scherbaum and Gordon Woo. I must thank them for their interests in my work and for their intellectual contributions. It is my pleasure to acknowledge Ezio Faccioli and John Douglas for their reviews and comments on my report.

My sincere thanks also go to Stephane Drouet for his assistance on the probabilistic seismic hazard models. I also would like to thank to Christophe Martin for his helps. Many thanks to Jérôme Lambert, Paola Traversa and Christophe Durouchoux for their assistances about the SISFrance data.

This work is done as a part of the SIGMA project. The main purpose of the project is to quantify and bring more insight to the uncertainties at all steps of probabilistic seismic hazard analysis. I am grateful to all teams of the project for the exchanges and especially for providing the data for my work.

I would like to thank my office mate Afifa Imtiaz for her friendly support, helpful advices especially during the last year of my PhD. I would also like to thank my labmates, to Ismael Riedel, Johannes Chandra and Elizabeth Hardwick for delightful talks, lunches, sharing, fun, and warm friendship. The hardest part of finishing this PhD will be moving far away from them.

I am very lucky to be in risk team of ISTerre that provided fruitful discussions during meetings. I also owe a debt of gratitude to all the members ISTerre for providing a good atmosphere. Thanks to Cécile Cretin and Abderrahman Salhi for administrative aids. Special thanks to Kamil Adoum for being available in short time to deal with technical issues in the last month of my PhD.

Many special thanks to my college and valuable friend, Abdullah Sandikkaya. It means a lot for me to have a friend like him with whom I can talk about both science and life. Many thanks to his lovely wife, Hilal Sandikkaya, for her accompany, cheerful conversations and for the delicious dinners she served.

I would also like to thank my mum, my dad and my sister for their deep supports of any kind. I cannot express how grateful I am to them with words. Their prayers were always with me. I am also grateful to my mother-in-law and father-in-law for supporting me and also to my sister-in-law for her care and advices.

Last but not the least, my greatest appreciation goes to my husband and best friend, Emrah. Without a doubt, I always knew that he believed in me. He has been caring and encouraging all the time during these three years. He could not be even more patient and supportive in spite of all the time my PhD took me away from him. Without him, I could not have finished this thesis.

Abstract

PSHA calculations rely on several models and assumptions in its components, such as the characterization of seismic sources, the establishment of recurrence laws in magnitude, and the choice of ground-motion prediction equations. The final output of a PSHA study is the hazard curve that gives annual rates of exceedances of different acceleration levels. All steps of the PSHA calculation bear uncertainties. Understanding the impact of these uncertainties on the final output of the PSHA is not straightforward. Until recently, little attention has been paid to testing the final output of PSHA models against observations. Acceleration datasets and intensity databases, partially independent from the PSHA calculations, can be used, as proposed in a handful of recent papers (Stirling & Gerstenberger 2006, Stirling & Gestenberger 2010, Albarello & D'Amico 2008).

This study is aimed at testing PSH models in France (MEDD2002, AFPS2006 and SIGMA2012) and also in Turkey (SHARE), developing a quantitative method for comparing predicted and observed number of sites with exceedance over the lifetime of the network. This method builds on the studies of Stirling & Gerstenberger (2010) and Albarello & D'Amico (2008). All sites are sampled, observation time windows are stacked, and the PSHA is evaluated over a large geographical area at once. The objective is to understand the possibilities and limits of this approach, as observation time windows are short with respect to the return periods of interest in earthquake engineering.

Results show that the AFPS2006 PSH model is consistent with the observations of the RAP accelerometric network over the acceleration range 40-100 $cm.s^{-2}$ (or 50-200 years of return periods). The MEDD2002 PSH model over-predicts the observed hazard for the return period of 100 years. For longer return periods (475 and 975 years), the test is not conclusive due to the lack of observations for large accelerations. No conclusion can be drawn for acceleration levels of interest in earthquake engineering.

The proposed method is applied to Turkey. The PSHA model can be tested using longer observation periods and higher accelerations levels than in France. The PSH model is tested for different selections of accelerometric sites, minimum inter-site distance and total observation period. For accelerations between 0.1 and 0.4g, the model is consistent with the observations for all tests. At lower acceleration levels, the agreement between the model and the observations varies depending on the decisions taken.

Finally, the PSHA models in France are evaluated using the macroseismic intensity database (SISFrance). Completeness time windows are estimated from statistics on the intensity data ($I \geq 5$, MSK). Twenty-five sites are selected, with completeness time periods for $I \geq 5$ extending between 66 and 207 years, located in the highest active zones in France. At 100 years return period, MEDD2002 models predicts more sites with exceedances than the observed number of sites. At return periods higher than or equal to 475 years, both models AFPS2006 cannot be discriminated as both are consistent with observations. Considering the uncertainties on the selection of sites, on the determination of completeness time periods, and on the equation selected for converting intensities into accelerations, the results based on macroseismic intensities should be considered very carefully.

Résumé

L'estimation probabiliste de l'aléa sismique est basée sur plusieurs modèles et hypothèses à chaque étape, tels que la caractérisation des sources sismiques et des distributions de magnitudes, et le choix d'équations de prévision du mouvement du sol. Le résultat final de ces études est la courbe d'aléa qui donne les taux annuels de dépassement pour différentes valeurs d'accélération. Chaque étape du calcul comporte des incertitudes. Comprendre l'impact de ces incertitudes sur le résultat final n'est pas évident. Jusqu'à récemment, peu d'études se sont intéressées à tester le résultat final des calculs d'aléa sismique. Des données accélérométriques ou d'intensités macrosismiques, partiellement dépendantes des calculs d'aléa sismique, peuvent être utilisées, comme l'ont proposé quelques articles récents (Stirling & Gerstenberger 2006, Stirling & Gestenberger 2010, Albarello & D'Amico 2008).

Cette étude vise à tester les estimations probabilistes de l'aléa sismique en France (MEDD2002, AFPS2006 et SIGMA2012) et aussi en Turquie (SHARE), en développant une méthode quantitative pour comparer les nombres prédits et observés de sites avec dépassement pendant la durée d'observation. Cette méthode est basée sur les travaux de Stirling & Gerstenberger (2010) et Albarello & D'Amico (2008). Les modèles sont évalués pour une zone étendue en sélectionnant tous les sites et en sommant les durées d'observation à chaque site. L'objectif est de comprendre les possibilités et les limites de cette approche, quand les durées d'observations sont courtes par rapport au temps de retour pertinent en génie parasismique.

Les résultats montrent que le modèle AFPS2006 est cohérent avec les observations du Réseau Accélérométrique Permanent (RAP) pour les accélérations entre 40 et 100 $cm.s^{-2}$ (temps de retour entre 50 et 200 ans). Le modèle MEDD2002 surestime l'aléa sismique pour un temps de retour de 100 ans. Pour des temps de retour plus longs (475 et 975 ans), il n'y a pas d'observation au dessus du seuil d'accélération. Cette méthode ne permet donc pas de tester les niveaux d'accélérations d'intérêt en génie parasismique.

La méthode proposée a aussi été appliquée pour la Turquie. Les modèles d'aléa sismique peuvent être testés avec des observations plus longues et des niveaux d'accélération plus élevés qu'en France. Le modèle est testé pour différentes sélections de stations accélérométriques, différentes valeurs de la distance minimum entre stations, et différentes durées totales d'observations.

Pour des accélérations entre 0.1 et 0.4 g, le modèle est cohérent avec les observations pour tous les tests. Pour des seuils plus bas, les résultats varient en fonction des décisions prises.

Enfin, les modèles probabilistes d'aléa sismique en France ont été évalués avec la base de données SISFRANCE d'intensités macrosismiques. Les périodes d'observations complètes sont estimées par une analyse statistique des données ($I \geq 5$, MSK). Nous avons sélectionné 25 sites avec des durées d'observations pour $I \geq 5$ variant entre 66 et 207 ans, localisés dans les zones les plus actives de France. Pour un temps de retour de 100 ans, le modèle MEDD2002 surestime le nombre de site avec dépassement. Pour des temps de retour de 475 ans et plus longs, les modèles MEDD2002 et AFPS2006 ne peuvent pas être distingués car ils sont tous les deux compatibles avec les observations. Ces résultats basés sur les données d'intensité doivent être considérés de façon très prudente considérant les incertitudes sur la sélection des sites, sur la détermination des durées d'observations et la complétude, et sur l'équation utilisée pour convertir les intensités en accélérations.

Contents

Chapter 1

Introduction

The hazard at a site is usually expressed in terms of the annual rate of exceedance of a ground motion level. If the observation time window is long enough at a site, the annual rate of exceedances could be obtained by simply counting the observed number of exceedances during the observation period. However, for all sites in the world, the complete observation time windows are too short to obtain the hazard curves empirically.

The probabilistic seismic hazards assessment (PSHA) exploits our knowledge in geology, geophysics, paleoseismology and seismology for estimating the expected ground motion levels in a future time window at a site. The final output of the PSHA is a hazard curve that expresses the hazard in terms of annual rates of exceedances corresponding to different acceleration levels (Figure 1.1). In building codes, the design value of conventional buildings is usually selected as the acceleration corresponding to 10% of exceedances probability in 50 years, which is equal to one occurrence on average every 475 years when assuming that the occurrences of ground motions follow a Poisson process. The design acceleration levels that should be considered for the safety of nuclear plants correspond to return periods of 10000 years and longer. Low levels of accelerations correspond to shorter return periods and they are exceeded more often than high acceleration levels. PSHA studies should provide as accurate information as possible to help governments in establishing safety regulations, evaluating seismic risk and developing emergency planning.

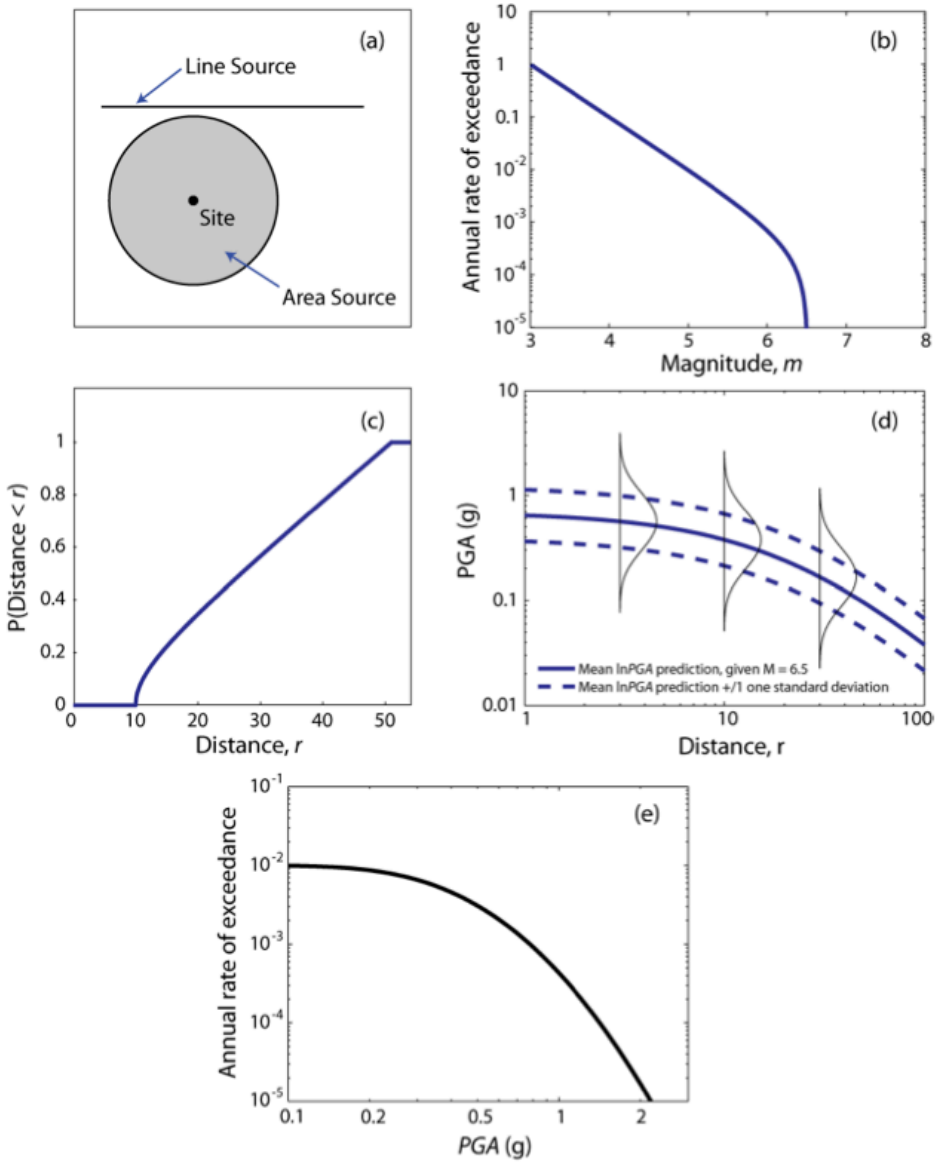

Figure 1.1: The basics steps followed during a probabilistic seismic hazard assessment study (from Baker 2008). (a) Identifying seismic sources that may generate an acceleration level of interest at a selected site. (b) Determining the frequency magnitude distribution considering all sources. (c) Determining the probability distribution of source to site distance. (d) estimating the resulting ground motion at the sites due to the likely distance and magnitude distributions. (e) Combine information from parts a-d to compute the annual rate or the probability of exceeding a given ground motion intensity over a time period.

In general, PSHA models are established following a classical Cornell-McGuire PSHA method (Cornell 1968, McGuire 1976). A PSHA calculation consists of the steps illustrated in Figure 1.1; 1) identifying the seismic sources around the selected site, 2) determining the frequency -magnitude distributions of each sources (line/fault or areal sources), 3) determining

the probability distance distribution between the possible earthquakes and the site, 4) estimating the resulting ground motion at the site due to all earthquakes. The final output of a PSHA calculation is the combination of different models and hypothesis, which bear some uncertainties. Different PSHA studies may follow different assumptions at each step depending on the information available and on the expert opinions. As a consequence, the exceedance probabilities of ground motion thresholds estimated at a specific site may vary between different PSHA calculations (Figure 1.2).

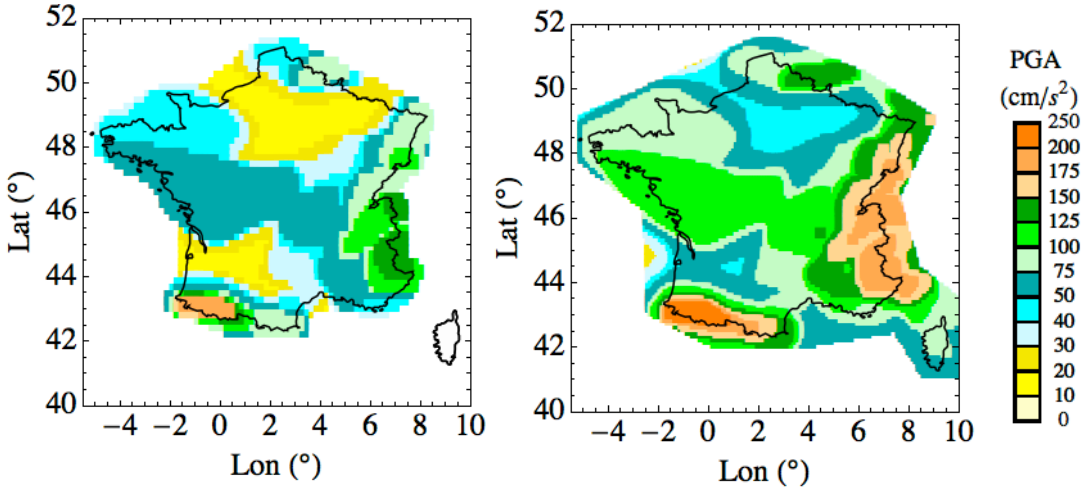

Figure 1.2: Example for the differences in the predicted ground motion levels given by two PSHA calculations for the same region. The hazard maps of peak ground accelerations (PGA) corresponding to 475 years of return given by AFPS2006 PSHA study (left, Martin & Secanell 2006) and MEDD2002 PSHA study (right, Martin *et al.* 2002, Sollogoub *et al.* 2007) for France.

A reliable PSHA must take into account and quantify uncertainties. The uncertainties in the description of the seismic sources (magnitude, distance, source characteristics) and in the ground motion they can produce are generally captured using a logic-tree. The final output of a PSHA study is a hazard curve, annual rates of exceedances of ground-motion thresholds at a site.

The comparison with observations can be performed at the intermediary steps of the probabilistic calculations. Several studies have evaluated the components of PSHA analysis using observations: testing seismic source models both in magnitude, time and space (e.g. Musson & Winter 2012; Rhoades *et al.* 2002), testing ground motion prediction equations (e.g. Delavaud *et al.* 2012, Beauval *et al.* 2012; Scherbaum *et al.* 2009). However, in the literature, there have been few attempts for evaluating the final hazard estimates of a PSHA.

PSH models can be evaluated using different types of observations, such as macroseismic intensities, accelerations recorded at instrumented sites, or maximum acceleration levels based on fragile geological features (precarious rocks, Anderson et al. 2011) (see Figure 1.3). Some methods have been proposed recently for testing PSHA against observations. Some of them rely on macroseismic intensities, like in Stirling & Gerstenberger (2006). Others rely on instrumental ground-motion data (Albarello & D'Amico 2008, Fujiwara *et al.* 2009, Stirling & Gerstenberger 2010). It is also possible to constrain the hazard models at long return periods using the data of fragile geological features (Anderson *et al.* 2011). Using fragile geological features requires identifying e.g. precarious rocks, and estimate since when the rock is in this state (dating). For now no such study has been led in France. In this study, we will focus on testing PSHA models using accelerometric and macroseismic intensity data.

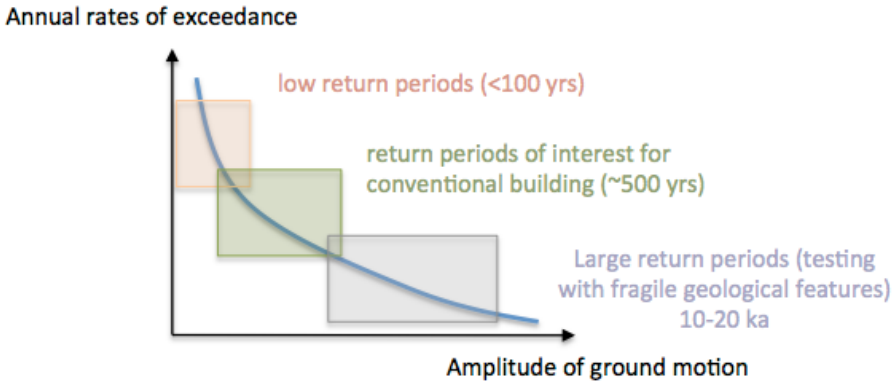

Figure 1.3: Simple scheme to illustrate how in theory the available observations could be used for constraining different parts of the hazard curve: accelerations should help contraining results at low return periods, macroseismic intensities at intermediate return periods (around 475 years), and fragile structure in equilibrium (Anderson *et al.* 2011) for large return periods (around 10 to 20 ka).

In order to test the hazard curve against observations, these observations must be as independent as possible from the different steps of the hazard calculations. Accelerometric data recorded on the French territory are partially dependent from the probabilistic calculations. They are partly included in the generating datasets of the GMPEs used in the PSHA, but they represent an extremely small percentage of these datasets. Historical intensity data are also partially dependent from the PSHA calculations, because macroseismic intensities have been used to estimate the magnitudes of historical earthquakes, but the individual data points are not used directly.

Due to the limited observation time windows available, the evaluation of a PSHA model is very challenging, even in high seismicity regions. The longest observation time windows for accelerometric stations consist of several decades at maximum around the world (maximum 80 years for the first station installed in the US, 16 years for the first station installed in France). Thus, comparing predictions and observations at one particular site is nearly impossible at acceleration levels of interest in earthquake engineering (Beauval et al. 2008).

PSHA studies are based on the ergodic assumption for estimating the repeatability of ground motions at a single site from spatial ground motion uncertainties (Anderson & Brune 1999). According to Anderson & Brune (1999), "*An ergodic process is a random process in which the distribution of a random variable in space is the same as the distribution of that same random variable at a single point when sampled as a function of time*". In other words, the properties of an ergodic process can be obtained considering very long observations at a single site or considering shorter observations at several independent sites. For compensating the limited observation lengths, one can consider several independent sites at once. The recent studies by Stirling & Gerstenberger (2010) and Albarello & D'Amico (2008), have followed this approach for testing PSHA against accelerometric data.

In the second chapter, we propose a testing methodology inspired from the studies of Stirling & Gerstenberger (2010) and Albarello & D'Amico (2008). The PSHA testing method is first implemented in France using different types of data: accelerations, synthetic accelerations, and macroseismic intensity. When performing the testing, a special attention is given to the understanding the limits of the tests. In this study, we introduce clearly the assumptions made and we test hazard models using different assumptions: different number of sites, different observation lengths, changing inter-site distances thresholds. Three probabilistic seismic hazard models recently established for France (MEDD2002, AFPS2006 and SIGMA2012) are tested against accelerometric data. Due to the short observation lengths at accelerometric stations, we also take advantage of an earthquake catalog, coupled to a ground-motion prediction equation, to extend the observation length.

Since France is a low-to-moderate seismicity country, the available data consist of mainly low acceleration levels. In the third chapter, we apply the same approach to a more active region, Turkey. The higher observed acceleration levels, the length of accelerometric observation period and the quantity of accelerometric stations make the Turkish accelerometric database appealing

for evaluating PSHA models. The Turkish data allow us to apply tests at higher ground motion levels (~0.4g) using different number of sites and different inter-site distances.

The evaluation of French PSHA models at return periods of interest (>475 years) is required for engineering purposes. In the last chapter we study the possibility of using SISFrance macroseismic intensity database for evaluating recent PSHA models of France (www.sisfrance.net, Scotti *et al.* 2004), following the same methodology. The uncertainties in handling macroseismic intensity data are evaluated and discussed.

Chapter 2

Testing Probabilistic Seismic Hazard Estimates Against Observations: Application In France Using Accelerometric Data

Hilal Oksuz-Tasan, Céline Beauval, Agnès Helmstetter

In revision in Geophysical Journal International

Contents

Summary

Probabilistic seismic hazard models (PSHM) are used for quantifying the seismic hazard at a site or a grid of sites. In the present study, a methodology is proposed to compare the distribution of the expected number of sites with exceedance with the observed number considering an acceleration threshold at a set of recording sites. The method is applied to France, where three existing PSH models are tested (MEDD2002, AFPS2006 and SIGMA2012). The French accelerometric database is checked to produce a reliable accelerometric dataset going down to low accelerations (minimum acceleration 1 cm/s^2). This database contains 62 rock stations with observation time windows varying from 2.8 to 16.6 years. In addition to this dataset, we also used a synthetic dataset inferred from the instrumental LDG catalogue spanning 34 years and combined with the ground-motion prediction equation Cauzzi & Faccioli (2008). The results show that all models over-estimate the number of sites with exceedance for low acceleration levels (below 30 to 70 cm/s^2 depending on the model and the dataset) or short return periods (smaller than 50 yrs for AFPS2006 and 475 yrs for MEDD2002). For larger acceleration levels, all models are consistent with the observations. However, for very large accelerations or long return periods, the observed number of exceedances decreases down to zero, especially for SIGMA2012 model covering only southeastern France. Nevertheless, the models cannot be rejected in this range since the 2.5% percentile of the distribution of predicted number of exceedances is also zero.

2.1 Introduction

Probabilistic seismic hazard models (PSHM) are used for quantifying the seismic hazard on a site or on a grid of sites. Probabilistic seismic hazard maps are now the basis for establishing seismic building codes in most parts of the world. These maps provide at geographical locations the ground motions with given probabilities of being exceeded in a future time period. Typically for conventional buildings, probabilities of exceedance of 2% to 10% over a 50 years time window are taken into account, corresponding to return periods of 2475 to 475 years (Poisson model). Very few studies have tested PSH models against observations using independent observations. Several recent Opinion papers in Seismological Research Letters are encouraging hazard analysts to carry out tests (Stein *et al.* 2011, Stirling,

2012). However, considering the observation time window in seismology (~100 years at maximum for instrumental networks, and several centuries for historical data), testing at the return periods of interest in engineering seismology is a real challenge. Validation of the full probabilistic hazard curve with observations at a site is strictly impossible as several thousands of years of observation would be required (Beauval *et al.* 2008). Nonetheless testing partially these models against observations is possible (Beauval 2011). Several authors have proposed ways to test the probabilistic estimates and the present study is building on these works and thoughts. PSH models can be evaluated using different types of observations, such as intensities, "synthetic" accelerations (converted from intensities or predicted from an earthquake catalog), true accelerations recorded at instrumented sites, or maximum acceleration levels based on precarious fragile structures (Baker *et al.* 2013). The methods to compare probabilistic estimates with observations are either focusing on a site or gathering several sites at once. They range from purely qualitative techniques to quantitative statistical methods.

Since the first application of the Cornell-McGuire probabilistic method (Cornell 1968, McGuire 1976), some authors have proposed to compare hazard curves with observed intensity rates. Macroseismic intensities bear large uncertainties, but they are available over much longer time windows than accelerations. In these studies, intensities are either true observed intensities at the sites, or they have been derived from earthquake catalogs using an intensity-magnitude attenuation relationship. An example of the latter case is presented in Papazachos *et al.* (1990) focusing on seismic hazard in Greece. An intensity-magnitude relationship was used to generate the sequence of intensity observations at a site, as if an "observer" was there continuously. This sequence was then converted into a recurrence curve at the site, taking into account completeness issues. The authors superimposed the "observed" rates on hazard curves evaluated in terms of intensities at a series of sites. More recently, Stirling & Petersen (2006) proposed a similar comparison of predictions with observations, with applications in New Zealand and in the United States, the main difference being that true macroseismic intensities were used. Intensities were converted into accelerations applying an equation. The authors discussed in great details the uncertainties that might influence the results and tried to understand the discrepancies. Another direction was explored in Mucciarelli *et al.* (2008), who reconstructed the intensity history at a site from observed intensities and calculated ones (based on epicentral information or neighboring intensity observation). They

chose not to include an intensity-acceleration conversion and compared PSH and intensity-based recurrences through the ranking of hazard evaluated at many sites in Italy. Most of these studies acknowledged the difficulty of calculating observed rates from potentially short time windows. To counteract this limitation, they analyzed the results considering all sites as a whole, a reasoning close to sampling in space. Although rather qualitative, these comparisons can highlight large discrepancies between observations and hazard estimates, and encourage understanding the causes and questioning the models. Such studies nourish the debates on the probabilistic seismic hazard analyses, on the building of the seismicity model, on the prediction of ground motions and on the final hazard values.

At present, hazard curves are most often provided in terms of accelerations. The first attempt to use recorded ground motion to superimpose acceleration rates on a hazard curve was published by Ordaz & Reyes (1999). Few stations in the world have been recording since 1968 like this station in Mexico City. However, as shown in Beauval *et al.* (2008), when focusing on one site only return periods much shorter than the observation time can be tested. Several authors proposed to compensate the short time periods of observations by sampling in space. Ward (1995) performed area-based probabilistic seismic hazard tests, based on a grid of sites where synthetic accelerations were predicted from an earthquake catalog. More recently, Fujiwara *et al.* (2009) carried out a comparison between predictions and observations, taking advantage of the dense Japanese accelerometric network. Considering a ground-motion threshold, they summarized the hazard map in one number, the average probability of exceedance over the grid of sites covering Japan, and compared this number with the percentage of accelerometric stations with exceedance (K-NET network). Using the recorded strong motions at the New Zealand network, Stirling & Gerstenberger (2010) calculated observed numbers of exceedance for two acceleration thresholds (100 and 200 cm/s^2) and compared these numbers with the value predicted by the probabilistic seismic hazard analysis. Number of exceedances was compared first on a site-basis, then considering all sites at once. Albarello & D'Amico (2008) took advantage of the Italian strong motion network. They used a 30-yr time recording window to test a PSH model against observations, considering all sites at once. The present study builds on these works, and develops a method for testing probabilistic seismic hazard estimates available at the sites of an accelerometric network, and for exploring the uncertainties of the method.

The aim here is to test the final output of the probabilistic calculations, the hazard

curve. Understanding the impact of the uncertainties of PSH components on the final output is not straightforward (e.g., Beauval & Scotti 2004), and we believe that the full PSH model needs to be tested. However, the comparison with observations can also be performed at the intermediary steps of the probabilistic calculations. Seismicity models, predicting the frequencies, size, and locations of future earthquakes, can be tested against earthquake catalogs. The Collaboratory for the Study of Earthquake Predictability (Schorlemmer & Gerstenberger 2007) experiment is currently developing robust statistical protocols to test earthquake forecasts against earthquake occurrences (Zechar *et al.* 2010, Rhoades *et al.* 2011). Moreover, a set of ground-motion prediction equations must be selected to feed the logic tree in the PSH calculation. The selection can be performed using accelerometric data from the region under study, i.e. testing the model against observations (e.g. Scherbaum *et al.* 2004). Such studies are underway in France, the difficulty here is to test ground-motion prediction equations developed from moderate-to-large events on low-magnitude datasets (see, e.g., Beauval *et al.* 2012). Testing the intermediate steps of the probabilistic calculation is complementary to testing the PSH output, but it should be underlined that conclusions from the former cannot be generalized to the latter. In New Zealand, test of predictions against observations has been done in details both at the level of the PSHA components (Rhoades *et al.* 2002) and at the level of the hazard curve (Stirling & Petersen 2006, Stirling & Gerstenberger 2010), and they came out with the following enlightening conclusion: "Our analysis implies that a PSH model may be consistent with the historical record of hazard despite component comparisons showing significant discrepancies. It therefore appears that the complexity of the PSH modeling process mutes the impacts of these components, and may even allow some to cancel others out" (Stirling & Gerstenberger 2009, p. 4).

In the first part of this article, we present the methodology followed to test probabilistic hazard estimates and explore uncertainties. The method is applied in metropolitan France, an example of low-to-moderate seismicity region, using datasets covering different observation time-windows: ground motion data recorded at the stations of the French Accelerometric Network (RAP), and synthetic ground motions predicted from an earthquake catalog. To minimize the influence of site classification on the results, only stations considered as rock stations are used. Three probabilistic hazard studies recently established for France are tested. The Ground Motion Prediction Equations (GMPE) used in these studies might include recordings from the RAP database, but these recordings would represent a very small

percentage of the generating dataset. Nonetheless, the dataset can be considered as approximately independent from the PSH calculations.

2.2 Method for Testing PSHM against Observations

The method developed in the present study is building from several previous works. As introduced by Ward (1995), the length of observation time windows can be compensated by considering several sites and sampling in space. Thus, the consistency of a PSH model with the observations is evaluated at several locations at once. Following Albarello & D'Amico (2008), sites need to be distant enough from each other. Acceleration occurrences must be independent from one site to the other, and the ground-motion occurrences at the different sites are assumed to belong to the same unique stochastic process. The acceleration thresholds with a given probability p of exceedance in a given time window are inferred from the hazard curves at all sites. Albarello & D'Amico (2008) considered only sites having the same lifetime (30 years, 68 sites). For each site, either the threshold has been exceeded during the observation time window (success with a probability p according to the PSH model), or there was no exceedance (probability 1-p). The situation is comparable to a sequence of independent yes/no experiments. Therefore the binomial distribution gives the expected number of sites with exceedances

$$P(n) = \binom{N_S}{n} p^n (1-p)^{N_S - n} = \frac{N_S!}{n!(N_S - n)!} p^n (1-p)^{N_S - n} \quad (1)$$

where $P(n)$ is the probability to observe n sites with exceedance out of the N_S sites, p is the probability of an experiment resulting in a success. If the observed number corresponds to a very low or very high probability (compared to a chosen confidence interval), the test indicates that the model over- or under-predicts the observations.

Stirling & Gerstenberger (2010) proposed another approach, adapted to the New Zealand accelerometric network where station lifetime varies a lot from one station to the other (from 6 to 44 years, 24 stations in 2009). The test aims at comparing the predicted and observed number of exceedances, while Albarello & D'Amico (2008) compare the number of sites with exceedance. At one site, for a given acceleration threshold g_0, a PSH model provides the mean annual rate of exceedance λ_i. The mean expected number of exceedances is obtained

by multiplying the rate λ_i by the duration of the observation time window t_i. Again, accelerations at a site are assumed to occur according to a stationary Poisson process. The Poisson distribution, fully defined by its mean, provides the probability of observing a given number n of accelerations above the threshold g_0 :

$$P(n) = \frac{\left(\lambda_i t_i\right)^n e^{-\lambda_i t_i}}{n!} \tag{2}$$

where t_i is the time window at the site i with annual rate of exceedance λ_i given by the PSH model. The authors defined the following simple statistical test: if the observed number falls within the tails of the distribution, defined by the percentiles 2.5 and 97.5%, the observations are considered consistent with the model (model is not "rejected"). Stirling & Gerstenberger (2010) first evaluated PSH models at individual sites and then gathering all sites. They wrote p. 1408 "The summed analysis is conducted because the site-specific comparisons often involve very few events and would yield meaningless results in many cases". The sites are far enough apart so that they can be considered independent in terms of ground-motion exceedances. As the sum of independent Poisson processes constitutes a Poisson process, the total number of exceedances observed over all sites is compared to the distribution defined by the following mean:

$$N_{total} = \sum_{sites} \lambda_i t_i \tag{3}$$

Stirling & Gerstenberger (2010) obtained different results when testing each site individually and when considering all sites at once (Equation 3). When testing each site individually, the model is not rejected at 22 out of 24 sites, i.e., the observed number of exceedances is within the confidence interval of the discrete Poisson distribution. However, when testing the whole network at once, i.e. comparing the total observed and predicted numbers of exceedances, the PSH model is rejected with 95% confidence, as it is predicting fewer exceedances than have been observed in the historical period. This suggests that testing the PSH model against the total number of exceedances is more meaningful than individual tests.

The French accelerometric network has been built progressively since 1995, and lifetime of stations varies from 2.8 to 16.6 years. The test must be able to handle varying

lifetimes to take advantage of the full database. A PSH calculation yields the probability that an acceleration level will be exceeded "at least once" over a time window. We prefer to focus on the number of sites with exceedance, rather than the exact number of exceedances, although both studies are possible. In total, 62 sites in France are included in the analysis. The Monte Carlo method is used to sample the site-specific Poisson distributions (Equation 2), characterized by their means ($\lambda_i t_i$), and generate numbers of acceleration exceedances for all sites (corresponding to time windows t_i). One run yields one set of 62 numbers of exceedance. Sampling the Poisson distributions many times, many sets of numbers of exceedances are generated. All are compatible with the PSH model. For each run, we count the total number of sites with exceedance. Finally, 10.000 runs provide 10.000 total numbers of sites with at least one exceedance (out of 62), and a probability distribution can be built. This distribution describes the expected number of sites with exceedance, for a virtual network having the same number of stations as the accelerometric network, and the same lifetimes. This probability distribution has a shape very close to a binomial distribution. Note that in the case of Albarello & D'Amico (2008), where all sites have the same lifetime, this distribution is binomial and can be obtained analytically. In Figure 2.1, as an example, the test is led considering 5 RAP stations and a given acceleration threshold.

2.3 Building the Accelerometric Dataset

In France, the first stations of the accelerometric network were installed in 1995 (French Accelerometric Network, RAP, Péquegnat *et al.* 2008). Since then, the number of stations has increased, reaching at present a total of 142 sites in Metropolitan France. Out of these 142 sites, 69 are identified as 'rock sites' (shear-wave velocity at 30 m depth larger than 760 m/s; see Régnier *et al.* (2010) and the information given on the RAP website). Most of these stations are located in the Pyrenees (19), Alps (33) and Lower Rhine Graben (5), regions with the highest seismic hazard in metropolitan France. The RAP stations are either in triggering mode or continuous recording stations. They consist of one three-component broadband accelerometric sensor (kinemetric episensors, except for some of the oldest stations having Guralp CMG5). They are connected to a 24-bit three-component digitizer sampling at 125 Hz. The useful frequency band is 0-50 Hz. Only offset correction is applied to the data without any additional filtering.

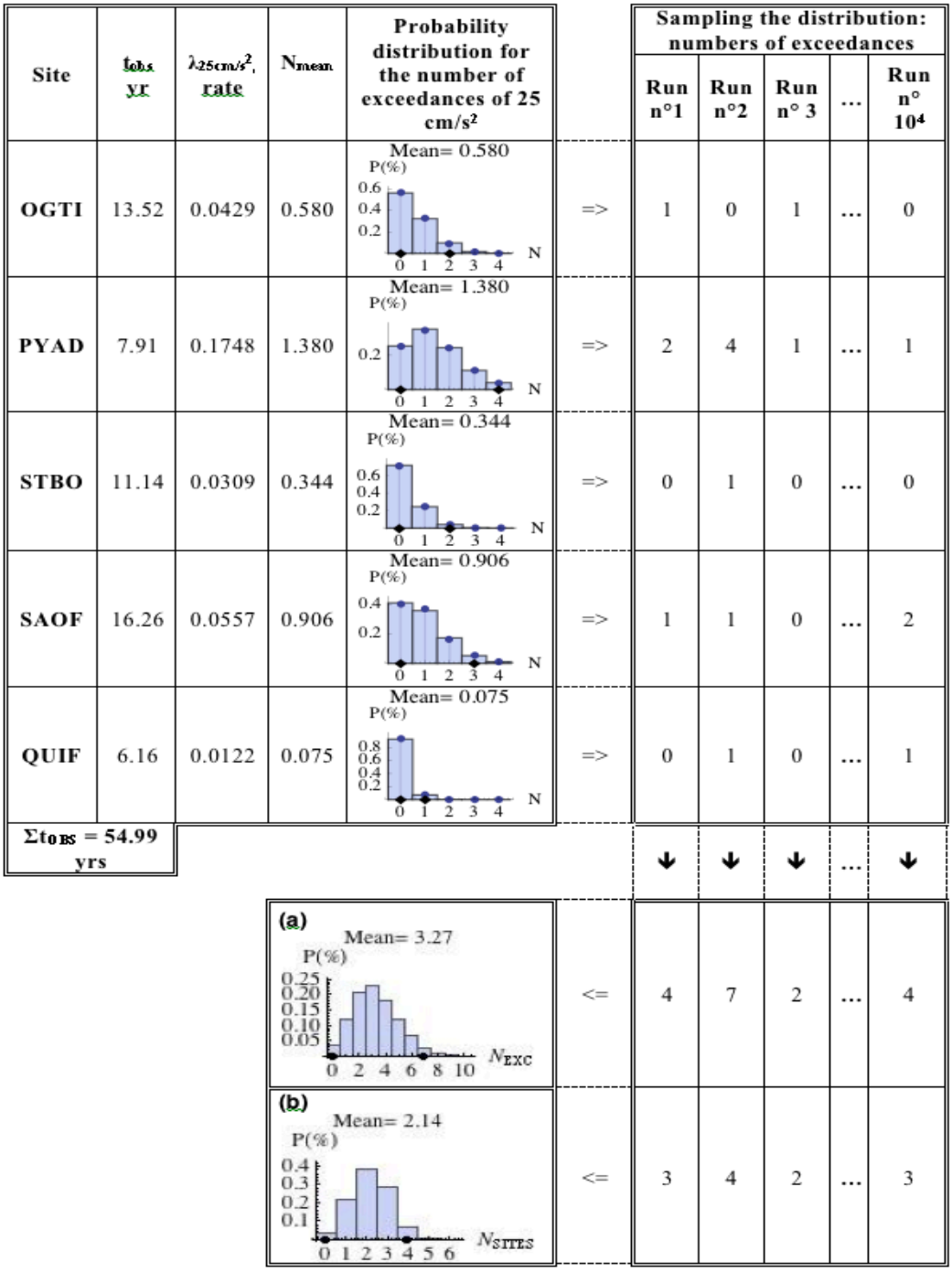

Figure 2.1: Scheme detailing the Monte Carlo process followed for generating a) the probability distribution for the number of exceedances (N_{EXC}) considering all sites, b) the probability distribution for the number of sites with at least one exceedance (N_{SITES}). The acceleration threshold is fixed (25 cm/s^2). Five accelerometric sites are considered in this example, with different observation windows, resulting in a total observation time window of 54.99 years. The probability distributions provide numbers of occurrences over 54.99 years. t_{OBS}: observation time length of the stations, $\lambda_{25cm/s}{}^2$: predicted annual rate of exceeding 25cm/s^2, N_{mean}: Predicted number of exceedances for a ground motion higher than or equal to 25cm/s^2 during t_{OBS}.

The database extends over 16 years, from June 1995 to July 2011, and contains 40431 recordings (horizontal two-components). To limit the size of the database, we selected only signals with Peak Ground Amplitude (PGA) higher than 1 cm/s^2, whatever the magnitude of the earthquake, reducing the total number of records to 2207. Stations in buildings and boreholes are not used. Note that a few events recorded only on one horizontal component and on the vertical component are kept.

After a careful check of the database, we identified several issues: bad association of records with responsible earthquake, shift of signal baselines, truncation of records, and low signal-to-noise ratio. For all signals, we checked the association of a record with an earthquake by comparing the P-wave arrival time observed on the signal with the arrival time estimated from the earthquake location and origin time given in the RAP database. If the observed and estimated arrival times differed by more than 10 seconds, we looked for an explanation. Either the clock of the station was not correct, or the record had not been associated with the right earthquake. For ten records, the associated earthquake was not correct and the appropriate one was extracted from the Renass earthquake catalog (See "Data and Resources" section). For 54 signals, the shift was likely due to a clock problem of the station. Indeed, in most cases the time shift was a multiple of 60 seconds, as often observed for clock problems.

Other issues encountered are shifts in the signal baselines and truncation of signals. Forty-two records contain a sudden shift in the baseline, which we corrected. Due to completeness issue, truncated records must be kept in the database. Twenty-four records were clearly truncated after the occurrence of the peak amplitude, and thus only the PGA could be estimated. Records that were truncated in the middle of the signal were kept and the amplitude considered as a minimum threshold for PGA (38 signals).

The final dataset used for testing PSH models contains 701 two-component records recorded at 47 rock sites, corresponding to 551 earthquakes (Figure 2.2). At the other 15 rock stations, no ground motion higher than 1 cm/s^2 occurred during their lifetime, these stations are nonetheless included in the analysis. For the sake of independency of sites, stations located closer than 10 km to another rock station are not considered further (7 stations). In this case, we kept the station with the largest expected number of exceedances during the station lifetime. The time windows of observations vary from one station to the other; 28 stations have been recording between 5 to 10 years, and 29 of them have been recording between 10 to

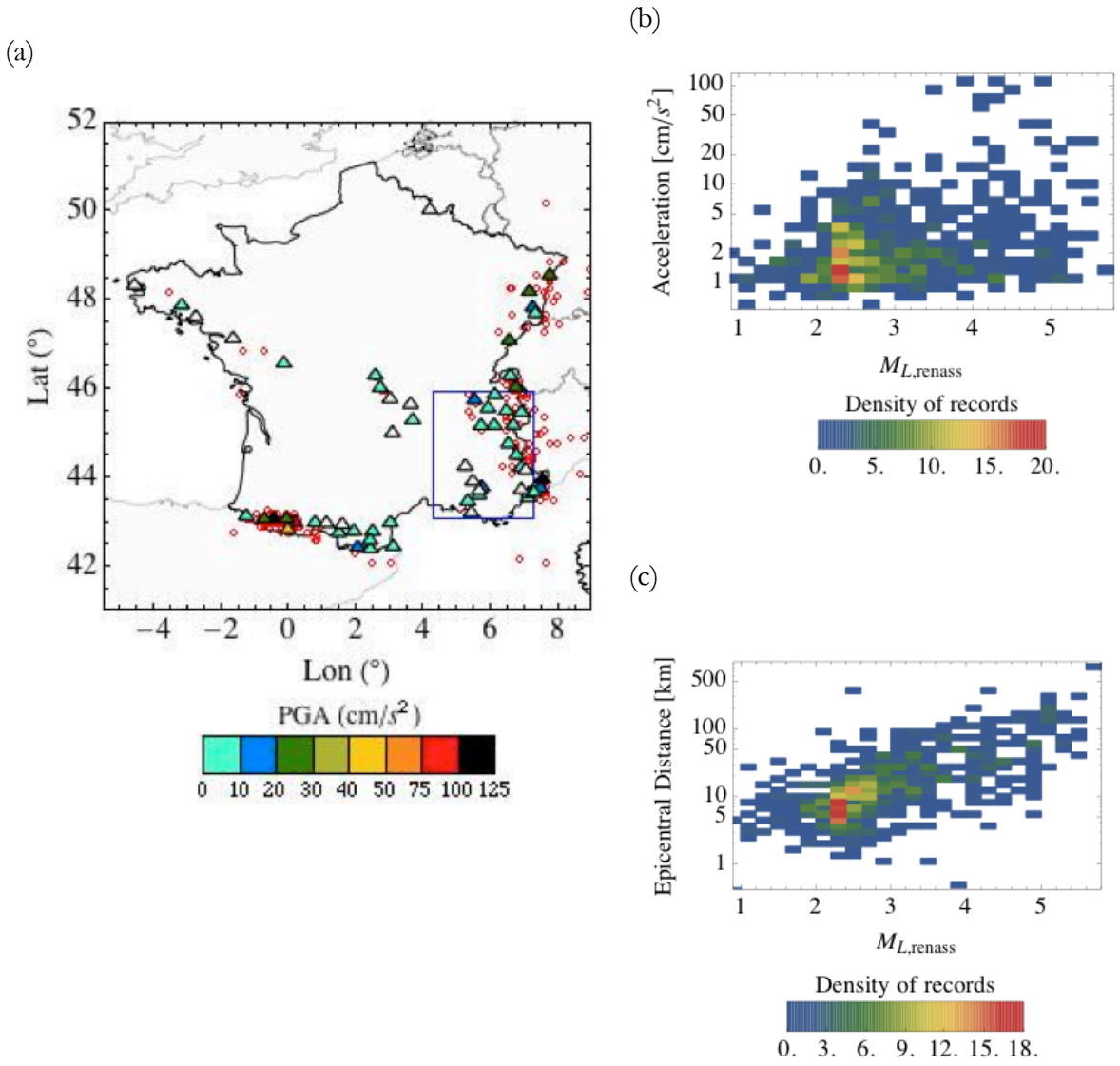

Figure 2.2: The accelerometric dataset built from the RAP raw database, for testing PSHA in France. (a) Colored triangles: the 47 rock stations which have experienced at least one PGA ≥1 cm/s^2 during their lifetime, white triangles: 15 remaining rock stations. Color scale: maximum acceleration recorded at each station. Circles: responsible earthquakes. Blue rectangle: region considered in the SIGMA2012 study. (b) Distribution of all PGA amplitudes against the magnitude of the corresponding earthquake (M_{L_Renass}). (c) Distribution of epicentral distances of these records against the magnitude of the corresponding earthquake.

16 years. Three rock stations have recorded a PGA higher than 100 cm/s^2, SAOF in the South-East Alps and PYBB/PYAD in the Pyrenees, whereas half of the stations recorded at maximum a PGA lower than 10 cm/s^2 (Figure 2.2). Magnitudes responsible for producing a PGA higher than or equal to 1 cm/s^2 (on at least one component of the accelerometric

stations) vary between 1 and 5.7 (Renass local magnitude, M_{L_Renass}). However, most of the data have been produced by magnitudes between 2 and 3.5 (70% of the total database, M_{L_Renass}) at stations located between 5 and 70 km from the epicenters (89%).

Table 2.1: The five missing records which occurred within identified gaps (completeness check performed for accelerations ≥ 10 cm/s^2, see the text).

Event Date (y/m/d)	Event Time (h:m:s)	M_L *	Station Name	Station Latitude (°)	Station Longitude (°)	Gap † (y/m/d)	Gap Length (days)	R_{HYP} ‡ (km)	PGA_M § (cm/s^2)	□ t ‖ (days)
2006/11/17	18:19:50	4.9	PYCA	43.024	0.183	2006/09/28 - 2006/12/09	72	20	12.7	4.01
2007/11/15	13:47:35	4.5	PYCA	43.024	0.183	2007/07/15 - 2008/02/23	223	17	10.5	4.01
2009/04/05	00:06:37	3.0	PYCA	43.024	0.183	2009/03/19 - 2009/05/09	51	6.1	10.9	4.01
2001/01/25	02:17:15	3.0	OGSI	46.057	6.756	2000/10/03 - 2001/03/09	157	8	10.7	8.10
2008/11/20	13:20:19	3.4	OGSI	46.057	6.756	2008/07/27 - 2008/12/12	138	6.6	10.1	8.10

*Renass local magnitude
†Starting and ending date of time windows identified as a gap in the operating lifetime of the stations
‡Hypocentral distance
§Median PGA level predicted by GMPE
‖Average inter-event time

For our analysis, it is of primary importance to use a complete database, or at least to identify gaps in the recording and estimate the fraction of missing records in our database. We identified potential gaps in a station recording by analyzing the inter-event times (times between successive earthquakes) of the acceleration sequence, based on the raw RAP database (no threshold on the acceleration). Mean inter-event times were calculated, and inter-event times larger than 10 times the mean were considered as gaps in the recording (station not functioning) (Figure 2.S5 in Electronic Supplement). The station lifetime was shortened accordingly (Table 2.S1 in Electronic Supplement). Another test can be applied to check the completeness of our database, using an earthquake catalog and a GPME. This test if however limited by the inherent variability of ground motions. Using the Cauzzi & Faccioli (2008) equation, which fits well the French dataset (Beauval *et al.* 2012), we looked for earthquakes in the Renass earthquake catalog that should have produced a median acceleration larger than 10 cm/s^2 at the stations considered. Fifty-eight couples event-station were identified. Eight records were missing (2 at OGSI, 5 at PYCA, 1 at PYAT). Five of them occurred within identified gaps (Table 2.1). For the three remaining earthquakes, we did not find an

explanation for the missing record (Table 2.2). The station seemed to be working correctly at the time of the earthquake, since it detected a few events in the preceding and following days. Even if the problem is mostly localized on one station (PYCA), this suggests that the fraction of missing records (after correcting from identified gaps in the monitoring) is around 5% (3/58).

Table 2.2: The three missing records for which no explanation was found (completeness check is done for accelerations ≥ 10 cm/s^2, see the text).

Event Date (y/m/d)	Event Time (h:m:s)	M_L*	Station Name	Station Latitude (°)	Station Longitude (°)	Date of previous and next events (y/m/d)	R_{HYP}† (km)	PGA_M‡ (cm/s^2)	□ t§ (days)
2004/07/22	20:16:00	3.1	PYCA	43.024	0.183	2004/07/18-2004/07/25	6.8	10.2	4.01
2009/10/15	22:27:51	3.9	PYCA	43.024	0.183	2009/10/06-2009/11/10	8.9	14.9	4.01
2001/07/11	23:44:07	2.9	PYAT	43.0942	-0.7133	2001/07/10-2001/07/14	5	13.2	3.19

* Renass Local Magnitude
† Hypocentral distance
‡ Median PGA level predicted by GMPE.
§ Average inter-event time

2.4 Testing PSH Models against Accelerometric Data in France

2.4.1 PSH models

Three PSH models are tested in the present study. The MEDD2002 model has been derived for the official French seismic building code (Martin *et al.* 2002, Sollogoub *et al.* 2007), which entered in 2010 into the French regulations. It is the first building code in France established from probabilistic seismic hazard methods following the Eurocode 8 standards. The AFPS2006 model was developed later on (Martin & Secanell 2006), involving a different group of experts who were questioning some of the decisions taken in MEDD2002. This group was claiming that the hazard estimated in the MEDD2002 study was too high, based on a test led against observations (Humbert & Viallet 2008). Both models rely on the same seismicity models; the main difference in AFPS2006 with respect to MEDD2002 is the treatment of magnitude conversions and the ground-motion prediction equations used. We refer to the reports for details on the models used and their implementation in a logic tree. We do not question any of the decisions taken in these studies. We simply use these models and test them, because they are hazard references for France. The AFPS2006 study is predicting hazard values that are always lower or equal to the values of MEDD2002 model (Figure 2.3,

example at three sites in France). The MEDD2002 results are only available for 4 return periods (100, 475, 975, 1975 years), whereas the AFPS2006 results are available for 10 return periods (5 to 10000 years). The stations locations usually do not fall on one of the grid nodes but in the middle of a cell (0.1°x0.1° for MEDD2002, 0.2°x0.2° for AFPS2006), therefore mean values are calculated using the 4 hazard values of the cell's corners.

Minimum magnitudes used in the probabilistic calculations vary. In MEDD2002 study, the minimum magnitude $M_{L,LDG}$, local LDG magnitude (LDG, 2012), used is 4 (corresponding to moment magnitude, M_w, around 3.5 according to Drouet *et al.* 2010), and the study uses this magnitude as a surrogate for M_S. In AFPS2006 study, minimum magnitude varies with the GMPE used, between 2.5 ($M_{L,LDG}$) and 5 (M_S). In the present study, all accelerations recorded at the stations are taken into account, regardless of the magnitude of the earthquake. Uncertainties are present at all steps of the PSH calculation and the magnitudes contributing to the PSHA cannot be related easily to the magnitudes of the acceleration recorded at the sites of the RAP. The original magnitudes of earthquake catalogs have been converted using equations established over restricted magnitude range or equivalence has been assumed between magnitude scales (Martin & Secanell 2006). Most ground-motion prediction equations used in the PSH studies tested here are imported from other regions, they have not been tested against local data and it is not possible to prove that they are adapted to the full magnitude range nor that their variability is truly representative at the sites considered. Besides, the level of studies on site effects varies greatly from one site to the other, and the uncertainty on the assigned class is expected to be large.

At last, the SIGMA2012 study was carried out within the SIGMA project (Carbon *et al.* 2012, Drouet 2012) and focused on southeastern France (see Figure 2.2, area of 240km×320km). The full hazard curves are provided for the stations locations. The acceleration range considered is from 1 to 1000 cm/s^2. This study uses two GMPE developed from earthquakes with a wide magnitude range: the Bommer *et al.* (2007) model, established from earthquakes with $M_w \geq 3$, and the Atkinson & Boore (2011) model, from earthquakes $M_w \geq 3.5$ (see Section "Selection of the GMPE"). Logic tree results are provided separately for each GMPE. The minimum magnitude used in the PSH calculation is the minimum bound of the GMPE generating dataset.

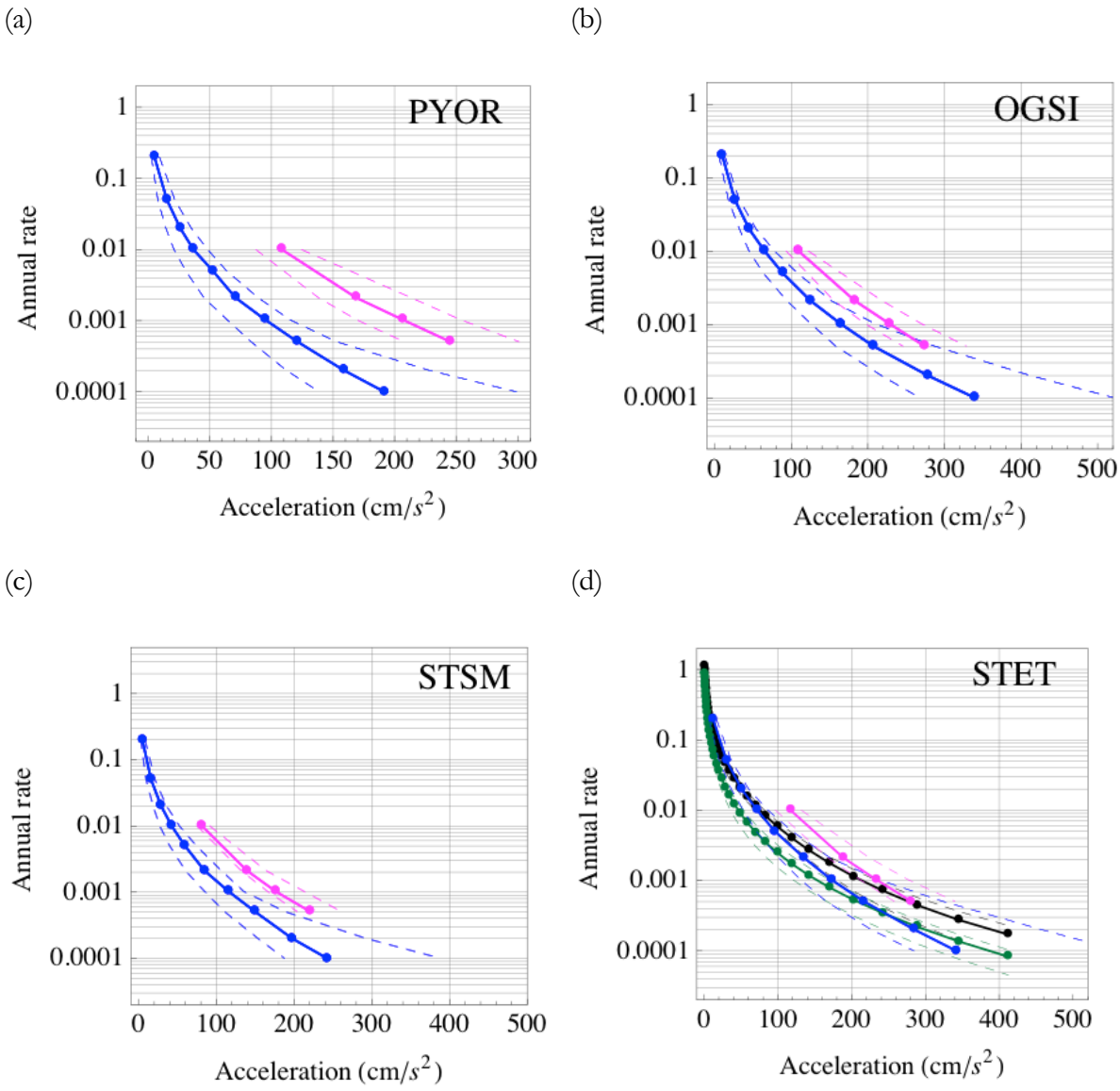

Figure 2.3: Example of hazard curves at 3 stations: (a) PYOR station in the Pyrenees, (b) OGSI station in the Alps, (c) STSM station in Alsace, (d) STET station in the southern Alps. Blue: AFPS2006 study (mean and percentiles 15 and 85), Pink: MEDD2002 study (mean and percentiles 25 and 75), Black: SIGMA2012-AtkinsonBoore2011, Green: SIGMA2012-Bommeretal2007 (mean and percentiles 16 and 84).

2.4.2 Test of PSH Models against the Newly Built Accelerometric Dataset

The PSH models provide median hazard curves, as well as percentiles deduced from the logic tree. Only the median hazard curve will be considered here. A series of acceleration thresholds is considered successively. The probability distributions for the number of sites with exceedance are obtained through Monte Carlo sampling, based on 10,000 runs (see Section

"Method for testing PSHM against observations"). Tests show that 10,000 runs are large enough to get stable results. These distributions indicate the expected number of sites (out of the 62 rock sites) with at least one exceedance of the acceleration level over the lifetime of the stations. The AFPS2006 and MEDD2002 studies provide hazard curves for a grid of sites covering metropolitan France. Both models can be tested against observations using the accelerometric history at the 62 rock sites, resulting in a total observation time window of 449 years (corrected lifetimes, see Table 2.S1 in the electronic supplement). As for SIGMA2012 study, the spatial area is reduced to southeastern France, 22 rock stations can be used, resulting in a total observation time window of 182 years.

The tests can be carried out only for the acceleration levels that have been considered in the PSHA calculations. The AFPS2006 study provides accelerations for 10 return periods between 5 and 10,000 years. Obviously, the accelerations corresponding to these return periods vary from one site to the other. We chose to lead the test for a fixed acceleration threshold, common to all sites. The useful range is defined by the maximum of minimum accelerations of hazard curves (23 cm/s^2 for the return period 5 yrs), and by the minimum of maximum accelerations of hazard curves (130 cm/s^2 for 10,000 yrs). The AFPS2006 model can thus be tested against observations in the range 23 to 130 cm/s^2. The example in Figure 2.4 shows the results for 23 cm/s^2. The sites with exceedance are highlighted on the map and the responsible earthquakes are indicated. The probability distribution has the shape of a binomial distribution, percentiles 2.5 and 97.5 correspond respectively to 9 and 21 sites with exceedance. In this case the model predicts more sites with exceedance than what has been observed. Note however that for acceleration thresholds larger than 40 cm/s^2, the test concludes on a consistency between predictions and observations, as will be discussed later on. The MEDD2002 study provides hazard results only for 4 return periods starting from 100 years to 1975 yrs (there was no possibility to obtain the full hazard curves, C. Martin, personal communication). Considering the 62 RAP sites, there is no common acceleration range between the 62 sites. For this reason, the MEDD2002 model is tested for a fixed return period rather than a fixed acceleration threshold. As for SIGMA2012 model, the authors did on purpose hazard calculations starting with an acceleration level equal to 1 cm/s^2 (Drouet 2012), so any level higher than 1 cm/s^2 can be considered in the testing.

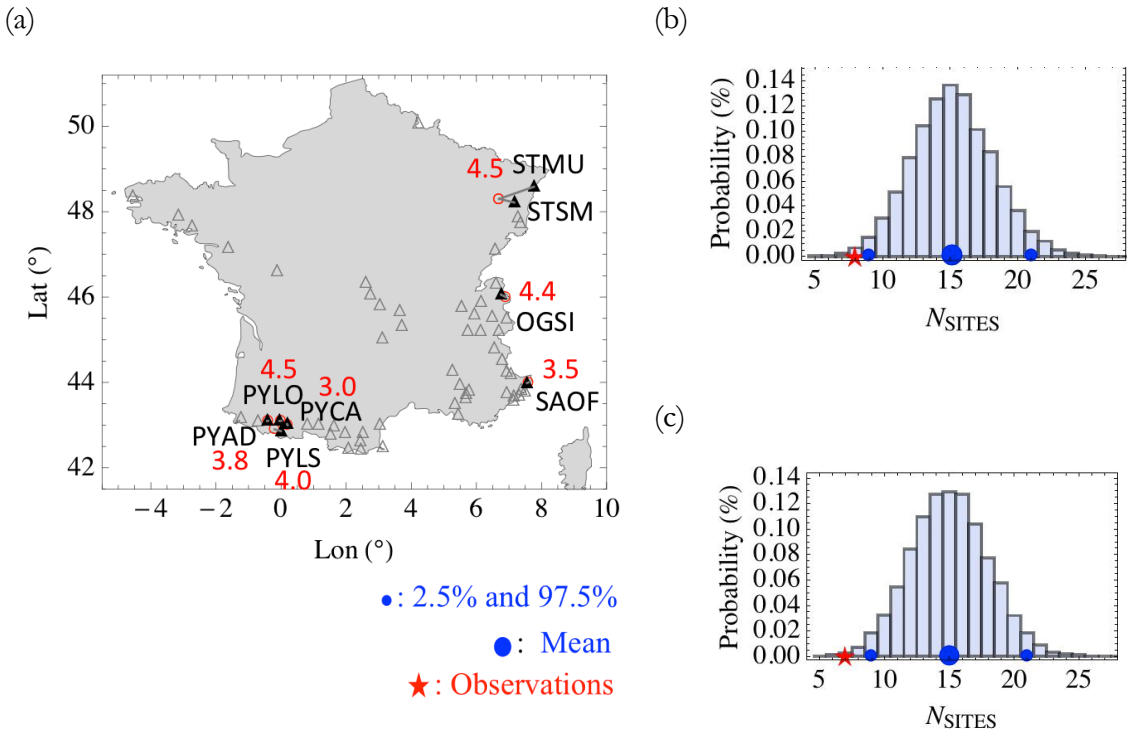

Figure 2.4: Testing the AFPS2006 model against the accelerometric dataset, example for the acceleration threshold A_0= 23 cm/s^2. (a) Locations of the 8 stations, out of 62, which recorded a ground motion higher than A_0 (black filled triangles, acronyms of stations indicated), and responsible events (circles, M_w indicated). Right: b) the observed number of sites where A_0 was exceeded is superimposed on the probability distribution predicted by the PSH model. In this example, the model over-predicts the observations; c) two records producing exceedance are related to the same earthquake (stations STMU and STSM), excluding one station from the analysis does not change the conclusions (predictions are for 61 stations).

Results of the testing are displayed in Figure 2.5. For each acceleration threshold, the observed number of sites with exceedance is superimposed on the expected number of sites, a probability distribution characterized by its mean and percentiles 2.5 and 97.5%. For the model AFPS2006 (Figure 2.5a), results show that observations are consistent with the model, i.e. within the tails, for all acceleration thresholds above 40 cm/s^2. For the two lowest levels tested (23 and 30 cm/s^2), the observed number of sites with exceedance is much lower than predicted by the model. Note that the test is carried out using the modified lifetimes of stations to account for gaps in the monitoring (Section "Building the accelerometric dataset"). We have estimated that about 5% of records with accelerations above 10 cm/s^2 may be missing from our database. This could explain part of the discrepancy between the expected and observed number of exceedances. We tested AFPS2006 also at fixed return periods (Figure 2.5b). We

found that the AFPS2006 model predicts more exceedances than observed at 20 years return period. Between 50 and 200 years, the model is consistent with the observed number of exceedances (within the tails). For 475 and 975 years, the test is not conclusive due to the lack of observed exceedances.

Results for MEDD2002 model are displayed for 100, 475 and 975 years (Figure 2.5c). The observed number of sites with exceedance (1) is lower than the 2.5 percentile at 100 years (2 exceedances) and the model is rejected. For 475 and 975 years, the model is not rejected, however there is no exceedance, and the 2.5 percentile is also zero. This is not surprising, since these return periods are large with respect to the total length of the observation time window. In such a case, very different models may be consistent with the observations. In order to obtain meaningful results, we need long enough time windows and/or a large enough number of sites so that the expected total number of exceedances is larger than zero.

The SIGMA2012 model can be tested for accelerations higher than 1 cm/s^2, but over a reduced spatial area. As we received two separate PSH model, one based on Bommer *et al.* (2007) (Betal07) and one based on Atkinson & Boore (2011) (AB2011), two tests are led against accelerometric data (Figs. 2.5d and 2.5e). Both models over-predict the observations for the low acceleration range; there are fewer sites with acceleration exceedance than expected from the PSH model. The over-prediction is stronger when AB2011 GMPE is used. Observed number of sites is lower than the 2.5 percentile for acceleration thresholds between 1 and 20/30 cm/s^2. For acceleration levels higher or equal to 30/40 cm/s^2, the observation and the percentile 2.5 equal zero, and no conclusion can be drawn.

Sampling the sites in space and testing the hazard estimates at all sites at once require that acceleration occurrences are independent. To reduce the correlation between records, stations closer than 10km from each other have been excluded prior to the analysis (section "Building the accelerometric dataset"). Moreover, the list of earthquakes responsible for the threshold exceedances was systematically checked. When two records at two stations were produced by the same earthquake, we simply discarded the site with the lowest acceleration recorded. They are few cases where this situation occurs. Moreover, discarding sites to ensure independence of sites brings minor changes to the plots and does not change the conclusions (see Figs. 2.4 and 2.5). At each station, the earthquakes responsible for the exceedance of thresholds have also been analyzed to avoid including accelerations related to clustered events.

We looked for events located within 10km of each other and within a time window of 30 days. Following this criterion, all events taken into account in the testing are independent.

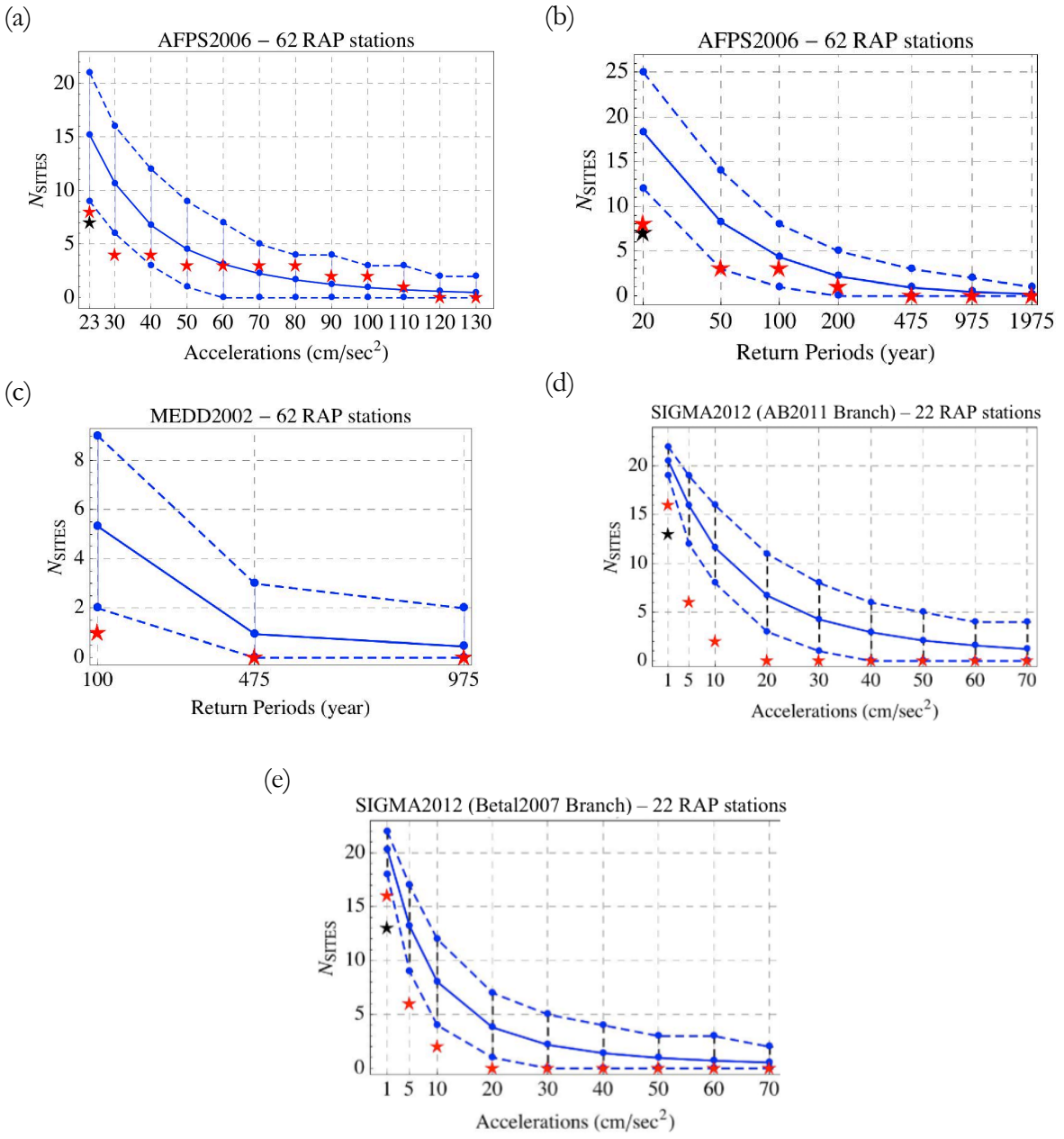

Figure 2.5: Testing the probabilistic seismic hazard models against accelerometric data in France: predicted and observed number of sites with exceedance. Blue curves: median and percentiles 2.5 and 97.5 of the predicted distributions, red stars: observed number of sites, black stars: reduced number of sites in the case of double-counting (see Figure 2.4). (a) Results for the AFPS2006 PSH model, considering a range of acceleration thresholds (62 rock sites, total time window 449 years). (b) Results for the AFPS2006 PSH model, considering a range of return period thresholds (62 rock sites, total time window 449 years). (c) Results for MEDD2002 model, considering 3 return periods (62 rock sites, total time window 449 years). (d) and (e) Results for SIGMA2012 model in

Southeast France (22 rock sites, in total 182 years, models Boore & Atkinson 2011 and Bommer *et al.* 2007).

2.5 Enlarging the Observation Time Windows: Using Accelerations Inferred from an Earthquake Catalog

Recorded accelerations are the most exact data to compare with hazard curves, but observation time windows are short, with the longest station lifetime reaching 16 yrs. An alternative to recorded ground motions is to use "synthetic" accelerations inferred from an earthquake catalog. Earthquake catalogs provide information over longer time periods than accelerometric networks. The test can be performed following exactly the same methodology; the "only" difference is that accelerations at sites have been obtained thanks to a ground-motion prediction equation. This test has advantages with respect to the testing on records, such as longer time windows and a complete database over these windows. However a strong assumption has to be made regarding the choice of the GMPE.

The LDG earthquake catalog, from the Laboratoire de Détection Géophysique (LDG, 2012) is the best candidate for this test. The first stations of the LDG network were installed in 1962. The catalog consists of 15993 earthquakes with magnitudes from 2.5 to 5.9 (M_{L_LDG}), and spatial extension 41° to 52° in latitude and -6° to 10° in longitude. For the purpose of this study, aftershocks should be removed from the catalog because the PSH model is not taking into account aftershocks and is predicting Poissonian rates. Therefore, the LDG catalog is declustered using the Reasenberg declustering algorithm (Reasenberg 1985). Some 4776 events (out of 15993 events in the catalog) are identified as clustered events and removed from the catalog. Then, the completeness is evaluated by plotting the cumulative number of earthquakes versus time (Figure 2.A1 of appendix). The catalog is considered complete for magnitudes $M_{L,LDG} \geq 2.5$ from 1978 on. Thirty-four years are available for the test.

The synthetic accelerometric history at a site is constructed using the earthquake catalog coupled with a ground-motion prediction equation. For all earthquakes in the catalog, the corresponding acceleration is calculated at the site. A GMPE adapted to the region under study must be selected. Based on the study by Beauval *et al.* (2012), and based on a new study detailed in Section "Selection of the GMPE" of this article, the Cauzzi & Faccioli (2008) model is selected for application in France. This equation depends on moment magnitude. For

around 160 events, an M_w has been calculated by Drouet *et al.* (2010). For the other events, magnitudes M_{L_LDG} are converted to M_w using the equation of Drouet *et al.* (2010). The variability σ of ground motions must be taken into account (e.g. Strasser *et al.* 2009). For one magnitude and one source-to-site distance, the GMPE provides a Gaussian probability distribution for the expected ground motion at the site. Therefore, through Monte Carlo sampling, many accelerometric histories are generated by sampling the Gaussian probability distributions. Instead of producing one set of accelerometric histories (median values), 10,000 sequences are generated, and the distribution for the "observed" number of sites with exceedance is obtained. Note that the Gaussian distribution must be sampled within meaningful limits. A higher level of truncation allows higher accelerations, and has a direct impact on the predicted probability distributions. The observed number of sites with at least one exceedance will be larger when truncating at $\pm 3\sigma$ than when truncating at $\pm 2\sigma$. So the testing will be performed for both truncation levels, to evaluate the influence on the results.

2.5.1 Selection of the GMPE

For this study, all records available at the 54 stations classified as 'rock' and recorded at least one PGA higher than 1 cm/s^2 are taken into account (class A, 746 records, 578 events). In Beauval *et al.* (2012), a set of GMPEs has been tested against a ground-motion dataset recorded by the RAP stations, with M_w ranging between 3.8 and 4.5, and epicentral distances up to 300km. The best-fitting GMPEs identified are the Cauzzi & Faccioli (2008) (CF2008) and the Akkar & Bommer (2010) (AB2010) equations. These models are tested here against our new dataset, going down to lower magnitudes and including only accelerations higher than 1 cm/s^2 (90% of data recorded within epicentral distance of 100 km). The CF2008 model has been developed from crustal Japanese data (80% of the dataset), with $M_w \geq 5$. The AB2010 model has been developed from data recorded in Europe and the Middle East, with $M_w \geq 5$. Both models are therefore applied below their magnitude validity limits. We refer to Beauval *et al.* (2012) for a detailed discussion on the regional dependence of GMPEs, and on the use of GMPEs outside their validity limits. Here the aim is to check the fit between these models and our newly built French accelerometric dataset. Moreover, two other models are tested, which could be better adapted to a lower magnitude dataset. The Atkinson & Boore (2011) equation has been developed from earthquakes with $M_w \geq 3.5$ recorded in western North American. This model is an update of the Boore & Atkinson (2008) NGA model extended towards lower

magnitudes. The Bommer *et al.* (2007) equation has been developed from earthquakes with $M_w \geq 3.0$ recorded in Europe and the Middle East. It was developed only to explore the effect of extending the magnitude range. We are considering this equation in the analysis because the SIGMA2012 study uses it.

Performing residual analyses enables us to evaluate the fit between models and observations. The residual is the difference between the observation and the prediction in terms of the logarithm, normalized by the standard deviation of the model. In Figure 2.6, histograms of the residuals are superimposed on the standard normal distribution representing each GMPE model. The Gaussian with mean and sigma calculated from the residuals is also superimposed on the histogram. Considering first the residual distributions, the best fitting model is Cauzzi & Faccioli (2008), since the mean of the residuals is close to 0 and the standard deviation close to 1.0. Akkar & Bommer (2010) model also provides a good fit to the data, with a mean slightly shifted towards higher values (slight under-prediction of the model) and a variability slightly larger than the dispersion predicted by the model. As for Bommer *et al.* (2007) model, it predicts well the dispersion in the dataset, but the model strongly under-predicts the amplitudes. Atkinson & Boore (2011) predicts a much lower variability in the dataset than is observed, although providing a rather good fit for the mean.

The residuals are plotted versus M_w and versus source-site distances to highlight potential trends (Figure 2.6). In the case of the CF2008 model, mean of residuals are rather stable with magnitude (no specific trend, and contained within $\pm\sigma$), and rather stable also with source-to-site distance. These remarks also hold for the AB2010 model, except that the residuals are more dispersed. In the case of the AB2011 model, a strong trend is observed for residuals depending on the distance, implying that the attenuation with distance as modeled in AB2011 does not reproduce observed attenuation of ground motions in France. At last, for Bommer *et al.* (2007) equation, there is no trend visible either with magnitude or distance. However most residuals are positive, indicating that the model under-predicts the recorded PGA.

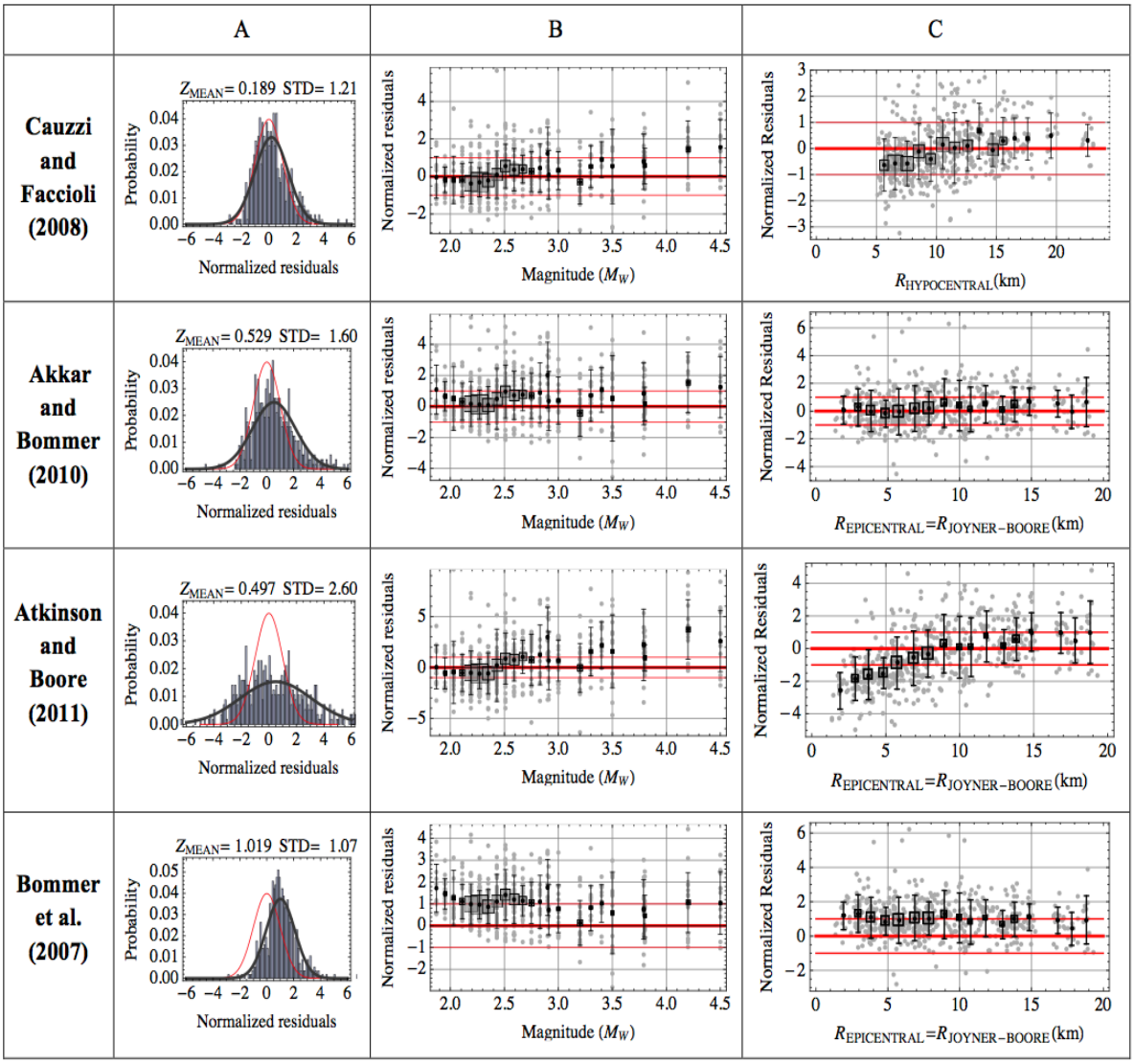

Figure 2.6: Testing 4 ground-motion prediction models against the newly built accelerometric French dataset. Column A: histogram of residuals superimposed on the standard normal distribution representing the model (red curve), a residual corresponds to [Log(observation)-Log(prediction)]/sigma. Column B: distribution of residuals versus magnitude (0.1 magnitude binning). Column C: distribution of the residuals with respect to source-site distance (1km distance binning). Squares: mean of residuals, size proportional to the number of residuals falling in each bin, errorbars correspond to ±1 standard deviation of model (normalized residuals). (Z_{MEAN}: Mean normalized residuals, STD: Standard deviation of normalized residuals.)

Based on these results, Cauzzi & Faccioli (2008) is confirmed as the best-fitting model and selected for the present study. The model has a large σ value, which fits well the rather large dispersion in the French dataset. This large dispersion is both natural (true variability of the ground motions) and due to some metadata bearing large uncertainties (magnitude

estimates, source location, site classification, etc.). Note that the sigma predicted by the CF2008 model is much larger than the sigma predicted by the Atkinson & Boore (2011) model (CF2008: 0.344, AB2011: 0.246, $\log_{10}$ units, for the PGA). Atkinson & Boore (2011) model fits well the median PGA for Californian small-to-moderate events ($3 \leq M_w \leq 5.75$), however the authors write "we do not propose any adjustments to the standard deviations given by Boore & Atkinson (2008) at this time. The standard deviations given in Boore & Atkinson (2008) are implicitly reflective of the variability seen in larger events ($M_w > 5.5$) […]. This is appropriate for the application of these GMPEs to seismic hazard analysis". Therefore, it is not a surprise that the model predicts a much lower variability than observed in our dataset.

2.5.2 Testing PSHM at the Sites of the RAP Stations with Synthetic Data

The test is first carried out exactly as in Section "Testing PSHM models against accelerometric data in France". At the 62 sites, locations of RAP stations, the synthetic time histories are 34 years long. Assuming that the accelerations belong to the same stochastic process, and sampling the sites in space, leads to a virtual site with a total observation time window equal to 2108 years. This time window is more than four times longer than the total observation time window merging the true-recorded periods at the same sites (449 years). The probability distribution for the observed number of exceedance is obtained by combining earthquakes in the LDG catalog with the CF2008 GMPE, which is sampled in the range $\pm 3\sigma$. The results are shown in Figure 2.7, which compares the probability distributions for the "observed" and predicted number of sites with exceedance.

The results obtained for the AFPS2006 and for the MEDD2002 models (Figs 2.7a and 7b) are very similar to results obtained from real data (Figs 2.5a and 2.5c). The predictions of the AFPS2006 model fit the synthetic observations above 40 cm/s^2. For the lowest acceleration levels (23-30 cm/s^2) the model overestimates the observations, the mean of the synthetic distribution is lower than the percentile 2.5 of the predicted distribution. The comparison with the predictions based on MEDD2002 model is once again difficult as the return periods tested are long and result in few observations at 475 and 975 yrs (Figure 2.7b). At 100 yrs, the model over-estimates the observations (like in the real case, Figure 2.5c). At 475 and 975 years, the mean of observations is within the tails, however both 2.5 percentiles correspond to 0 sites with exceedance.

In the case of the SIGMA2012 model, focusing on the South-East of France, results are displayed separately for the logic tree based on the GMPE of Atkinson & Boore (2011), and for the logic tree based on the GMPE of Bommer *et al.* (2007). Like in the real case (Figure 2.5d), the model based on the equation AB2011 over-estimates the observations for accelerations lower than 60 cm/s^2. Above this level, mean of observations fall on the 2.5 percentiles of the distribution predicted (Figure 2.7c). In the synthetic case, the total time window is longer (748 instead of 182 years) and the mean of observations is now higher than 0 over the whole acceleration range. As for hazard values relying on the equation Betal2007 (Figure 2.7d), the observed mean is within the percentile 2.5 and the mean of the predicted distribution over the whole acceleration range. Over the range 1-20 cm/s^2, this result differs with the result obtained in the real case (Figure 2.5e), where the model over-predicts the observations. This could be due to many (combined) reasons: 1) over-prediction of the rates corresponding to small acceleration levels by the SIGMA2012 model, 2) incompleteness of the observed accelerometric database for small acceleration levels, 3) few earthquakes and unusual quietness in the Alps over the observation time window (1995-2011), 4) shortness of the observation time window.

All the "observed" probability distributions presented in Figure 2.7 are obtained by sampling the CF2008 Gaussian PDF between $\pm 3\sigma$. Results obtained from sampling between $\pm 2\sigma$ are slightly different, with slightly lower numbers of sites with exceedance, but the main features remain identical (Figure 2.S1 in Electronic Supplement). Moreover, independency of sites is required in these tests. When 10000 synthetic datasets are generated, the independency of exceedances at 62 stations is controlled by checking the earthquakes causing exceedance. If one earthquake generates a ground-motion exceedance at more than one station, these stations are considered as dependent and the total number of sites with exceedance is decreased. The results obtained considering the independency of sites are also shown in Figure 2.7. Removing correlated accelerations has no influence on the results.

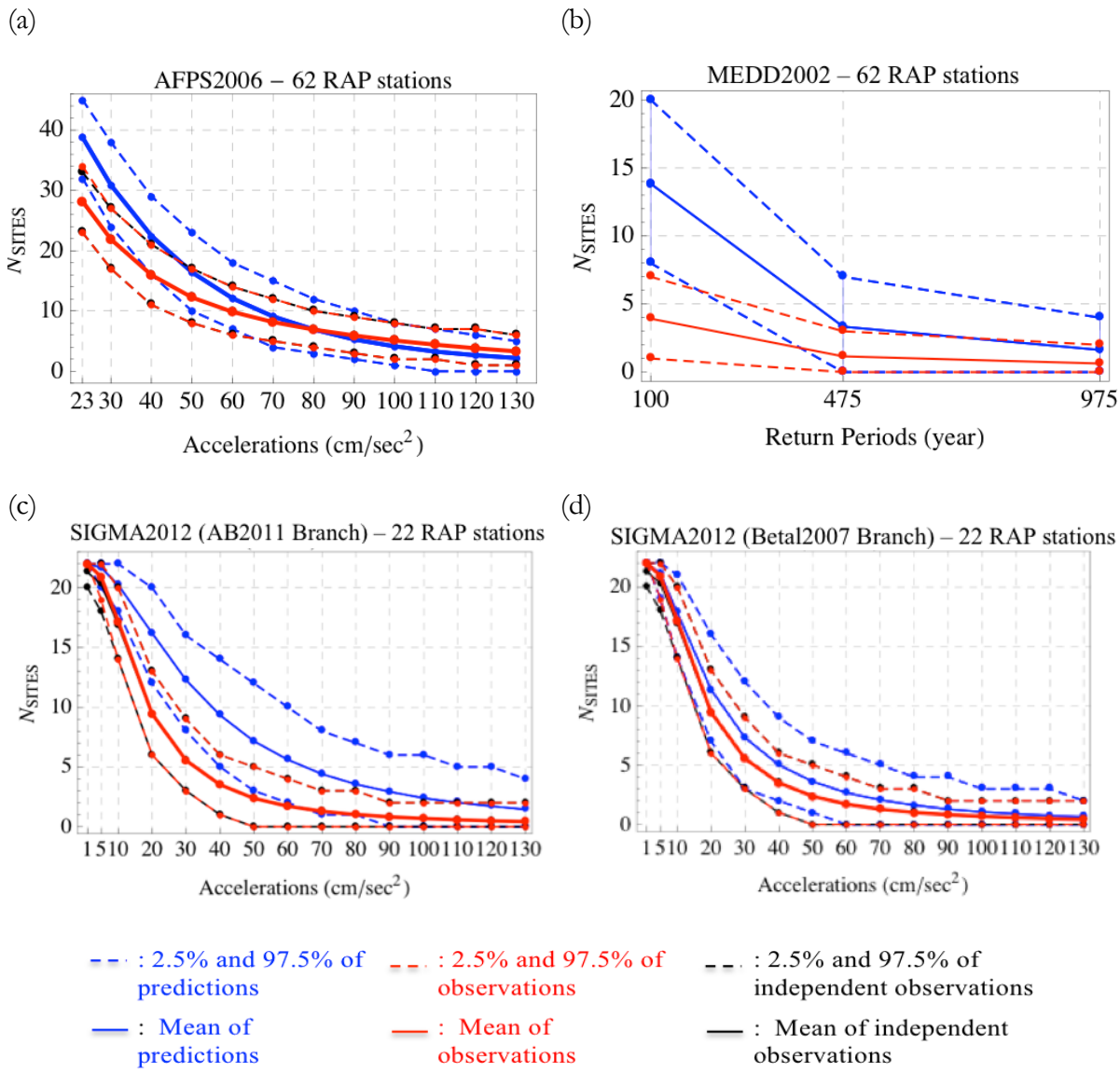

Figure 2.7: Testing the probabilistic seismic hazard models against synthetic accelerometric data: predicted and "observed" number of sites with at least one exceedance. Blue curves: predicted distributions, mean and percentiles 2.5 and 97.5. Red curves: observed distributions, mean and percentiles 2.5 and 97.5. Black curves: reduced number of sites in the case of double-counting (see Figure 2.4). (a) AFPS2006 model (62 rock sites with 34 years, total time window 2108 years). (b) MEDD2002 model, considering 3 return periods (62 rock sites, total time window 2108 years). (c) SIGMA2012-AtkinsonBoore2011 and (d) SIGMA2012-Bommeretal2007 (22 rock sites with 34 years, total time window 748 years). The synthetic data were generated using the LDG catalog and sampling the Gaussian of the CF2008 GMPE between ±3σ (see the text).

The LDG catalog consists of earthquakes with $M_{L,LDG} \geq 2.5$. While generating synthetic accelerations histories, all earthquakes are used. In order to understand the effect of this magnitude threshold on the results, the tests on the AFPS2006 model are performed again

increasing the minimum bound for magnitude of earthquakes. Results based on the LDG catalogue taking into account $M_{L,LDG} \geq 3.5$ are displayed in Figure 2.8 (sampling the GMPE Gaussian between $\pm 3\sigma$, see Figure 2.S2 for a sampling between $\pm 2\sigma$). The results still highlight a consistency between predictions and observations for the upper acceleration range (above 60 cm/s^2), and an over-prediction of the model for the lower acceleration range. However, the model is now strongly over-predicting the number of sites with exceedance, the mean of observations is much lower than the predicted 2.5 percentile. In the synthetic tests, the magnitudes between 2.5 and 3.5 are contributing largely in the range 23-50 cm/s^2.

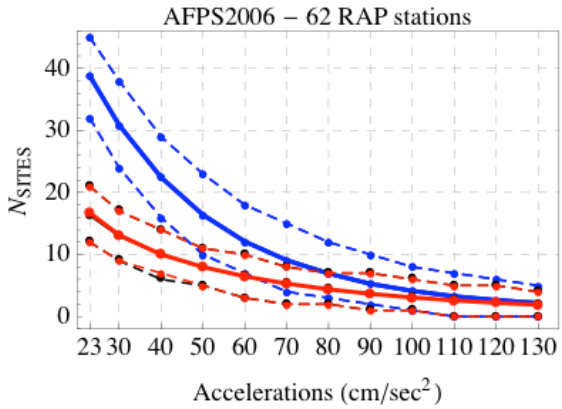

Figure 2.8: See legend of Figure 2.7(a). AFPS2006 model, events in LDG earthquake catalog with $M_{L,LDG} \geq 3.5$ are used for generating synthetic data.

2.5.3 Testing at Stations used in Humbert & Viallet (2008)

The results from the MEDD2002 study are provided over a grid covering France for 4 return periods from 100 to 1975 years. However, based on the same logic tree, other calculations have been performed at the locations of 20 accelerometric RAP stations (Humbert & Viallet 2008). We recently got these hazard curves from Geoter (C. Martin), for MEDD2002 and also for AFPS2006. These curves provide annual rates for accelerations higher than 1 cm/s^2. Humbert & Viallet (2008) led a comparison between PSH results and observations for a subset of the RAP stations (classified as 'rock', located in the Alps and Pyrenees). They compared the observed number of accelerations higher than one acceleration threshold, 10 cm/s^2, with the predicted distributions (median and percentiles 15 and 85%), considering all sites at once, similarly to Stirling & Gerstenberger (2010). Based on the result obtained for this acceleration threshold, Humbert & Viallet (2008) concluded on a strong overestimation of the

PSH model with respect to observations, conclusions that they extrapolated to the whole model (all return periods). Based on this result, different groups in France are calling for a revision of the national seismic hazard map based on MEDD2002 model.

The methodology described in "Testing PSH models against accelerometric data" is applied again to the records of the RAP stations selected in Humbert & Viallet (2008). Note that the accelerometric database we used is not exactly the same as Humbert & Viallet (2008), because the present database is more complete (see Section "Building the accelerometric dataset"). Now the number of rock stations is reduced to 20 (Figure 2.9e), reducing the observation time window from 449 to 162 years. Observed numbers of sites with exceedance are superimposed on expected numbers of sites (Figs 2.9a and 2.9b). The results obtained for AFPS2006 at these 20 sites are similar to the results obtained using 62 sites (Figure 2.5a). Both MEDD2002 and AFPS2006 models over-predict the observations for accelerations up to 20 cm/s^2. For 20 and 50 cm/s^2, MEDD2002 predicts more exceedances than observed whereas AFPS2006 model is consistent with the observations. For acceleration levels between 60 cm/s^2 and 100 cm/s^2, observations are consistent with both models (within the tails of the distributions). Whereas for accelerations higher than or equal to 110 cm/s^2, both the observed number and the percentile 2.5 equal 0, therefore models cannot be rejected.

Finally, another test is performed using a synthetic accelerometric dataset derived from Monte Carlo sampling of the LDG earthquake catalog (Figs 2.9c and 2.9d for a sampling of CF2008 between $\pm 3\sigma$). In this case, 34 years are available at each station, resulting in a longer total observation time window. The results obtained from this synthetic dataset are consistent with the results obtained from the true records, predictions are rather well fitting the "observations" above 70-80 cm/s^2 for MEDD2002 and above 20-30 cm/s^2 for AFPS2006, up to the highest level tested 200 cm/s^2. The synthetic observed dataset covers a longer time window (680 years) than the merged RAP lifetimes (162 years), which explains why higher acceleration levels can be tested in this case.

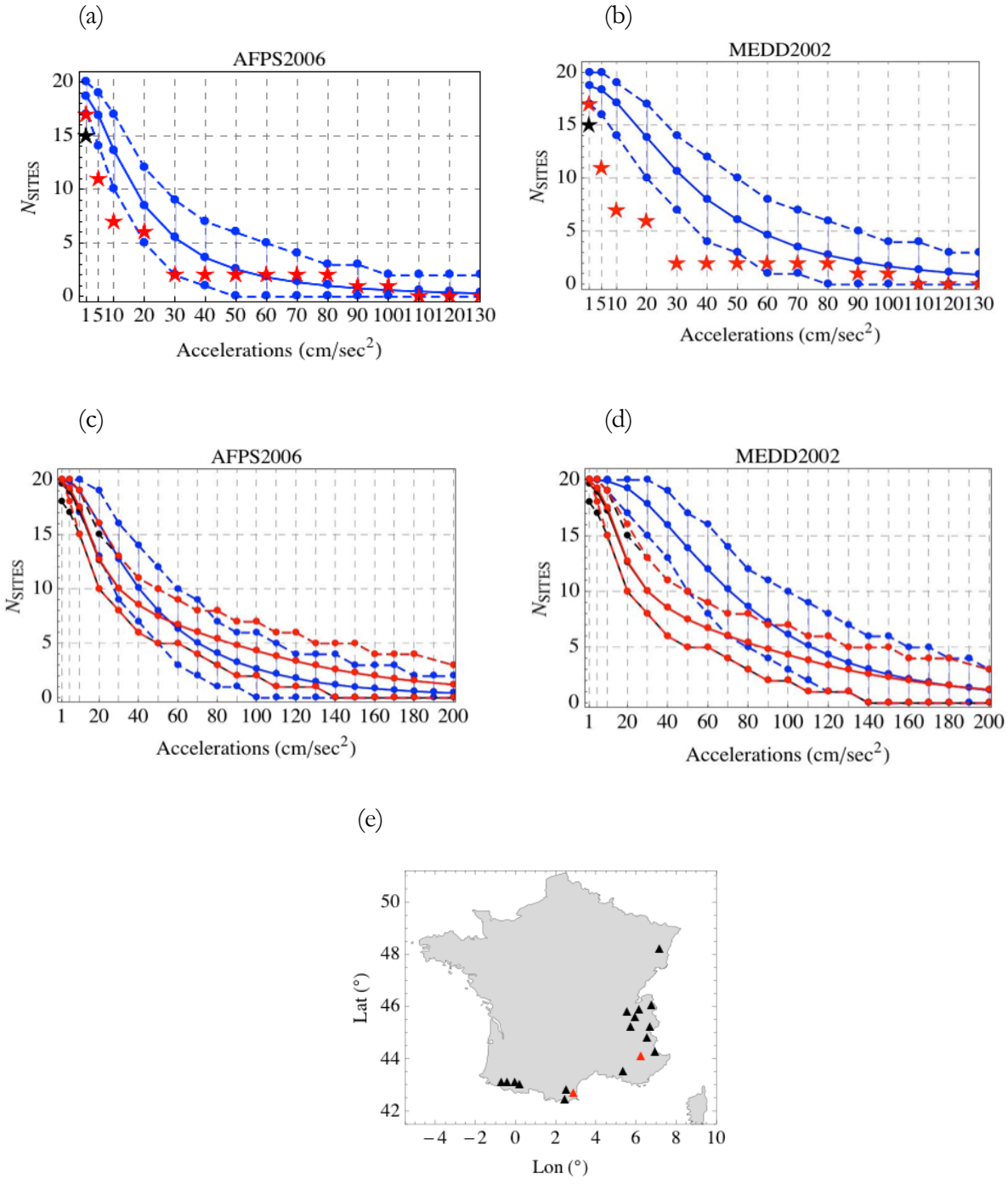

Figure 2.9: Testing PSH models MEDD2002 and AFPS2006 at the 20 RAP stations used in Humbert & Viallet (2008). (a) Results for AFPS2006 based on accelerations recorded at the RAP stations (162 years), (b) results for MEDD2002 based on accelerations recorded at the RAP stations, (c) results for AFPS2006 based on a synthetic dataset inferred from the LDG catalog at the same 20 stations (34 years each, in total 680 years), (d) results for MEDD2002 based on the same synthetic dataset, (e) locations of the 20 RAP stations (black: 18 rock sites, red: 2 soil sites).

Considering only the threshold 10 cm/s^2, we would conclude on an over-estimation of the PSH models with respect to observations, like Humbert & Viallet (2008). However, the test carried out on a wider acceleration range shows that results obtained for one level should not be extrapolated to other levels or longer return periods. The present tests demonstrate that conclusions are valid only for the acceleration range tested. Considering true-recorded data as well as synthetic accelerometric histories, models MEDD2002 and AFPS2006 cannot be rejected, respectively above 60 and 30 cm/s^2.

2.6 Stability in Time

The PSH models have been tested against the RAP accelerometric data recorded between 1995 and 2011. One question posed is whether this time period is representative for the acceleration levels involved, or in other words, if the observed number of sites with exceedance are stable when considering different observation time windows. Taking advantage of the LDG catalog, this hypothesis can be checked, as the catalog provides 34 years of synthetic observations at each RAP station. The LDG catalog is divided into five sliding time periods of 16 years (from 1978 to 2011). Each period is extending over the same duration as the RAP network. However, some stations of the network covers 16 years, while others cover much shorter durations. Within each period, the accelerometric history at each station is generated using a sub-division of the period, equal to the observation time available at that station. Again, the Cauzzi & Faccioli (2008) equation is used to build the synthetic accelerometric histories.

The same testing procedure is applied to the five time periods. Results obtained for the AFPS2006 study are displayed in Figure 2.10 (sampling between ±3σ, see Figure 2.S3 in ES for ±2σ). For each period, the synthetic distribution for the "observed" number of sites with at least one exceedance is superimposed on the predicted distribution. The results are stable from one period to the other. Below 40-60 cm/s^2 predicted means are always lower than "observed" means, similarly to the results displayed in the real case (Figure 2.5a) and when using 34 yrs of synthetic data (Figure 2.7a). Above these levels, both the means and the percentiles approximately fit, for the five time periods. These results based on a sampling over France tend to prove that 16 years of data is a representative period for the acceleration levels considered in the testing.

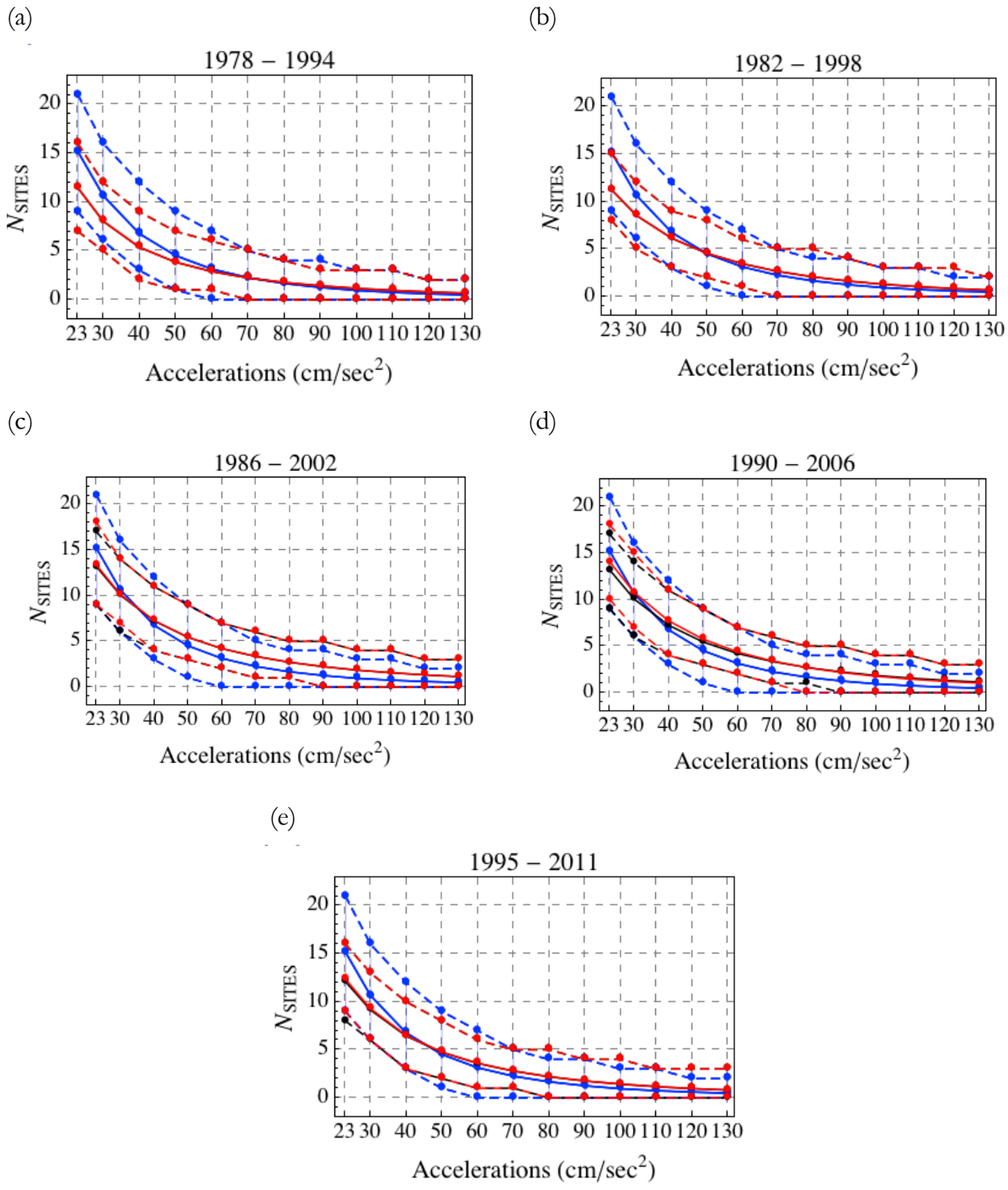

Figure 2.10: Testing AFPS2006 model against synthetic accelerometric data at 62 sites, and evaluating the stability of the results, with respect to the time window used. Five sliding windows are considered between 1978 and 2011, with length equal to the lifetime of the RAP network (16 yrs). Each station is attributed the same lifetime as in the real case. For each 16-yrs period, synthetic datasets are generated by coupling the LDG catalog with the ground-motion prediction equation CF2008 (sampled between $\pm 3\sigma$). Total observation time window is 449 years, like in the real case.

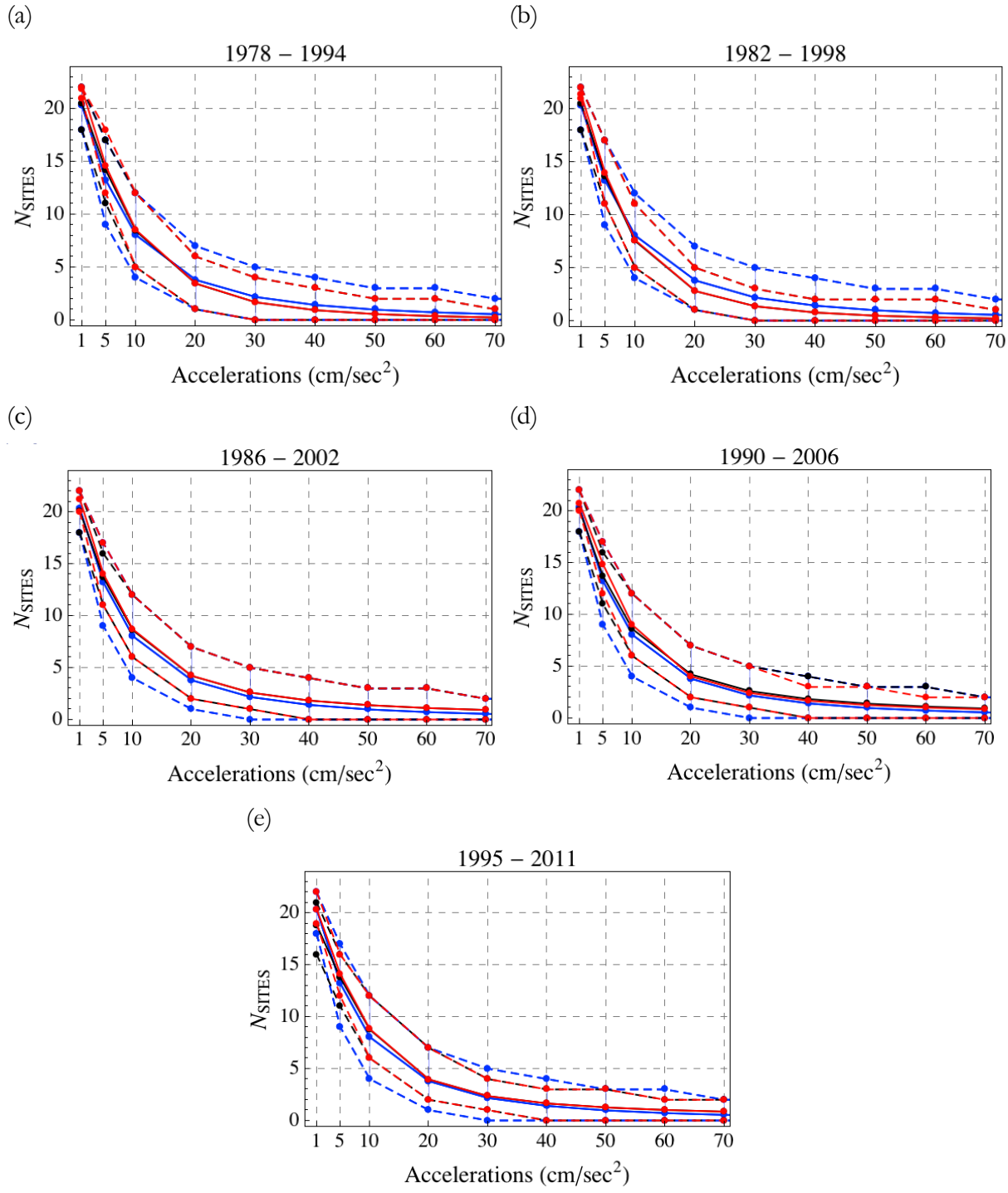

Figure 2.11: Same as Figure 2.12, testing the SIGMA2012 model (branch Bommer *et al.* 2007) considering 22 RAP rock stations in southeast France. Total observation time window is 182 years.

Results obtained for the SIGMA2012 study are displayed in Figure 2.11 (branch using the Bommer *et al.* 2007 equation, ±3σ). In this case, the total time length is much reduced (182 years, 22 sites), however the observed distributions are still stable from one period of 16 years

to the other. The results for each 16 yrs period are comparable to the results based on 34 years of synthetic data (Figure 2.7d). As for the model SIGMA2012 based on the Atkinson & Boore (2011), observed distributions are also rather stable over the different time periods (Figure 2.S4). The fit with the model is slightly better than in the 34-years synthetic case (Figure 2.7c).

2.7 Conclusion

We have carried out an extensive experiment to test probabilistic seismic hazard models against accelerometric datasets. Sites are sampled in space to compensate for the short observation time windows. Models are tested against different datasets, true-recorded accelerations and synthetic amplitudes based on an earthquake catalog combined with a GMPE equation. The sites sampled vary from one test to the other, distributed all over France or located only in the southeastern part of the country. Varying observation time windows are considered. The maximum time window available is 16 years for the RAP accelerometric database, while the time window is 34 years when considering the LDG earthquake catalog. When applied over a wide region and a large number of sites (30 or more), these different tests provide rather similar results.

Three PSH models have been considered in the present study. Expected numbers of sites with exceedance are compared to observed numbers of sites. A model is judged consistent with the observations if the observed number is within the percentiles 2.5 and 97.5 of the predicted distribution. If both observation and predicted numbers equal 0, the test is not conclusive, the model cannot be rejected. The AFPS2006 model is consistent with the observations of the RAP network over the acceleration range 40-100 cm/s^2 and 50-200 years of return periods (62 sites, 449 yrs in total). When using synthetic accelerations over 34 yrs at the same 62 sites (2108 yrs in total, applying the Cauzzi & Faccioli 2008 GMPE), the model predicts a number of sites with exceedance that is consistent with the "observations" over the range 40 to 130 cm/s^2.

The MEDD2002 model is provided all over France only for 4 return periods, from 100 to 1975 years. For 100 years, there is only one site with exceedance, which is less than predicted. For longer return periods (475 and 975 years), the test led over the 16 years of the RAP network is not conclusive, since for these return periods both observed and predicted numbers equal zero. Using the synthetic dataset (62 sites, 2108 years in total), the

"observation" time window is increased. The model still over-predicts the observations at 100 years, but is consistent with the observations for 475 and 975 years. Moreover, another comparison is carried out considering the 20 RAP sites used by Humbert & Viallet (2008), where hazard curves are provided over the acceleration interval 1 to 200 cm/s^2. Based on the true-recorded dataset (162 yrs in total), the model over-predicts the observations below 60 cm/s^2, and is consistent with the data over the range 60 to 100 cm/s^2. Above 100 cm/s^2, the comparison is not conclusive because both the numbers of observed sites and the 2.5% percentiles of the predicted distribution are equal to 0. Based on 34 years of synthetic data (in total 680 yrs), the same results are found; the model predicts a number of sites with exceedance consistent with the observed one over the range 70-200 cm/s^2.

In the case of the SIGMA2012 models, the tests are led over a restricted spatial area and results are less clear. When considering the accelerometric data recorded at the accelerometric sites (22 sites, 182 yrs in total), both models over-predict the observations for acceleration thresholds lower than 30-40 cm/s^2. When testing the models against the synthetic dataset (22 sites, 748 yrs in total), the model based on Atkinson & Boore (2011) GMPE still over-predicts observations below 70 cm/s^2, whereas the model based on Bommer *et al.* (2007) GMPE predicts numbers of sites which are now compatible with the observations for the whole acceleration range.

At last, by leading the tests systematically for a wide range of accelerations, we have shown that the results obtained for one acceleration level should not be extrapolated to other levels. The conclusions drawn are only valid for the thresholds tested, and should not be generalized to the whole probabilistic hazard model, like it has been done in the past (Humbert & Viallet 2008).

We have begun to apply the same methodology to the French intensity database. Such study will enable to test higher ground motions over longer time windows, but the results will also depend on some assumptions required (completeness of intensity histories at sites, conversions of intensities into accelerations …). Any testing method relies on some assumptions, and the discrepancies between observations and predictions can generally have more than one explanation. We believe that firm conclusions on the validity of a PSH model will only be possible if applying for the same region several techniques, using different observables, recorded over different time windows.

2.8 Data and Resources

The accelerometric database built within this article is based on data available online (French Accelerometric Network, http://www-rap.obs.ujf-grenoble.fr/, last accessed May 2013). The Renass earthquake catalogue is provided by the Réseau National de Surveillance Sismique (RéNaSS, http://renass.u-strasbg.fr/, last accessed May 2013). The LDG earthquake catalog (2012) is provided by LDG upon request. For declustering the earthquake catalogs, we used the Code cluster 2000, http://earthquake.usgs.gov/research/software/index.php, (Reasenberg, 1985).

2.9 Acknowledgments

Hilal Tasan's PhD grant is funded by the Seismic Ground Motion Assessment (SIGMA) project. We are grateful to the French Accelerometric Network (RAP) for providing the accelerometric records, and to the Laboratoire de Détection et de Géophysique (LDG) for sharing the earthquake catalog. We are thankful to Philippe Guéguen and Pierre-Yves Bard for fruitful discussions.

2.10 Supplement

Table 2.S1: List of 62 rock RAP stations used in this study. *

Station Name	Latitude (°)	Longitude (°)	Recording Lifetime (years)	Modified Recording Lifetime (years)	Number of records with PGA ≥ 1 cm/s²	Maximum recorded PGA (cm/s²)
ANTF	43.564	7.123	8.6	3.0	2	2.6
ARBF	43.492	5.332	11.7	4.3	1	1.6
CAGN	43.667	7.146	8.1	3.8	6	2.8
ESCA	43.831	7.374	7.8	6.1	3	2.9
IRJO	43.630	5.660	15.6	15.6	1	5.8
IRPV	43.803	5.759	14.1	0.8	2	11.8
IRSE	44.530	6.780	6.7	6.7	1	2.0
MENA	43.784	7.489	12.5	7.9	18	16.1
NBOR	43.690	7.301	10.6	10.6	3	3.8
OCCD	45.319	3.699	8.0	5.4	1	1.0
OCMN	46.328	2.589	5.7	5.7	1	2.4
OCSJ	46.051	2.733	7.9	5.2	2	3.1
OGAG	44.788	6.540	16.1	6.9	2	2.3
OGCH	45.589	5.933	14.1	5.1	3	1.8
OGGM	45.204	6.117	16.6	7.3	1	1.7
OGLE	45.533	6.473	13.6	13.0	1	4.5
OGMA	45.774	5.535	12.3	10.4	7	15.7
OGAN	45.892	6.136	14.4	9.6	1	1.2
OGMO	45.208	6.685	14.8	10.6	8	9.0
OGMU	45.195	5.727	14.5	9.0	4	1.4
OGSI	46.057	6.756	15.4	12.1	18	27.7
OGTB	46.319	6.596	12.5	12.5	5	2.9
OGTI	45.494	6.925	13.5	13.5	17	6.2
PYAD	43.097	-0.428	7.9	6.6	220	100.9
PYAS	43.012	0.797	9.1	9.1	4	2.9
PYAT	43.094	-0.713	7.7	6.7	63	22.6
PYBA	42.474	3.117	9.3	6.0	3	2.4
PYBE	42.819	1.951	7.3	5.9	3	1.6
PYCA	43.024	0.183	7.9	5.6	127	84.6
PYFE	42.814	2.507	10.1	9.3	5	3.3
PYLL	42.453	2.065	7.6	5.3	2	10.1
PYLO	43.097	-0.049	7.4	6.3	20	26.5
PYLS	42.860	-0.008	10.0	8.7	34	40.8
PYOR	42.783	1.507	8.8	8.0	7	2.7
PYPM	42.416	2.439	10.6	7.9	1	6.8
PYP1	43.156	-1.241	6.8	6.8	1	0.93
PYPR	42.614	2.429	7.6	5.4	3	1.9
PYPT	43.009	3.033	9.9	9.9	1	2.1
QUIF	47.910	-3.160	6.2	2.2	1	2.0
SAOF	43.986	7.553	16.3	13.5	12	117.9
SMFF	46.600	-0.130	6.3	6.3	4	2.4
STBO	47.861	7.262	11.1	5.4	10	10.9
STET	44.260	6.929	12.1	9.5	25	6.6
STFL	47.112	6.563	11.3	3.6	5	22.6
STMU	48.584	7.766	9.9	3.6	28	28.1
STRB	47.723	7.341	5.7	3.0	7	8.1
STSM	48.215	7.159	11.6	8.7	4	25.4

BAIF	50.059	4.208	2.8	2.8	0	0
BRGM	43.237	5.438	9.7	9.7	0	0
UBBR	48.358	-4.562	3.5	3.5	0	0
UBNA	47.156	-1.637	2.8	2.8	0	0
UBVA	47.645	-2.746	2.9	2.9	0	0
CALF	43.753	6.922	15.8	12.0	0	0
IRIS	44.190	7.050	6.6	6.6	0	0
OCOL	45.676	3.636	6.0	6.0	0	0
OCOR	45.798	3.028	7.4	6.5	0	0
OCSF	45.034	3.097	4.0	4.0	0	0
OGBB	44.281	5.259	12.2	12.2	0	0
OGCA	43.732	5.672	15.1	6.5	0	0
PYFO	42.968	1.607	10.6	10.6	0	0
PYLI	43.002	1.136	9.3	9.3	0	0
RUSF	43.941	5.484	10.5	5.2	0	0

* 47 stations experienced at least one PGA ≥1 cm/s^2 during their lifetime, 15 stations have not recorded any PGA > 1 cm/s^2 during their lifetime. Modified recording lifetime should be closer to the true lifetime of the station (obvious gaps where station might not be functioning have been retrieved).

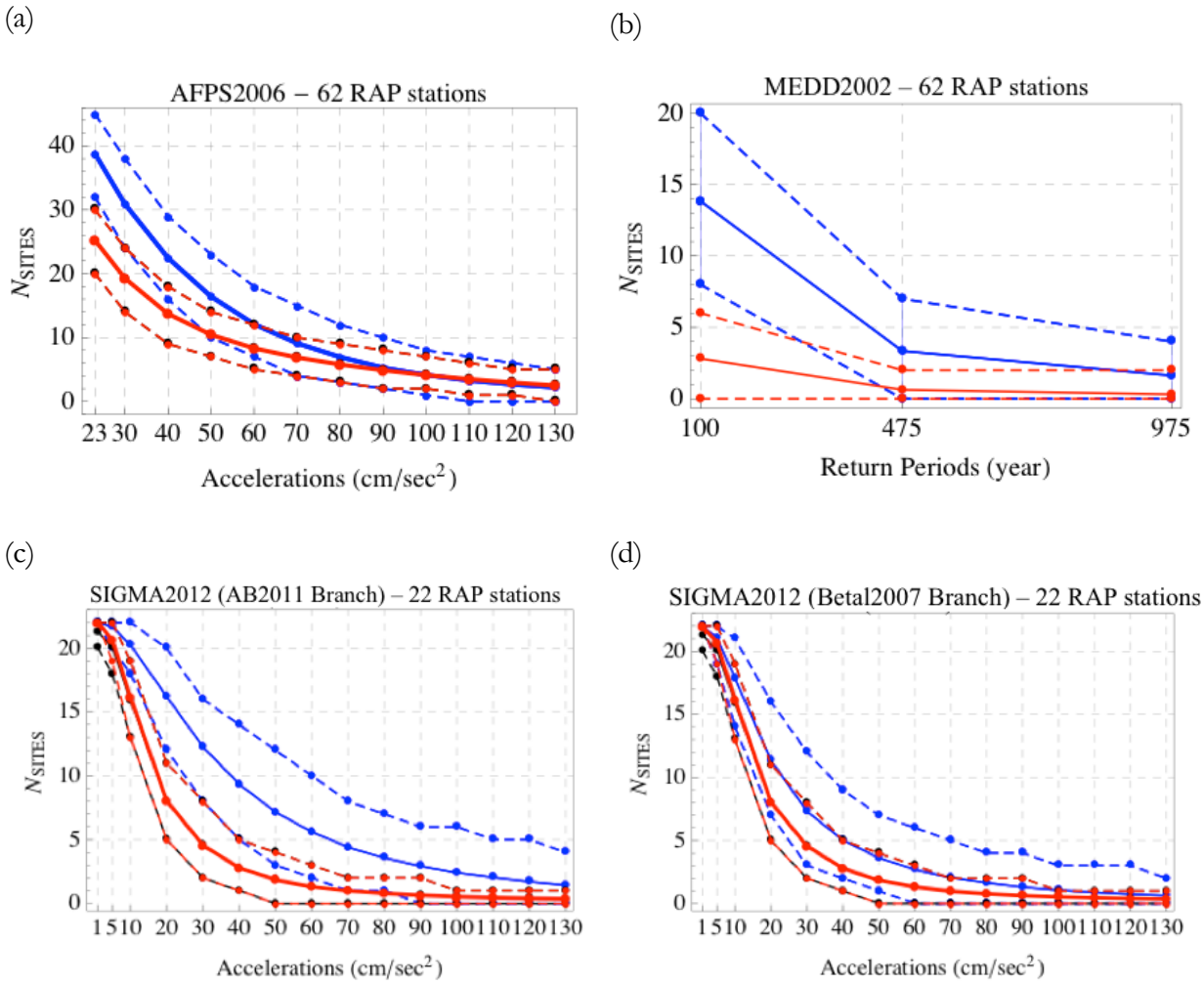

Figure 2.S1: Testing the probabilistic seismic hazard models against synthetic accelerometric data: predicted and "observed" number of sites with at least one exceedance. Blue curves: predicted distributions, mean and percentiles 2.5 and 97.5. Red curves: observed distributions, mean and percentiles 2.5 and 97.5. (a) AFPS2006 model (62 rock sites with 34 years, total time window 2108 years). (b) MEDD2002 model, considering 3 return periods (62 rock sites, total time window 2108 years). (c) SIGMA2012-AtkinsonBoore2011 and (d) SIGMA2012-Bommeretal2007 (22 rock sites with 34 years, total time window 748 years). The synthetic data were generated using the LDG catalog and sampling the Gaussian of the Cauzzi & Faccioli (2008) (CF2008) GMPE between ±2σ (see the text).

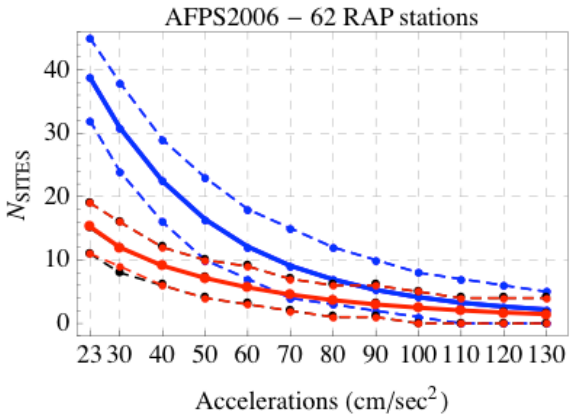

Figure 2.S2: Same as Figure 2.S1(a), testing the AFPS2006 model considering 62 RAP rock stations in southeast France. Only magnitudes $M_{L,LDG} \geq 3.5$ are used for the test.

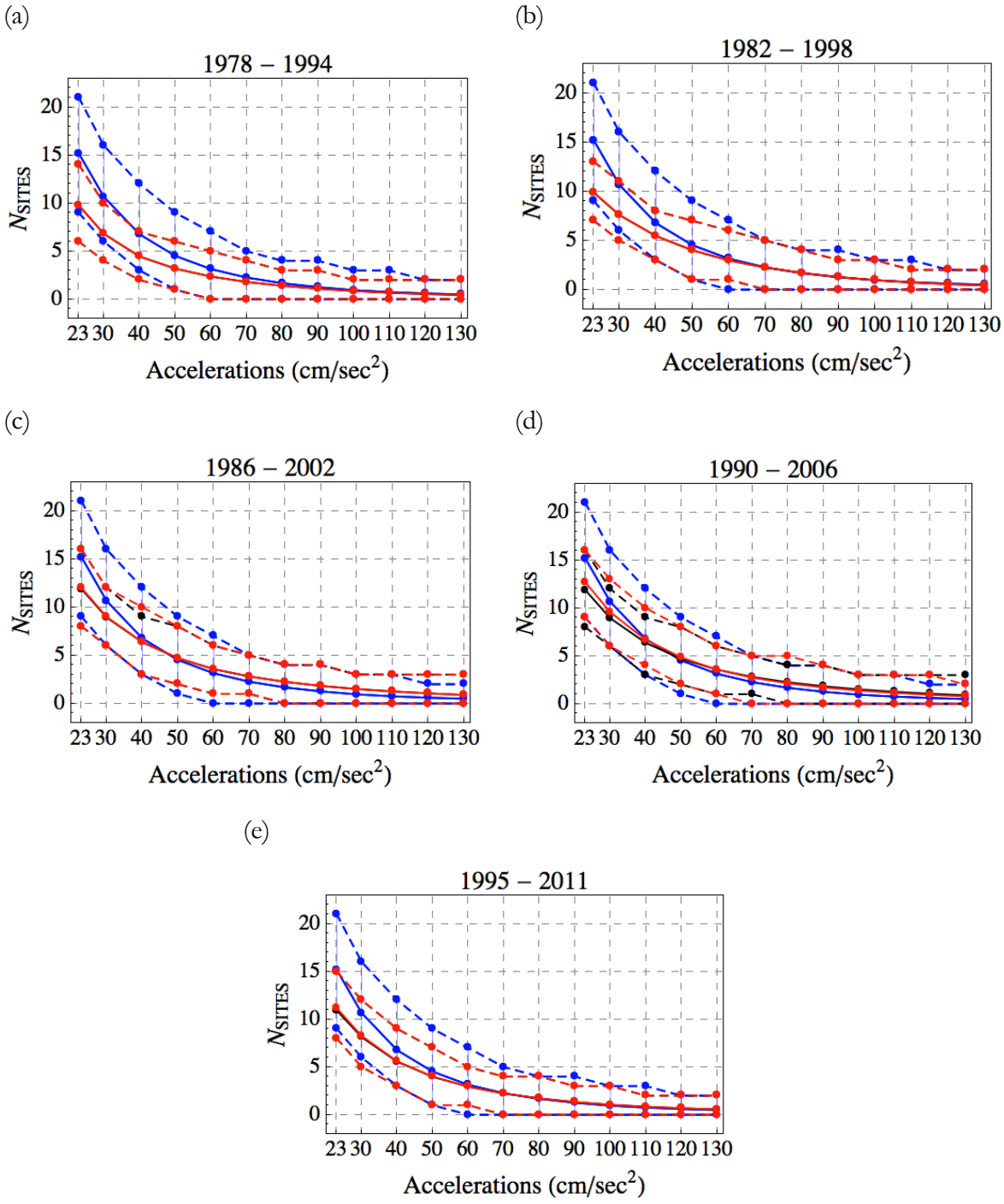

Figure 2.S3: Testing AFPS2006 against synthetic accelerometric data at 62 sites, and evaluating the stability of the results, with respect to the time window used. Five sliding windows are considered between 1978 and 2011, with length equal to the lifetime of the RAP network (16 yrs). Each station is attributed the same lifetime as in the real case. For each 16-yrs period, synthetic datasets are generated by coupling the LDG catalog with the ground-motion prediction equation CF2008 (sampled between $\pm 2\sigma$). Total observation time window is 449 years, like in the real case (Figure 2.5a).

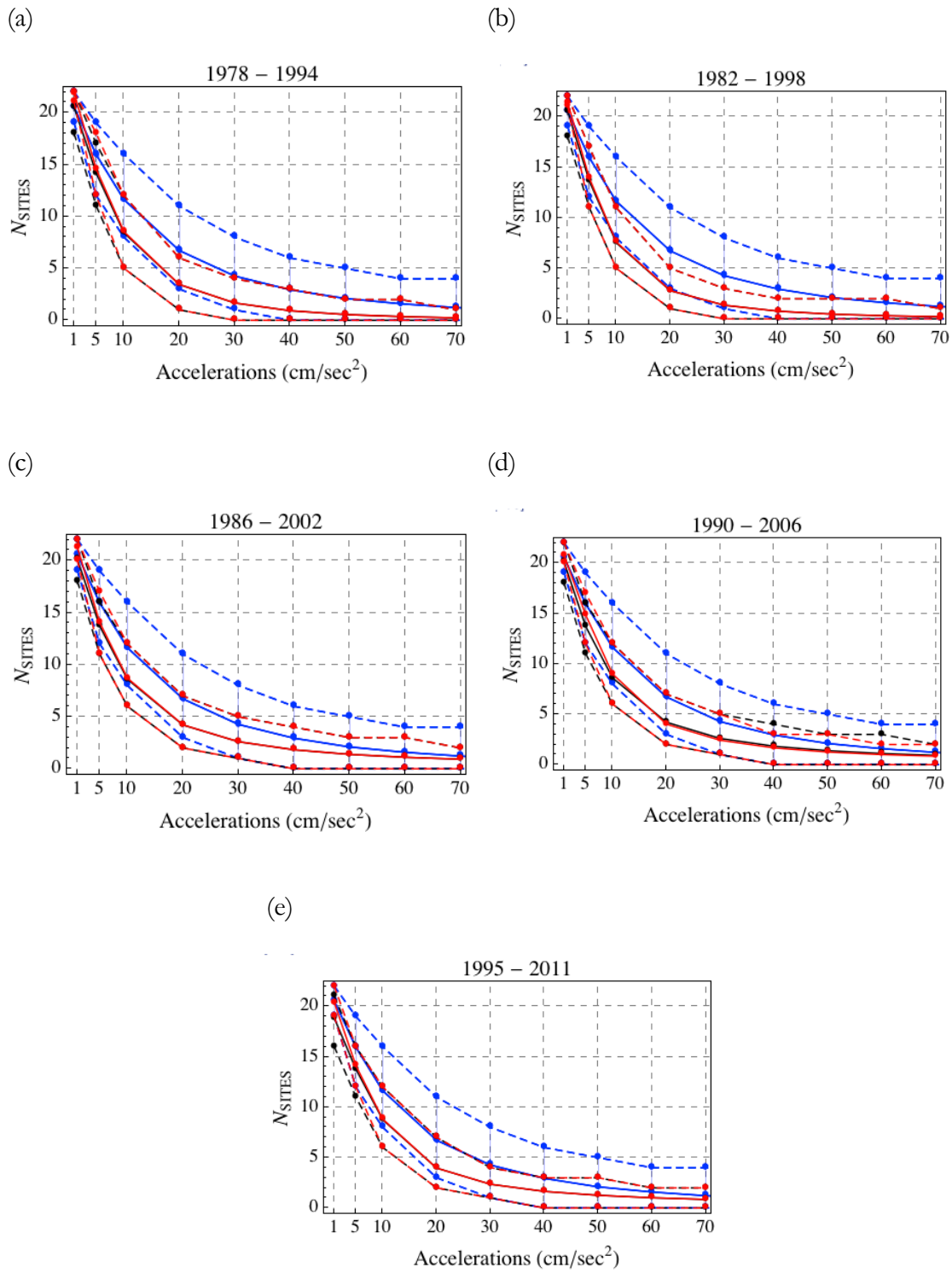

Figure 2.S4: Same as Figure 2.S3, testing the SIGMA2012 model (branch SIGMA2012 Atkinson & Boore 2011) considering 22 RAP rock stations in southeast France. Total observation time window is 182 years. Synthetic datasets are generated by coupling the LDG catalog with the ground-motion prediction equation CF2008 (sampled between ±3σ).

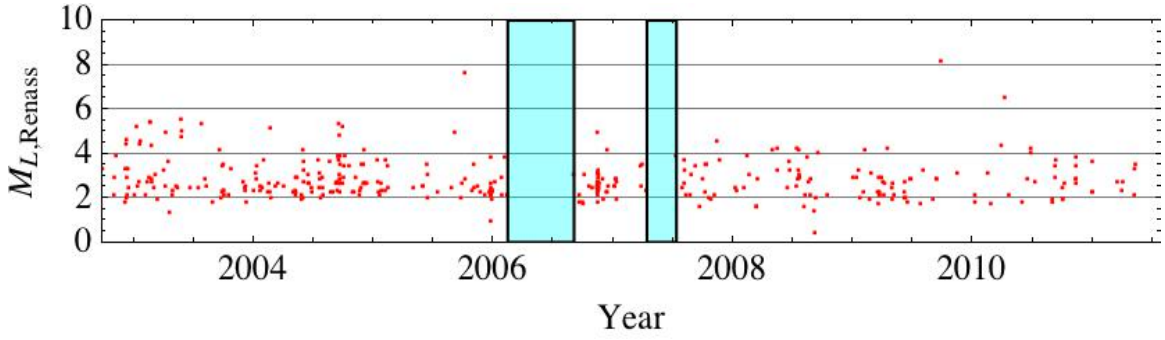

Figure 2.S5: The time history at PYOR station over its observation lifetime (8.8 years). Cyan fillings represent the gaps, which are the inter-event times larger than 10 times the mean inter-event time. Total length of gaps is 0.8 years. Thus the modified observation lifetime at PYOR stations is 8.0 years.

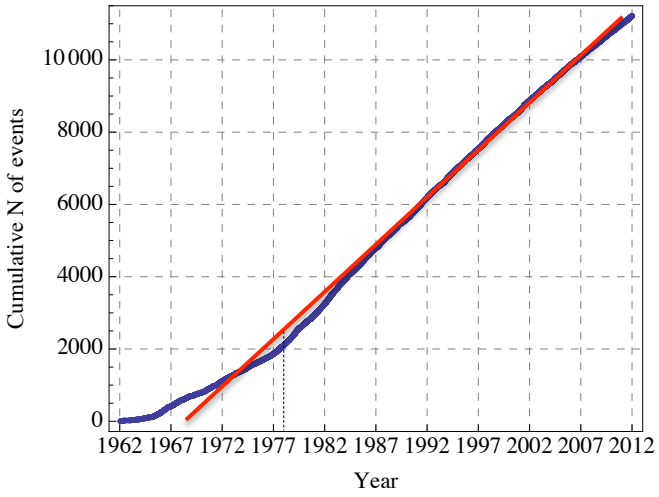

Figure 2.S6 : Cumulative number of events in declustered LDG catalogue over years. (total number of earthquakes is 11217.

Chapter 3

Evaluating the SHARE hazard model in the Turkish area using accelerometric data

Currently being integrated in the paper that is in revision in GJI.

Contents

3.1 Introduction

Turkey is an interesting region for the purpose of this study considering its abundant number of stations, high level of observed acceleration (PGA up to around 0.5 g) and the duration of observations (going back to earliest 1973). A higher number of records with higher accelerations (>100 cm/s^2) than acceleration observed in France allow us to test the hazard curve for stronger ground motions levels (or longer return periods).

In the following sections, we recall briefly the procedure used to compare the observations and the predictions. The **S**eismic Hazard **Har**monization in **E**urope (SHARE) hazard model will be introduced in detail. We will present the data used for testing. Then we will discuss the approaches developed to determine the observation lifetimes. The results will be introduced for varying number of sites, observation time lengths selected and minimum inter-site distances.

3.2 Method

As explained in section 2.2 of Chapter 2, our testing methodology is based on previous studies by Stirling & Gerstenberger (2010) and Albarello & D'Amico (2008). Albarello & D'Amico (2008) focused on the comparison of empirical and predicted number of sites with exceedance (N_{SITES}), whereas Stirling & Gerstenberger (2010) focused on the number of exceedances (N_{EXC}). It is possible to apply the test on either N_{SITES} or N_{EXC} (see Figure 3.1 of Chapter 2). In the previous chapter, we tested the French hazard models. Due to the low level of observed accelerations in France, at most sites considered the exceedances of acceleration levels were due to a single observation. Therefore we tested only the number of sites with exceedances (N_{SITES}). In this study, we follow the same methodology as in Chapter 2 except that we test both N_{SITES} and N_{EXC}.

We used different criteria to select the accelerometric stations, described in section 3.4.1. We also tested different methods to estimate the duration of observations at each station, explained in section 3.5.

3.3 PSH model: the Seismic Hazard Harmonization in Europe

With the collaboration of eighteen institutions and contribution of researchers with expertise spanning different fields, geology, seismology and engineering etc., a PSHA study has been established covering the whole European territory within the "Seismic Hazard Harmonization in Europe" project (SHARE, www.share-eu.org, Giardini *et al.* 2013) in the Framework Program 7 of the European Commission. In the SHARE study, the region under study stretches from mid-Atlantic ridge and Iceland in the west, to Romania and Turkey in the east. In general, hazard models are established regionally, for one country, by local institutions. The aim of SHARE project is to integrate countries in a unified framework and also to treat and assemble the data in a homogeneous way. The compiled earthquake and seismogenic fault databases are publicly available on the SHARE website http://www.share-eu.org, as well as the source geometries and characteristics.

The SHARE-PSHA considers the epistemic uncertainties using a logic tree approach, as frequently done in a PSHA. For active shallow crustal regions considered in SHARE-PSHA, four ground motion prediction equations (GMPEs) are selected for predicting ground motions at periods smaller than or equal to 3s (including the PGA); 1) Akkar & Bommer (2010) with logic tree weight (W) of 0.35, 2) Cauzzi & Faccioli (2008) with W=0.35, 3) Zhao *et al.* (2006) with W=0.1 and 4) Chiou & Youngs (2008) with W=0.2 (Delavaud *et al.* 2012). These GMPEs used are not necessarily established using the data from Turkey. Akkar & Bommer (2010) model is established using the data from Europe, the Mediterranean region, and the Middle East. Cauzzi & Faccioli (2008) is established using worldwide data dominated by Japanese data. Zhao *et al.* (2006) is generated using Japanese data. Chiou & Youngs (2008) is generated using a worldwide data.

The earthquake activity rates are estimated using three approaches (3 branches of logic tree): 1) Area source model (Cornell, 1968): the regions under study are divided into areal sources depending on their seismicity, geology, tectonics etc. The seismic activity is assumed to be homogenously distributed inside the seismic zone. 2) The fault-source and background model: this is a hybrid model that combines fault sources and background sources. 3) A kernel-smoothed model: This method is based on a kernel type probability density estimation technique of the activity rates inferred from the regional earthquake catalogs using information on past earthquakes and slip rates. The maximum magnitude M_{MAX} (largest magnitude of

earthquake that is expected to be seen in the source) is determined in three unified ways for all regions (Woessner *et al.* 2012).

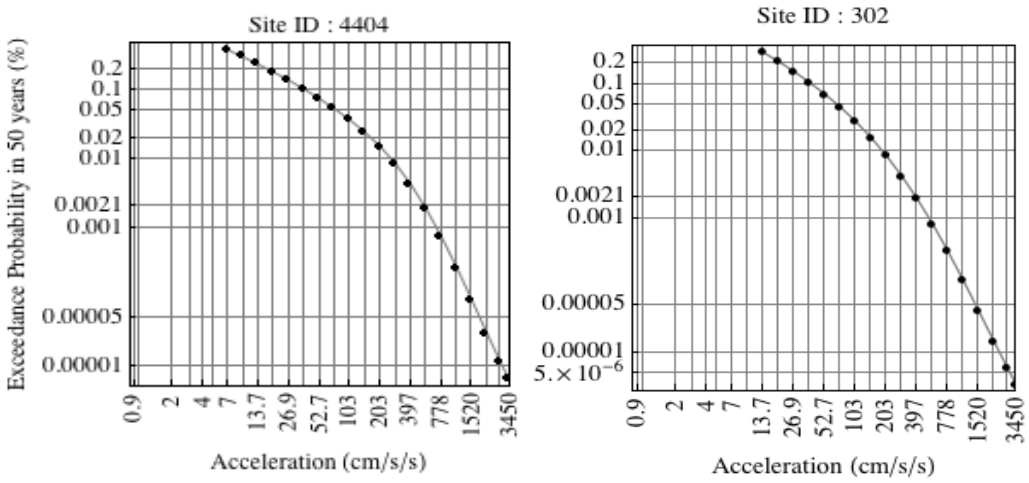

Figure 3.1: Examples for mean hazard curves of SHARE-PSHA at sites 4404 (Poturge province) and 302 (Dinar province)

The SHARE-PSHA model provides the weighted average of all logic tree branches considering different assumptions and models, e.g. GMPEs, M_{MAX} and seismogenic sources. The results are available for a wide range of accelerations starting from 0.9 cm/s^2 (smallest value at some sites) up to 3450 cm/s^2 (see Figure 3.1 for two examples at two sites). The hazard values are provided on a grid in every 0.1°x0.1° cell. At each site considered, the mean value of the 4 hazard values of the cell's corners are calculated to obtain the hazard values at sites selected in this chapter. The minimum magnitude used in the probabilistic calculation is M_W=4.5. The PGA values are provided for site conditions with V_{S30} of 800 m/s. In this study, we will test the median of weighted average of all logic tree branches of SHARE-PSHA model for Turkey.

We can see the predicted accelerations corresponding to 475 years of return period given by the SHARE-PSHA in Figure 3.2, and given by other probabilistic studies applied for Turkey in Figure 3.3; Kalkan *et al.* (2008), Erdik *et al.* (1999) and The Global Seismic Hazard Assessment Program (GSHAP). It would also be interesting to test these models. However, Kalkan *et al.* (2008 & 2009) study is available only for vicinity of Istanbul province (Marmara region). SHARE model can be accepted as an updated version of GSHAP model for Turkey and the hazard maps given in Erdik *et al.* (1999) were calculated in connection with GSHAP program. An elaborated PSHA study relying on most current data and GMPEs is going on

(personal communication with Sinan Akkar). However, until the results from the project are available, we test only the SHARE-PSHA.

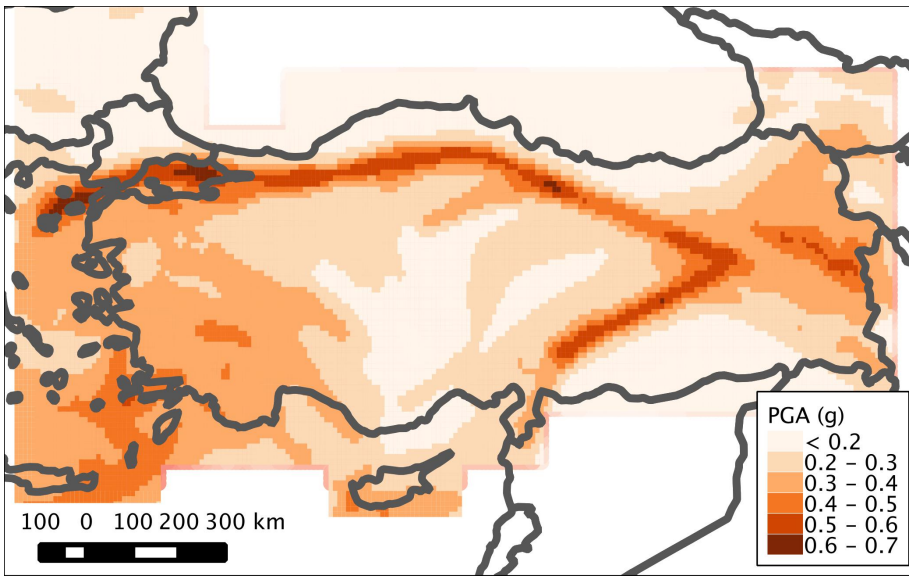

Figure 3.2: The SHARE seismic hazard map for 475 years of return period.

3.4 Accelerometric data

The accelerometric data is taken from the Turkish National Strong Motion Observation Network (TR-NSMN), which has been operating under the General Directorate of Disaster Affairs of Turkey since 2009 (kyh.deprem.gov.tr). The first station of TR-NSMN was installed in 1973 and the first earthquake recorded is the Denizli Earthquake, which occurred on 19 August 1976. The number of stations has been increasing ever since. Especially after the two devastating earthquakes that hit Marmara region, the 17 August 1999 M_W7.6 Kocaeli Earthquake and the 12 November 1999 M_W7.2 Duzce Earthquake, the General Directorate of Disaster Affairs of Turkey started deploying several accelerometric stations around the active regions of Turkey. In the beginning of 2013, around 400 stations were operating mainly in the active regions.

However, many stations detected very few events. The number of observations per station is often smaller than in the French accelerometric database, although the seismic hazard in Turkey is much stronger. As shown in Figure 3.4, 38% of stations considered for testing observed less than 10 records. We suspect that the small number of observations at some

stations is due to the presence of gaps in the monitoring, but unfortunately we have no information on the operational time of each station.

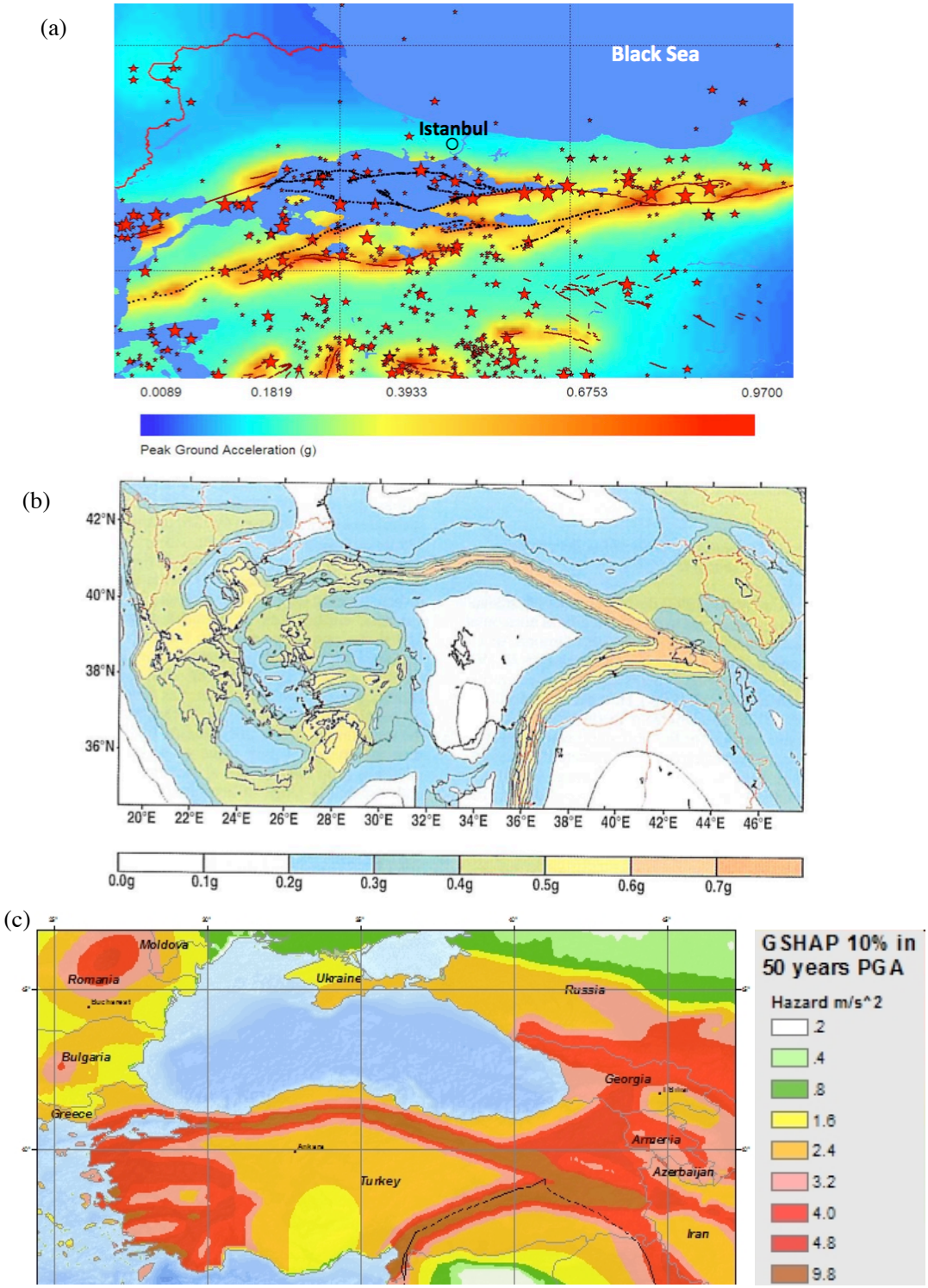

Figure 3.3: Seismic hazard map for 475 years of return period given by other studies. (a) Kalkan et al. (2008) (b) Erdik et al. (1999) (c) GSHAP (http://earthquake.usgs.gov/earthquakes/world/turkey/gshap.php)

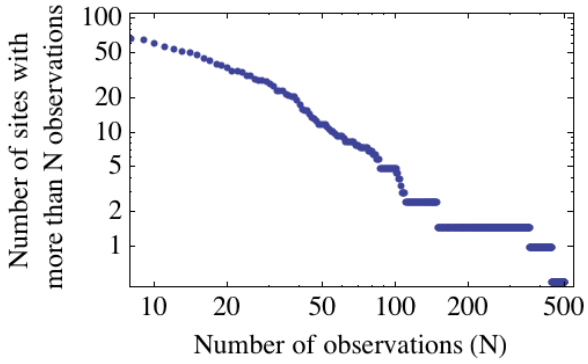

Figure 3.4: Distribution of the number of raw observations (no acceleration threshold) at 204 sites with known V_{S30} values.

3.4.1 Selecting accelerometric stations

The testing methodology imposes some constraints on the selection of stations:

- V_{S30} must be known in order to estimate rock ground motions at sites that are not rock stations.

- The operating lifetime of the stations should be known, or enough records should be available to estimate the observation time window from the observations.

- The stations should be far enough so that observations at each station can be considered independent from the other stations.

We first select only stations with known V_{S30} values. In RESORCE database (Akkar *et al.* 2014, Sandikkaya *et al.* 2010), the average shear-wave velocity in the top 30m soil profile (V_{S30}) beneath some TR-NSMN accelerometric stations were studied through field surveys. We use these V_{S30} values when available. For some other stations, V_{S30} values are given on TR-NSMN website. The total number of stations with known V_{S30} values is 291.

At stations with no or only one observation, it is not possible to estimate the operating time without any external information. Among the 291 TR-NSMN stations, 26 stations observed only one earthquake and 61 stations have no record. These 87 stations have thus been excluded from our analysis (Figure 3.5).

Testing a PSHA model requires independency of the observations at accelerometric stations to be able to consider several sites at once (ergodic assumption). The sites are selected aiming to keep a minimum inter-site distance (R_{MIN}) between each other. When several sites are closer than R_{MIN}, we keep only the site with the highest predicted annual rate of exceedance given by the PSHA model. If these sites also have the same annual rate of exceedance, only the site with the longest observation time window is kept. We tested different values of R_{MIN} between 0 and 60 km.

Even when removing nearby stations, there are still a few earthquakes detected by several stations above the considered acceleration threshold. In order to remove dependent observations, when two records at two stations are produced by the same earthquake, we simply discard the site with the lowest acceleration.

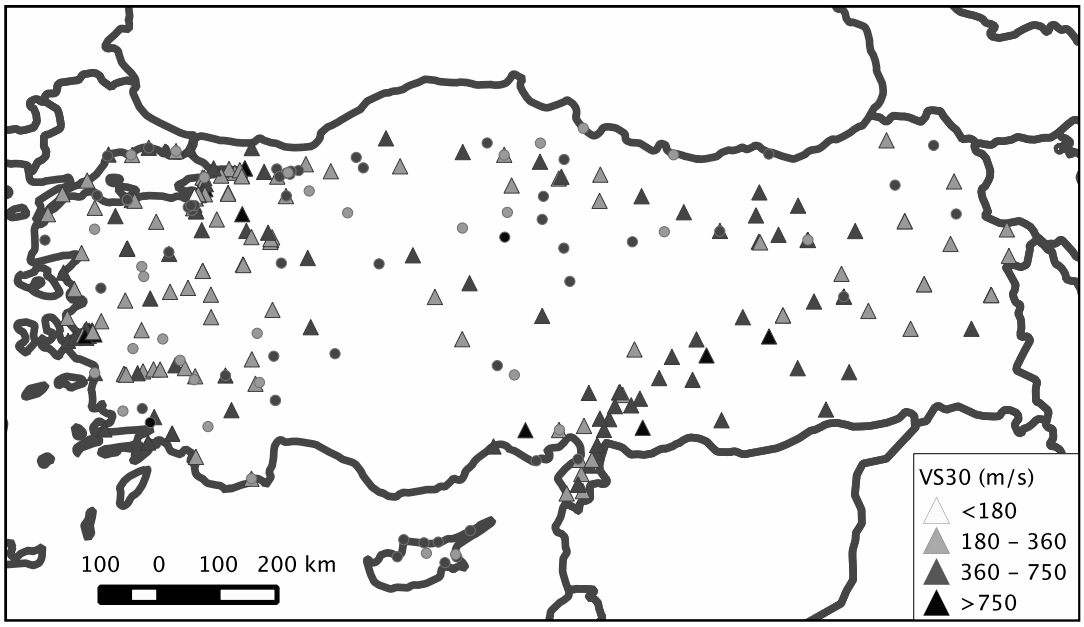

Figure 3.5: Triangles: 204 stations with known V_{S30} values. Circles: 87 stations with only one/no observation (excluded). Gray shadings: the V_{S30} values of the stations.

3.4.2 Selecting and processing accelerometric records

In this study we are interested in testing the SHARE hazard model at acceleration levels higher than 50 cm/s^2. We obtain the raw (unprocessed) records given by TR-NSMN without any filtering on magnitudes. All records observed between 1976 until the date when

we retrieved the data (13/03/2013) with a PGA≥50 cm/s^2 (in at least one of their horizontal components) are extracted from the database.

The main source of our accelerometric dataset is the RESORCE ground-motion database built within the SIGMA project (Reference Database for Seismic Ground-Motion in Europe, Akkar *et al.* 2014). RESORCE is a single integrated accelerometric databank for the broader European area, consisting of earthquake and station metadata information, and accelerometric data. The Turkish component of RESORCE relies strongly on the T-NSMP strong-motion database, covering the time window between 1976 and 2011, and including ground motions from magnitudes 2.8 to 7.6 (Mw). In RESORCE, the waveform of raw accelerometric data were visually inspected one by one in terms of waveform quality and frequency content to implement a well-established data processing technique into the entire strong-motion databank (see Akkar *et al.* 2014 for details on the band-pass filtering and post-processing scheme). Source-to-site distance measures (e.g. R_{JB}, R_{RUP}) are provided. We obtained 100 records with a geometrical mean of processed horizontal components higher than or equal to 50 cm/s^2 observed at stations with known V_{S30} values. For 56 records, the processed records are already available in RESORCE. We processed 44 additional records that are found in TR-NSMN and that are not in RESORCE using the same methodology explained in Akkar *et al.* (2014). 23 of these 44 records are recent records, which occurred after 2007.

3.4.3 Calculating the rock ground motion at sites

Less than 6% of the Turkish stations are actually located at rock (Eurocode8 class A). The SHARE-PSHA provides the hazard values for rock site conditions (V_{S30} 800 m/s), but there are too few rock sites to test the model. To increase the number of sites, we decided to consider also the soil sites. Therefore it is necessary to estimate the rock ground motions that would be recorded if the stations were on a site with V_{S30} of 750 m/s (PGA_{750}).

Sandıkkaya *et al.* (2013) proposed a nonlinear site amplification function for shallow active crustal regions derived using the SHARE database (Yenier *et al.* 2010, www.share-eu.org/sites/default/files/D4%201_SHARE.pdf last accessed on 04/04/2014). The data used in Sandıkkaya *et al.* (2013) is mainly from Greece, Italy and Turkey and also small amount of data come from Taiwan, Japan and California. The dataset used for deriving the site-amplification function consists of events with magnitude between 4 and 7.9, source to site distance (Joyner-Boore distance, R_{JB}) shorter than 200 km and maximum focal depth of 30 km.

Sandıkkaya *et al.* (2013) recommended to use this equation for V_{S30} between 150 m/s and 1200 m/s. The equation of Sandikkaya *et al.* (2013) to calculate the period-independent reference ground motion level is given in Equation 3.1. F_N and F_R are the dummy variables to account for the faulting style. F_N is 1 for normal faulting and zero for other faulting styles; F_R is 1 for reverse faulting and zero for other faulting styles. The equation to calculate the site amplification factor is given in Equation 3.2.

To use the site amplification equation of Sandikkaya *et al.* (2013), we must know 1) the moment magnitude and the faulting style of earthquakes, 2) V_{S30} of the sites and 3) R_{JB} distance. We searched the required parameters in different sources following the hierarchical order of agencies explained in Table 1 of Akkar *et al.* (2010), (data from these agencies are last retrieved on October 4th, 2013). We estimate the PGA_{750} values of the records observed at soil sites (sites with V_{S30} smaller than 750 m/s) and also at rock sites (sites with V_{S30} higher than 750 m/s) for the homogeneity of the dataset. Among the observations at stations with known V_{S30} values, required parameters could be obtained for most records (77 out of 110 records), mainly from RESORCE database. For the 33 records with missing parameters, we made some assumptions on the missing parameters discussed in section 3.8.1.

To calculate PGA_{750} using the site-amplification equation of Sandikkaya *et al.* (2013), we follow these steps;

1) The period-independent reference PGA (PGA_{REF}) is predicted from the moment magnitude, faulting style and R_{JB} of the earthquake (Equation 3.1)

$$for\ M_W \leq 6.75; \quad \ln(PGA_{REF}) = 3.17101 + 1.15371\,(M_W - 6.75) + 0.0803\,(8.5 - M_W)^2 + [-1.49513 + 0.13602(M_W - 6.75)]\,ln\left(\sqrt{R_{JB}^2 + 13.39544^2}\right) - 0.35736F_N + 0.06573F_R$$

$$for\ M_W > 6.75; \quad \ln(PGA_{REF}) = 3.17101 - 0.31204(M_W - 6.75) + 0.0803(8.5 - M_W)^2 + [-1.49513 + 0.13602(M_W - 6.75)]\,ln\left(\sqrt{R_{JB}^2 + 13.39544^2}\right) - 0.35736F_N + 0.06573F_R \quad \textbf{(3.1)}$$

2) Using the V_{S30} of the sites and PGA_{REF} calculated in step 1, the amplification (Amp) at the period-independent reference site condition (V_{REF}) is calculated by

$$ln(Amp) = \begin{cases} a(T)ln(V_{S30}/V_{REF}) + b(T)ln\left[\frac{PGA_{REF}+c(V_{S30}/V_{REF})^n}{(PGA_{REF}+c)(V_{S30}/V_{REF})^n}\right] \; for \; V_{S30} < V_{REF} \\ a(T)ln(V_{S30}/V_{REF}) \quad for \; V_{REF} \leq V_{S30} < V_{CON} \\ a(T)ln(V_{CON}/V_{REF}) \quad for \; V_{S30} \geq V_{CON} \end{cases} \quad \textbf{(3.2)}$$

In this study, the following values of parameters are used : reference velocity V_{REF}=750 m/s, a(T)=-0.41997, b(T)=-0.28846, c=2.5, n=3.2 and V_{CON}=1000 m/s. The standard deviation of ln(Amp) is also provided for V_{REF} of 750 m/s in Sandikkaya *et al.* (2013).

3) The geometrical mean of the two horizontal components observed at the site (PGA_{SITE}) is divided by the amplification Amp, obtained at step 2, to calculate the first estimation of PGA_{750} value (Equation 3.3).

$$PGA_{750} = \frac{PGA_{SITE}}{Amp} \quad \textbf{(3.3)}$$

4) The PGA_{750}, obtained at step 3, is taken as PGA_{REF} and steps 2&3 are repeated iteratively until the PGA_{750} converges.

As shown in Equation 3.2, if $V_{S30}>V_{REF}$, calculated PGA_{750} is higher than $PGA_{SITE.}$ If $V_{S30}<V_{REF}$, calculated $PGA_{750}<PGA_{SITE.}$ Since most sites have V_{S30} smaller than 750 m/s, estimated values of PGA_{750} are generally smaller than observed PGAs (PGA_{SITE}). There are 69 records with PGA_{750} higher than or equal to 50 cm/s^2 compared to 100 records in the dataset of PGA_{SITE}. We use the dataset of PGA_{750} to evaluate the SHARE hazard model. As illustrated in Figure 3.6, the sites that observed at least one PGA_{750} higher than or equal to 50 cm/s^2 are mainly found along the western part of the North Anatolian Fault Zone, in the East Anatolian Fault Zone and in the Aegean Graben System.

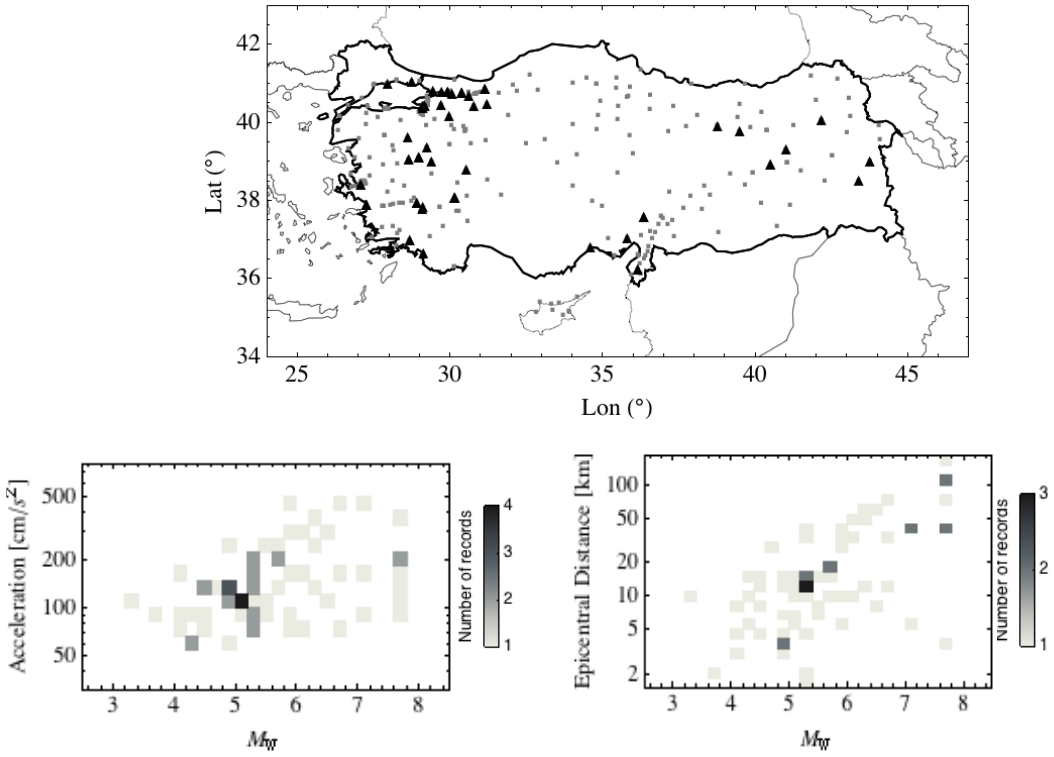

Figure 3.6: (a) 291 accelerometric stations (points) with known V_{S30} values. Black triangles are 42 stations (out of 291) that observed a PGA_{750} equal to 50 cm/s^2 or above (see text). (b) PGA-moment magnitude and (c) epicentral distance-moment magnitude distribution of 69 records with $PGA_{750} \geq 50$ cm/s^2.

3.5 Identifying complete observation periods at accelerometric stations

For comparing the predicted and observed rate of exceedances at a station, we must be sure that all ground shakings stronger than the selected threshold are present in the dataset during the observation time window (completeness of observations). Therefore, the operation time window of the station (installation/removal dates) and the time windows when the station was out of order (due to breakdown, stoppage or any other reasons) during its lifetime should be known. We contacted the TR-NSMN agency to obtain this information. However neither the information about the discontinuities in observation nor the operation time windows (installation/removal dates) of the stations could be obtained.

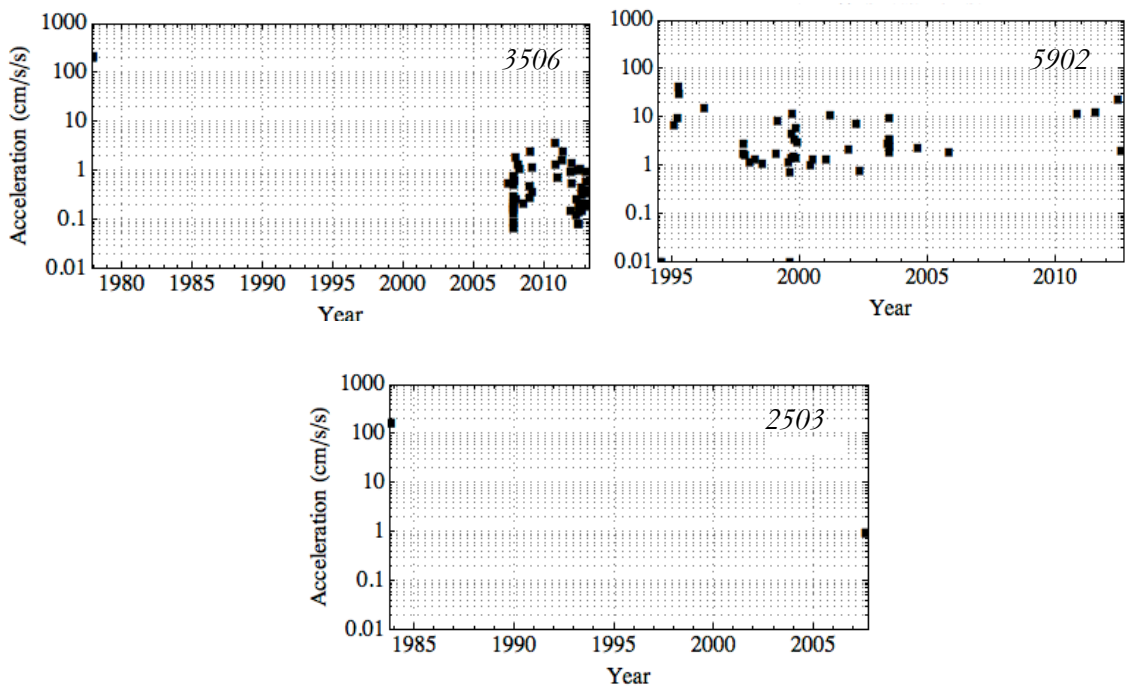

Figure 3.7: Example for observation history at three sites (top left: site 3506, top right: site 5902, bottom: site 2503) that have an unexpectedly long time period with no records.

The simplest way to calculate the operating time window at a station is to assume that it is the period between the first and the last recordings. When we look at the observations at some stations, we see some conspicuous time periods without any records. (Figure 3.7). However, it is difficult to decide whether a gap is due to the absence of strong ground shakings or due to the interruption of observation at the station. Therefore, we applied two methods to identify the gaps, which avoid arbitrary decisions.

The first method is based on the statistical analysis of inter-event times at each site. The second method uses predicted accelerations that should have been observed at each station, estimated using an earthquake catalog and a GMPE developed from Turkish strong motion data.

3.5.1 Method 1: Identifying the gaps using inter-event times

In this section, we follow the same methodology as in the second chapter to identify the gaps. This method is based on the inter-event times of the observations at each site. The method relies on the assumption that the occurrences of earthquakes in a region follow a Poisson distribution i.e., that these events are independent.

For a Poisson process, the probability of having an inter-event time significantly longer than the average inter-event time is very small. The probability of observing a time interval longer than t is $P(t)=exp(-t/t_{av})$, where t_{av} is the average inter-event time. In this study we define inter-event times longer than 10 times the average value as gaps. This corresponds to a very small probability of $exp(-10)=4.5x10^{-5}$ of finding such a gap by chance.

This method assumes that earthquakes follow a Poisson process. However, the observations at some stations are strongly clustered (see Figure 3.8). Therefore, for calculating the average inter-event times of observations at each site, we consider only the observations of mainshocks, which can be considered as independent.. Using the original catalog without declustering would under-estimate the average inter-event time and therefore detect too many gaps. To determine which observations are the records of mainshocks and which are records of dependent earthquakes, we decluster the earthquakes listed in TR-NSMN using the method of Reasenberg (1985) (Figure 3.9).

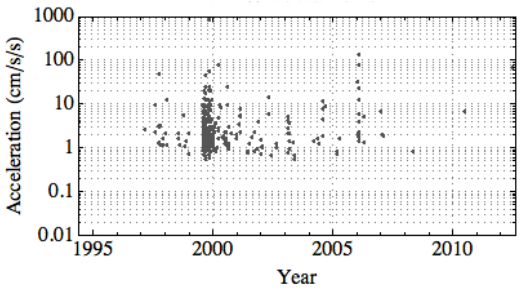

Figure 3.8: Example: observation history at station 5401 (Sakarya province, Marmara Region). Observations indicate a strong clustering especially after the M_W=7.6 17 August 1999 Kocaeli Earthquake (R_{JB}= 3.08 km) and the M_W=7.2 12 November 1999 Duzce Earthquake (R_{JB}= 40.5 km).

The declustering process analyses the inter-event times, inter-event distances and the magnitudes of earthquakes. We decided to use this earthquake catalog since it is the most complete for small earthquakes (smaller than 4). However, for some earthquakes given in the TR-NSMN earthquake catalog, some parameters are missing (728 earthquakes out of 5157). We checked some of these earthquakes in the ISC catalog and we found that these earthquakes have very small magnitudes (around 2). Considering only the earthquakes with known location and magnitude, we identify the earthquakes that occurred in a cluster (swarms, sequences of aftershocks or foreshocks). We use the following parameters for the declustering method: number of crack radii (distance factor) of 15, independence probability of 0.99, minimum

look-away time of 10 days and maximum look-away time of 20 days. We identified 470 clusters consisting of 3246 events among 4429 earthquakes, representing 73% of the earthquakes in the catalog. The distributions of the number of events per day in the catalog before and after declustering are shown in Figure 3.9 (b). The declustered catalog consists of the earthquakes that do not belong to any cluster (1183 earthquakes) and the earthquake with the highest magnitude of each cluster (470 earthquakes), representing 51% of the catalog. We use only the observations from the earthquakes in the declustered catalog to calculate the average inter-event times and identify the gaps.

(a)

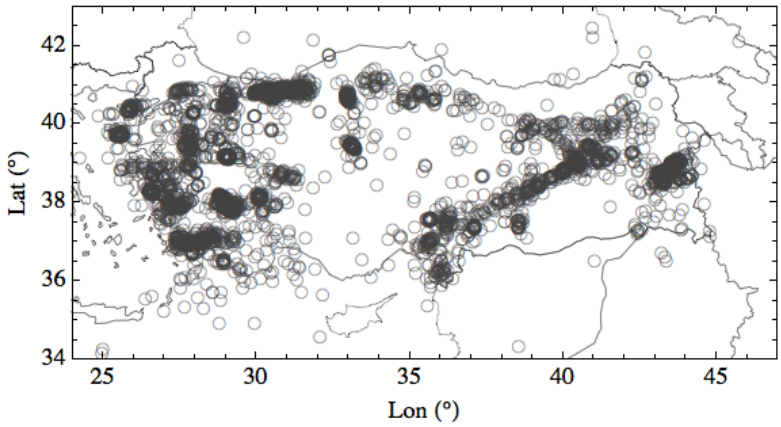

(b)

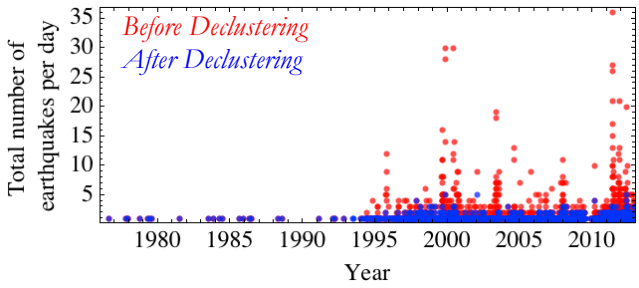

Figure 3.9: (a) Location of earthquakes in the TR-NSMN earthquake catalog (1976-2013) and (b) total number of earthquakes per day as a function of time before and after declustering.

We follow the steps below to identify the gaps using inter-event times of observations from the earthquakes in the declustered catalog:

1) The average inter-event time (t_{av}) is calculated using the time windows between the observations of mainshocks at a station.

2) The gaps, time windows between mainshocks longer than 10*tav, are identified.

3) The gaps identified in step 2 are excluded from the list of all inter-event times. The steps 1&2 are repeated iteratively excluding the gaps identified previously. The iterations are stopped when no more additional gaps are identified between two consecutive iterations.

4) Since we used only the inter-event times between mainshocks to identify the gaps, after identifying the gaps, we checked if any record of dependent foreshocks/aftershocks occurred during the identified gaps. We found that at three stations foreshocks/aftershocks fall within a gap. These events occurred only a few hours before/after the mainshock. For these 3 cases, the start/end dates of the gaps are modified, taking the date of fore/after shocks instead of mainshocks. We also found that none of the observations from 728 earthquakes that could not be included to the declustering calculations do not fall within the identified gaps.

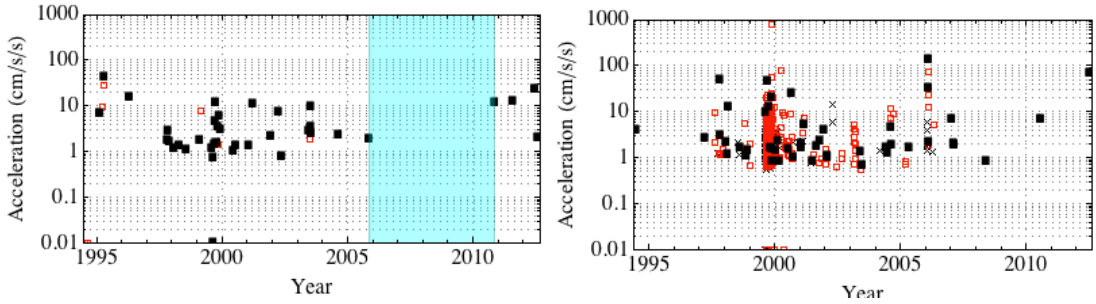

Figure 3.10: Examples of the identification of gaps using inter-event times of observations at stations. (a) The time history at station 5902 over its observation lifetime (18.03 years). The shaded area represents the gap, defined as an inter-event time longer than 10 times the mean inter-event time. Total length of the gap is 5 years. The modified observation lifetime at this station is 13.03 years. (b) The time history at station 5401. No gaps are identified considering the inter-event times of mainshocks. Observations from mainshocks and aftershocks are shown with different markers. ■ : Raw (not processed) observed PGA due to mainshocks, □ : Raw observed PGA due to dependent events, × : Records of earthquakes with unknown location and magnitude.

We show the results of gap identification for two examples in Figure 3.10. The mainshocks and dependent events are shown with different symbols. In Figure 3.10 (left), the shaded area between around 2006 and 2011 is identified as a gap. In Figure 3.10 (right), no gap is identified at station 5401. For all stations considered, Table 1 summarizes the original observation time lengths (time laps between first and last observation, T_{OBS}) and after retrieving the gaps ($T_{OBS\text{-}GAP1}$).

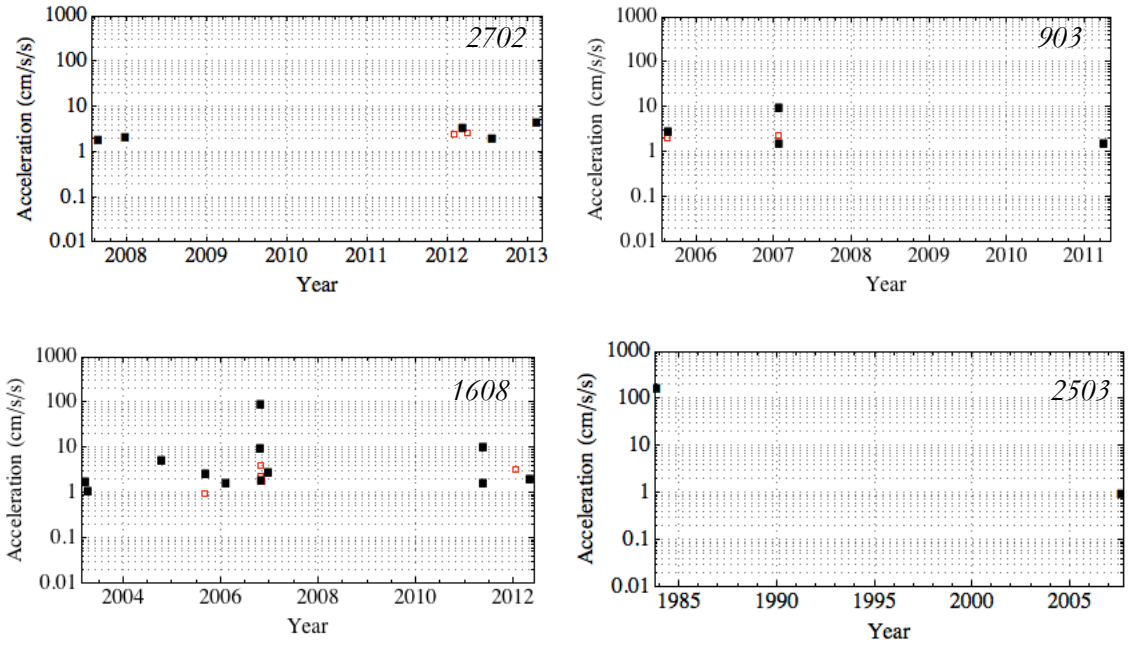

Figure 3.11: Example of time histories at four stations (top left) station 2702 with 7 records, (top right) station 903 with 6 records, (bottom left) station 1608 with 17 observations, (bottom right) station 2503 with 2 observations. There are no gaps identified at these stations using the method based on inter-event times. ■ : Raw (not processed) observed PGA due to mainshocks, □ : Raw observed PGA due to dependent events.

When calculating the gaps using inter-event times, there must be a sufficient number of observations at a station to calculate precisely the average inter-event time. At stations with few observations, if there is a long gap, the average inter-event time will be over-estimated. As a result, the gap may not be identified due to the biased average inter-event time. For example, the observation history at three stations are shown in Figure 3.11. There are no gaps identified at these stations using the method based on inter-event times. Thus, another criterion is required to identify gaps at stations with few records. For this reason, we used another method presented in section 3.5.2.

3.5.2 Method 2 : Identifying gaps using synthetic observations

This method identifies gaps based on synthetic acceleration data. We use synthetic data generated using an earthquake catalog and a GMPE. For further information on the earthquake catalog and the estimated PGA, see the Section 3.8 (Supplement). The minimum magnitude of the earthquake catalog is M_W4. We generate the synthetic dataset at 204 accelerometric stations using the GMPE Akkar & Çagnan 2010 (AC2010), based on an accelerometric dataset from Turkey. The magnitude validity range of AC2010 is 3.5-7.6 (M_W).

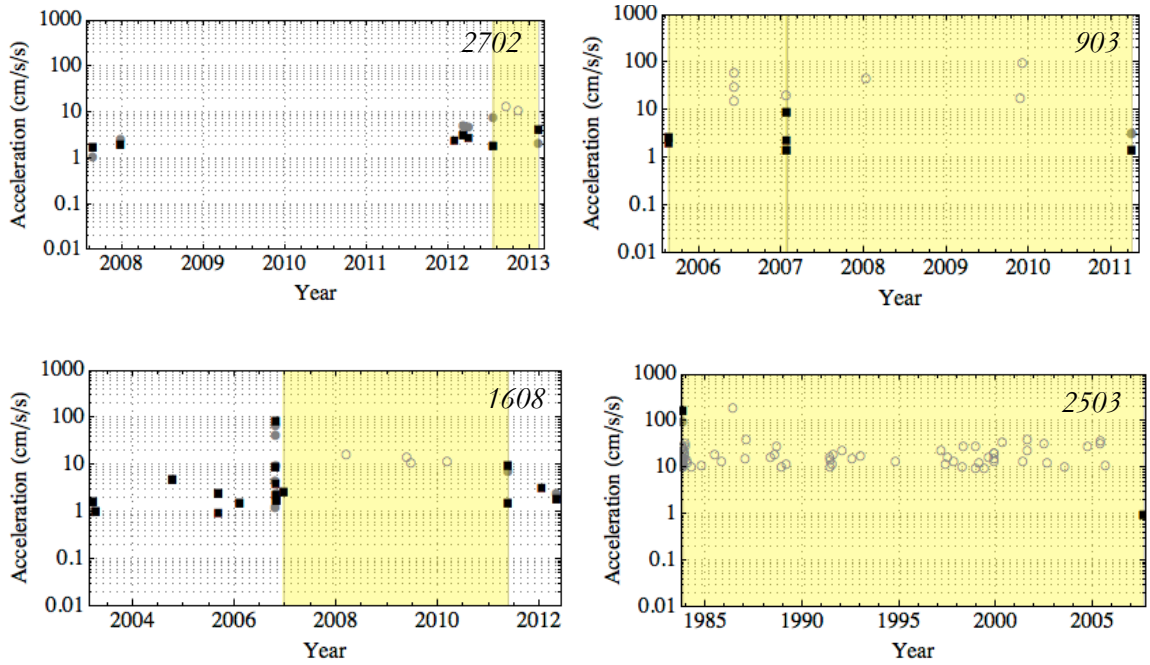

Figure 3.12: Example for time histories at four stations (top left) station 2702, (top right) station 903, (bottom left) station 1608, (bottom right) station 2503. Shaded areas indicate the gaps identified based on missing data with PGA ≥ 10cm/s^2. ■: Raw (not processed) observed PGA, •: the PGA_{MEDIAN} predicted by the GMPE.

We use the original observation lifetimes and the local site conditions V_{S30} at each site. We search for synthetic observations with $PGA_{MEDIAN} \geq 10$ cm/s^2 that are missing in the accelerometric dataset. We believe that observations with $PGA_{MEDIAN} \geq 10$ cm/s^2 should have been detected by the accelerometric stations if the stations were operating at the time of the earthquake. Indeed, the dataset contains many much smaller values of PGA, sometimes smaller than 1 cm/s^2, suggesting that the detection threshold is much smaller than 10 cm/s^2. The time period between the previous observation before and the next observation after the date of one missing data (including observations from foreshocks/aftershocks) is defined as a gap.

The gaps identified using this method are shown in Figure 3.12 for 4 stations as an example. As shown in Figure 3.11, the first method based on inter-event times does not detect any gap at these stations. For station 2702 (Figure 3.12, top, left), the original observation time window is 5.5 years. The method based on missing data identifies the time window between 22/07/2012 and 12/02/2013 as a gap due to two missing data with $PGA_{MEDIAN} \geq 10$ cm/s^2 that occurred between these two dates. Thus the corrected observation time window after retrieving the identified gap is 4.9 years. Stations 903 and 2503 (Figure 3.12, top-right and

bottom-right respectively) have an original operation length of 5.6 years. The corrected operation time windows of the stations are zero. These stations may be temporary stations or they may have been operating occasionally. The stations that have no length of corrected observation period are excluded from calculations (15 stations out of 204). Excluding the 15 stations that have no length of corrected observation period, the number of the stations considered further in this study decreased to 189 (Table 1). The corrected lifetimes obtained using the first method are generally longer than those obtained using the second method, except for stations 905 and 5902. We believe that the gaps identified using the first method provide a lower bound for the true gaps duration whereas the gaps identified using the second method are an upper bound.

Table 1: List of 189 accelerometric stations considered further in this study

Station ID	Latitude (°)	Longitude (°)	V_{S30} (m/s)	TINI	TFINI	T_{OBS} (years)	$T_{OBS-GAP1}$ (years)	$T_{OBS-GAP2}$ (years)	Maximum recorded PGA_{SITE} (cm/s²)*	Number of records with $PGA_{SITE} \geq$ 50 cm/s²	Maximum PGA_{750} (cm/s²)*	Number of records with $PGA_{750} \geq$ 50 cm/s²
301	30.53	38.78	226	1998.3	2013.1	14.87	14.87	9.19	103.4	1	82.5	1
905	27.27	37.86	369	1986.4	2013.1	26.72	6.97	10.25	113.9	7	91.5	4
1201	40.50	38.90	529	1997.5	2011.7	14.15	14.15	12.64	388.3	2	358.6	2
1206	41.01	39.29	356	2007.7	2012.6	4.99	4.99	4.99	143.9	1	119.4	1
1606	29.12	40.36	301	2003.2	2013.1	9.89	9.89	6.52	169.1	1	139.6	1
1608	29.18	40.41	366	2003.2	2012.3	9.12	9.12	4.70	83.0	1	66.4	1
1609	29.17	40.43	229	2003.3	2013.0	9.75	9.75	6.68	78.9	1	59.9	1
1612	29.72	40.44	197	1999.6	2000.6	1.02	1.02	0.78	106.4	1	88.3	1
2002	29.11	37.81	356	1994.3	2012.4	18.17	18.17	13.94	165.4	2	136.5	1
2007	28.92	37.93	233	2003.3	2012.5	9.25	6.18	5.18	114.5	3	90.9	2
3102	36.16	36.21	470	1981.5	2006.1	24.64	11.68	11.27	143.1	2	122.9	2
3506	27.08	38.39	771	1977.9	2013.1	35.20	5.69	5.69	221.1	2	223.7	2
1101	29.98	40.14	901	2006.8	2011.5	4.74	4.74	4.74	87.4	1	96.2	1
4106	29.45	40.79	701	1999.6	2013.0	13.39	13.39	5.13	183.4	1	182.6	1
4107	29.93	40.76	305	1999.7	2013.0	13.32	2.65	2.65	448.7	1	444.1	1
4113	29.73	40.78	300	2010.4	2013.0	2.58	2.58	2.58	97.9	1	76.8	1
4304	29.40	38.99	343	2006.8	2012.8	6.02	6.02	3.71	98.1	3	76.9	1
4305	28.98	39.09	259	2006.8	2012.8	6.01	6.01	2.78	196.2	5	170.5	4
4306	29.25	39.34	304	2010.6	2012.8	2.22	2.22	2.20	73.7	1	56.4	1
4504	28.65	39.04	336	2006.8	2013.0	6.22	6.22	6.22	288.2	3	261.2	2
4604	36.36	37.57	611	1997.1	2012.6	15.50	15.50	15.15	265.2	2	253.9	2
4803	29.12	36.63	248	2007.5	2012.5	4.97	4.97	3.97	177.0	1	154.9	1
302	30.15	38.06	198	1995.7	2013.1	17.40	17.40	5.33	295.4	12	318.5	9
4804	28.69	36.97	372	1985.9	2008.5	22.60	22.60	11.71	108.3	2	86.0	2
5401	30.38	40.74	412	1994.5	2012.5	18.06	18.06	18.04	261.8	6	228.5	5

5402	30.62	40.67	272	2000.6	2009.3	8.73	8.73	5.51	87.4	1	67.2	1
6501	43.40	38.50	363	1995.1	2013.2	18.06	18.06	4.64	187.0	1	159.6	1
6503	43.77	38.99	293	1997.8	2012.3	14.51	14.51	1.52	174.0	2	144.6	1
1607	29.10	40.39	176	2003.2	2012.9	9.68	9.68	7.88	190.1	2	190.9	1
8101	31.15	40.84	282	1999.6	2007.1	7.47	7.47	6.12	455.6	2	466.1	2
1801	32.88	40.81	348	1977.8	2006.5	28.76	6.37	6.36	62.8	1	48.9	0
3401	29.01	41.06	595	1995.1	2010.8	15.65	15.65	15.54	50.8	1	47.3	0
502	35.85	40.67	443	1995.9	2006.9	10.99	10.99	10.99	57.8	1	46.7	0
2301	39.19	38.67	407	1995.0	2011.5	16.52	16.52	14.82	55.0	1	44.7	0
4902	42.53	39.14	311	1997.8	2012.2	14.40	14.40	1.18	55.9	1	42.1	0
907	28.47	37.91	301	2003.6	2012.5	8.92	8.92	4.15	54.8	1	40.9	0
4302	30.00	39.42	243	1998.2	2007.7	9.54	9.54	8.92	54.7	1	39.4	0
3502	27.23	38.46	270	1995.8	2007.9	12.10	12.10	12.03	54.0	1	39.4	0
1601	29.08	40.23	249	2003.3	2013.0	9.75	9.75	9.75	53.5	1	38.6	0
1006	28.00	40.33	321	2000.6	2013.0	12.38	12.38	4.90	50.4	1	37.3	0
3409	28.76	41.03	283	2010.8	2012.8	2.04	2.04	2.04	50.3	1	36.1	0
6512	43.76	38.99	293	2012.3	2013.1	0.74	0.74	0.32	0	0	0	0
4906	42.53	39.14	311	2012.5	2012.7	0.25	0.25	0.25	0	0	0	0
1007	27.94	40.34	417	2003.3	2003.5	0.24	0.24	0.24	0	0	0	0
2902	39.44	40.12	612	2011.7	2012.1	0.35	0.35	0.35	0	0	0	0
402	44.09	39.55	271	2006.0	2007.0	0.97	0.97	0.34	0	0	0	0
3801	35.50	38.69	407	2008.9	2009.0	0.17	0.17	0.17	0	0	0	0
902	27.80	37.85	271	2003.7	2004.0	0.28	0.28	0.28	0	0	0	0
5801	38.11	40.17	413	2011.7	2012.0	0.31	0.31	0.31	0	0	0	0
6004	37.33	40.39	376	2012.5	2013.0	0.50	0.50	0.50	0	0	0	0
1001	27.86	39.65	662	1997.7	2008.5	10.76	10.76	9.72	0	0	0	0
4802	27.44	37.03	747	1999.2	2008.5	9.37	9.37	9.31	0	0	0	0
1701	26.40	40.14	192	1997.4	2013.0	15.61	15.61	15.61	0	0	0	0
2501	41.26	39.90	375	1994.9	2009.1	14.19	14.19	12.73	0	0	0	0
1613	29.23	39.92	401	2006.8	2013.1	6.34	6.34	6.34	0	0	0	0
2401	39.51	39.74	314	1993.1	2011.9	18.88	18.88	13.32	0	0	0	0
1502	30.22	37.70	294	1998.2	2012.4	14.29	14.29	13.80	0	0	0	0
4401	38.34	38.35	481	1994.5	2013.0	18.52	18.52	18.50	0	0	0	0
5902	27.52	40.98	409	1994.5	2012.6	18.03	13.03	18.03	0	0	0	0
3510	27.04	38.41	313	2010.6	2013.1	2.56	2.56	2.54	0	0	0	0
3701	34.04	41.01	362	1999.4	2011.6	12.21	12.21	11.78	0	0	0	0
901	27.84	37.84	311	1998.2	2002.1	3.87	3.87	3.87	0	0	0	0
1009	28.63	39.58	561	2006.8	2013.0	6.22	6.22	6.22	0	0	0	0
4810	28.24	36.84	393	2011.3	2013.0	1.78	1.78	1.73	0	0	0	0
3503	26.89	39.07	193	2006.8	2013.0	6.22	6.22	6.15	0	0	0	0
1604	29.13	40.18	457	1997.8	2001.5	3.68	3.68	3.67	0	0	0	0
3516	26.89	38.37	460	2010.8	2013.1	2.30	2.30	2.28	0	0	0	0
3524	27.11	38.50	459	2010.9	2013.1	2.28	2.28	2.26	0	0	0	0
3511	27.26	38.42	827	2010.8	2013.1	2.30	2.30	2.30	0	0	0	0

2603	30.45	39.88	629	2006.9	2012.5	5.58	5.58	5.58	0	0	0	0
6401	29.40	38.67	285	1998.2	2012.5	14.32	14.32	13.80	0	0	0	0
3530	27.22	38.45	270	2010.3	2013.1	2.81	2.81	2.79	0	0	0	0
3523	26.77	38.33	414	2010.8	2013.1	2.30	2.30	2.28	0	0	0	0
4811	28.69	36.97	372	2012.3	2013.1	0.87	0.87	0.87	0	0	0	0
4901	41.50	38.76	315	1994.7	2012.2	17.53	17.53	6.42	0	0	0	0
3521	27.08	38.47	145	2010.9	2013.1	2.28	2.28	2.26	0	0	0	0
3520	27.21	38.48	875	2010.8	2013.0	2.20	2.20	2.20	0	0	0	0
3519	27.11	38.45	131	2010.8	2013.1	2.29	2.29	2.27	0	0	0	0
3514	27.16	38.48	836	2010.8	2013.1	2.29	2.29	2.29	0	0	0	0
3525	27.11	38.37	745	2010.8	2013.1	2.30	2.30	2.30	0	0	0	0
4501	27.38	38.61	340	1998.2	2011.4	13.21	13.21	12.03	0	0	0	0
104	35.81	37.02	223	1998.5	2011.5	13.00	13.00	3.68	0	0	0	0
1003	27.86	39.65	456	2006.8	2013.0	6.19	6.19	3.35	0	0	0	0
603	33.12	39.56	450	2008.2	2011.7	3.48	3.48	3.19	0	0	0	0
1014	27.64	40.11	397	1983.5	2013.0	29.51	6.22	3.46	0	0	0	0
3515	27.09	38.46	171	2010.8	2013.1	2.29	2.29	2.22	0	0	0	0
1208	41.05	38.97	485	1997.7	2007.2	9.45	9.45	5.90	0	0	0	0
2602	30.50	39.79	326	2006.8	2012.9	6.07	6.07	3.66	0	0	0	0
201	38.27	37.76	391	2008.0	2013.0	5.03	5.03	5.03	0	0	0	0
4606	37.14	37.39	484	2004.5	2012.9	8.35	8.35	8.16	0	0	0	0
3512	27.15	38.40	468	2011.0	2013.1	2.16	2.16	2.16	0	0	0	0
3522	27.20	38.44	249	2010.8	2013.1	2.29	2.29	2.22	0	0	0	0
3513	27.17	38.46	196	2010.8	2013.0	2.20	2.20	2.13	0	0	0	0
2606	30.50	39.75	346	2010.6	2012.9	2.26	2.26	2.26	0	0	0	0
3518	27.14	38.43	298	2010.8	2013.0	2.21	2.21	2.10	0	0	0	0
4505	28.28	38.94	629	2012.3	2012.8	0.52	0.52	0.52	0	0	0	0
2406	40.38	39.78	417	2003.3	2006.9	3.56	3.56	3.53	0	0	0	0
6001	36.56	40.33	324	1999.4	2013.2	13.80	13.80	13.80	0	0	0	0
4506	28.12	38.48	273	2007.9	2012.6	4.75	4.75	4.75	0	0	0	0
904	28.05	37.86	367	2003.3	2007.3	4.04	4.04	3.79	0	0	0	0
908	28.34	37.91	267	2003.3	2008.0	4.75	4.75	4.75	0	0	0	0
4301	29.99	39.43	267	2006.8	2012.3	5.53	5.53	5.53	0	0	0	0
909	28.15	37.88	355	2003.3	2012.6	9.32	9.32	9.06	0	0	0	0
1615	29.29	40.42	349	2003.2	2011.4	8.17	8.17	8.17	0	0	0	0
8002	36.56	37.19	430	2010.9	2012.9	2.07	2.07	2.07	0	0	0	0
4111	29.59	40.68	300	2010.4	2013.0	2.65	2.65	2.65	0	0	0	0
4105	29.97	40.67	289	2008.2	2012.5	4.32	4.32	4.32	0	0	0	0
2601	30.53	39.81	231	2006.8	2011.5	4.73	4.73	3.51	0	0	0	0
2404	38.77	39.91	413	2011.7	2012.9	1.22	1.22	1.22	0	0	0	0
4801	28.36	37.21	468	2007.8	2012.7	4.84	4.84	2.76	0	0	0	0
309	31.24	38.53	387	2007.3	2012.5	5.22	5.22	5.22	0	0	0	0
910	27.80	37.85	271	2010.8	2012.5	1.76	1.76	1.76	0	0	0	0
4603	36.93	37.58	466	1995.3	2004.2	8.92	8.92	8.92	0	0	0	0

1005	26.69	39.31	387	2006.8	2013.0	6.22	6.22	6.22	0	0	0	0
4112	29.84	40.72	352	2010.4	2013.0	2.65	2.65	2.65	0	0	0	0
208	37.65	37.79	469	2011.2	2013.0	1.78	1.78	1.78	0	0	0	0
2701	36.64	37.03	421	1994.0	2012.7	18.71	18.71	7.27	0	0	0	0
4502	27.82	38.91	292	2007.6	2012.9	5.30	5.30	1.23	0	0	0	0
2405	40.39	39.78	320	1992.2	2003.1	10.87	10.87	5.87	0	0	0	0
4608	36.84	37.38	390	2006.3	2012.9	6.56	6.56	6.56	0	0	0	0
2607	30.15	39.82	274	2006.8	2011.4	4.58	4.58	4.58	0	0	0	0
1616	29.26	40.45	572	2004.4	2011.4	7.01	7.01	5.10	0	0	0	0
1603	29.13	40.18	457	2006.8	2013.0	6.22	6.22	6.22	0	0	0	0
4605	37.20	38.20	315	1996.9	2001.5	4.63	4.63	4.63	0	0	0	0
2307	39.93	38.70	329	2011.4	2013.1	1.72	1.72	1.72	0	0	0	0
2604	30.51	39.77	296	2006.8	2012.3	5.54	5.54	1.04	0	0	0	0
5904	27.12	40.61	225	2012.2	2013.0	0.83	0.83	0.83	0	0	0	0
4607	37.30	37.49	671	2006.3	2012.9	6.60	6.60	6.60	0	0	0	0
4403	37.89	38.10	654	1996.8	2007.0	10.15	10.15	10.15	0	0	0	0
3105	36.51	36.80	618	2004.6	2012.9	8.28	8.28	8.28	0	0	0	0
1301	42.28	38.50	273	1997.4	2011.8	14.39	14.39	2.02	0	0	0	0
3109	36.41	36.58	272	2004.6	2012.9	8.28	8.28	3.09	0	0	0	0
1904	34.94	40.55	193	2008.8	2012.9	4.11	4.11	2.63	0	0	0	0
4104	29.97	40.68	757	2010.7	2012.5	1.77	1.77	1.77	0	0	0	0
4110	30.15	41.07	380	2010.4	2012.5	2.14	2.14	2.14	0	0	0	0
1614	28.39	40.03	265	2006.8	2012.3	5.54	5.54	5.54	0	0	0	0
1610	29.51	40.07	252	2012.3	2013.0	0.73	0.73	0.73	0	0	0	0
1013	27.02	39.59	223	1983.5	2013.0	29.51	29.51	5.17	0	0	0	0
6301	38.80	37.17	652	2008.5	2010.7	2.20	2.20	2.20	0	0	0	0
4601	36.98	37.54	346	2004.5	2012.9	8.41	8.41	5.00	0	0	0	0
703	30.15	36.30	299	2000.8	2012.4	11.63	11.63	11.63	0	0	0	0
604	33.52	38.96	291	2008.2	2011.4	3.20	3.20	3.20	0	0	0	0
2703	37.35	37.06	758	2008.7	2012.8	4.12	4.12	4.12	0	0	0	0
3104	36.49	36.69	688	2004.6	2012.9	8.28	8.28	8.28	0	0	0	0
3101	36.16	36.21	470	2006.1	2013.1	6.97	6.97	2.35	0	0	0	0
4102	30.03	40.78	1013	2010.7	2013.0	2.27	2.27	2.27	0	0	0	0
2702	36.73	37.18	599	2007.6	2013.1	5.47	5.47	4.91	0	0	0	0
1102	30.05	39.90	407	2006.8	2011.5	4.73	4.73	4.73	0	0	0	0
7701	29.31	40.56	375	2004.4	2013.0	8.65	8.65	8.65	0	0	0	0
4701	40.72	37.33	709	2008.7	2012.6	3.93	3.93	3.93	0	0	0	0
1605	29.10	40.27	495	2003.2	2012.5	9.25	9.25	5.72	0	0	0	0
3111	36.22	36.37	338	2005.6	2012.7	7.15	7.15	2.77	0	0	0	0
3107	36.18	36.58	310	2004.5	2012.7	8.18	8.18	1.53	0	0	0	0
7801	32.62	41.20	703	2000.1	2001.7	1.53	1.53	1.53	0	0	0	0
1211	41.05	38.97	463	2011.8	2012.7	0.93	0.93	0.93	0	0	0	0
7702	29.27	40.59	359	2004.8	2011.4	6.61	6.61	4.90	0	0	0	0
8001	36.27	37.08	350	2005.1	2012.9	7.86	7.86	1.31	0	0	0	0

1703	27.26	40.23	304	2012.3	2013.0	0.74	0.74	0.74	0	0	0	0
1710	26.67	40.42	286	2012.4	2013.0	0.64	0.64	0.64	0	0	0	0
2302	39.68	38.39	907	2011.5	2012.7	1.19	1.19	1.19	0	0	0	0
1017	27.86	39.65	662	2012.2	2013.0	0.83	0.83	0.83	0	0	0	0
7201	41.15	37.87	450	2010.2	2012.5	2.27	2.27	2.27	0	0	0	0
1505	29.78	37.32	367	2012.4	2013.0	0.57	0.57	0.57	0	0	0	0
1611	29.72	40.43	251	2004.4	2013.0	8.65	8.65	0.68	0	0	0	0
1617	29.30	40.49	1598	2004.4	2013.0	8.65	8.65	1.99	0	0	0	0
4404	38.52	38.12	1380	2011.5	2012.4	0.92	0.92	0.92	0	0	0	0
2901	39.50	40.45	469	2010.2	2011.6	1.40	1.40	1.40	0	0	0	0
3501	27.17	38.46	196	1992.8	1995.1	2.24	2.24	0.69	0	0	0	0
4103	30.03	40.79	1013	2008.2	2012.5	4.32	4.32	4.32	0	0	0	0
3408	28.26	41.07	639	2010.8	2013.0	2.26	2.26	1.03	0	0	0	0
2608	31.18	39.52	476	2008.0	2011.4	3.42	3.42	3.42	0	0	0	0
2507	42.17	40.04	316	2012.0	2013.1	1.10	1.10	1.10	0	0	0	0
506	35.80	40.64	284	2010.8	2013.2	2.41	2.41	2.41	0	0	0	0
118	35.19	37.02	946	2008.0	2011.5	3.46	3.46	3.46	0	0	0	0
3108	36.37	36.50	539	2008.3	2012.9	4.53	4.53	4.53	0	0	0	0
3103	36.25	36.12	344	2006.1	2008.3	2.20	2.20	2.20	0	0	0	0
401	43.02	39.72	295	2007.1	2011.8	4.76	4.76	4.76	0	0	0	0
1903	34.80	40.98	255	2011.7	2012.2	0.52	0.52	0.52	0	0	0	0
7704	29.25	40.66	195	2008.2	2013.0	4.82	4.82	1.97	0	0	0	0
4001	34.16	39.16	460	2008.7	2012.8	4.03	4.03	4.03	0	0	0	0
3110	35.95	36.08	210	2004.3	2008.3	3.99	3.99	3.99	0	0	0	0
6005	36.57	40.70	327	2010.9	2013.2	2.32	2.32	2.32	0	0	0	0
7703	29.28	40.65	278	2010.4	2012.3	1.90	1.90	1.90	0	0	0	0
2101	40.20	37.93	519	2010.2	2010.7	0.53	0.53	0.53	0	0	0	0
6901	40.21	40.26	519	2011.0	2011.8	0.82	0.82	0.82	0	0	0	0
801	41.84	41.18	350	2011.1	2013.0	1.94	1.94	1.94	0	0	0	0
3601	43.08	40.60	270	1995.8	1997.8	2.10	2.10	2.10	0	0	0	0
7601	44.05	39.93	216	1998.1	1998.7	0.67	0.67	0.67	0	0	0	0
6801	34.03	38.35	208	2008.9	2011.5	2.59	2.59	2.59	0	0	0	0

* The maximum observed PGA levels at stations that have not seen an exceedance of 50 cm/s^2 are shown as zero in this table since their data are not processed.

Lat & Lon : Latitude and longitude in degrees.

T_{OBS}: The observation length calculated as the time difference between the most recent and the most ancient observations at the station

$T_{OBS\text{-}GAP1}$: The observation time window calculated considering the gaps identified using the inter-event times (method 1)

$T_{OBS\text{-}GAP2}$: The observation time window calculated considering the gaps identified using the missing synthetic data with $PGA_{MEDIAN} \geq 10$ (method 2)

PGA_{SITE}: PGA observed at the local site condition of the site

PGA_{750}: PGA at V_{S30}=750m/s calculated dividing the PGA_{SITE} by the amplification calculated (see text for further information)

TINI : date of first observation at the stations (considering all level of accelerations observed)

TFINI: date of last observation at the stations (considering all level of accelerations observed)

We found 21 records with $PGA_{MEDIAN} \geq 50$ cm/s^2 in the synthetic data that are missing in the accelerometric dataset. One of the missing records occurred during a gap previously identified in method 1 (method based on interevent times). Twenty missing synthetic records with $PGA_{MEDIAN} \geq 50$ cm/s^2 occurred outside the gaps identified in section 3.5.1. In the accelerometric database, there are 100 records with $PGA_{SITE} \geq 50$ cm/s^2 (geometric mean) recorded at 204 stations. The fraction of missing data in the dataset for accelerations higher than 50 cm/s^2 is thus 20% (20/100) when the observation time period obtained deducing the gaps in the first method is used.

The synthetic data is generated at the location of selected accelerometric stations and during the same time interval as in the acceleration database. We compute the synthetic acceleration using also the V_{S30} =750m/s (PGA_{750} in Table 2) to evaluate the amount of missing records in the data used for testing (dataset of PGA_{750}). Only eight missing records out of 20 have a median PGA_{750} (predicted for V_{S30}=750m/s) higher than 50 cm/s^2. Considering the 69 observations with $PGA_{750} \geq 50$ cm/s^2 in the accelerometric dataset observed at 204 sites, the ratio of missing records in the dataset used for testing (dataset of PGA_{750}) is 8/69=12%.

In our study, we will test the PSHA model also using the observation time windows obtained deducing the gaps detected in the second method to take into consideration the missing records.

Table 2: The synthetic records (predicted using earthquake catalog and a GMPE) that are not observed at sites considered (at local site conditions) and that occurred outside the observation gaps

Earthquake Date	Earthquake Time	Station ID	Lat (°)	Lon (°)	V_{S30} (m/s)	Median predicted PGA_{SITE} (cm/s^2)	Median Predicted PGA_{750} (cm/s^2)	Main Shock	Lat (°)	Lon(°)	Depth	M_W
10/23/11	10:41:41	6501	38.5	43.4	363	151.9	119.5	1	38.75	43.4	5	7
2/17/09	5:28:28	4305	39.09	28.98	259	151.8	105.5	1	39.11	29	8	5.3
5/19/11	21:12:12	4305	39.09	28.98	259	108.9	67.8	0	39.11	29	6	4.9
8/17/99	0:16:16	4101	40.77	29.92	826	101.1	104.7	0	40.78	29.9	10	5.3
5/19/11	21:21:21	4305	39.09	28.98	259	99.4	60.9	0	39.11	29	5	4.9
12/4/09	6:02:02	903	37.97	28.75	390	97.4	75.2	1	37.92	28.8	4	5.4
11/12/99	0:00:00	1404	40.4	30.78	348	83.6	60.7	1	40.8	31.2	10	7.2
8/31/99	8:10:10	4101	40.77	29.92	826	83.4	86.4	0	40.76	29.9	4	5.1
10/20/03	6:27:27	6503	38.99	43.77	293	67.3	44.4	1	38.91	43.7	9	5.2
10/1/95	22:21:21	302	38.06	30.15	198	66	30.9	0	38.08	30.1	34	4.5
6/18/02	14:58:58	2401	39.74	39.51	314	65	44.6	1	39.72	39.5	10	4.6
6/5/06	4:23:23	903	37.97	28.75	390	62.7	47.3	1	37.94	28.7	7	4.9

8/17/99	9:02:02	8101	40.84	31.15	282	61.2	38.9	0	40.81	31.1	10	4.7
8/23/98	8:18:18	4902	39.14	42.53	311	58.7	40	1	39.1	42.5	25	4.7
3/2/10	0:43:43	4305	39.09	28.98	259	56.1	33.2	1	39.16	29	8	4.8
11/12/99	21:38:38	8101	40.84	31.15	282	54.2	34.4	0	40.84	31.1	11	4.5
10/23/11	20:45:45	6501	38.5	43.4	363	53.1	38.7	0	38.63	43.1	8	6
10/20/03	6:27:27	6503	38.99	43.77	293	51.3	33.6	0	38.91	43.7	9	5
10/24/06	14:00:00	1605	40.27	29.1	495	51	42.6	1	40.42	29	14	5.5
8/17/99	4:20:20	5401	40.74	30.38	412	50.9	39.2	0	40.69	30.4	13	4.7

Station ID: The identity number of the station given by TR-NSMN.
V_{S30}: Average shear wave velocity at the upper 30m depth of soil below the surface.
Median PGA: The median PGA value predicted using AC2010 GMPE
M_W: Moment magnitude

3.6 Testing the SHARE Hazard Model

3.6.1 Testing SHARE model using accelerometric data

At the selected stations (Table 1), there are 56 observations with $PGA_{750} \geq 50$ cm/s^2. We first test the SHARE-PSHA model at 137 sites that satisfy a minimum inter-site distance of R_{MIN}=10 km. The SHARE-PSHA is provided for accelerations ranging between 52.7 cm/s^2 and 3450 cm/s^2. The PSHA model is tested at the acceleration levels 52.7, 73.8, 103, 145, 203, 284, 397, 556 and 778 cm/s^2 given by the model, so that no interpolation of the model is needed. We do not consider accelerations higher than 778 cm/s^2 since there is no observed exceedance above this acceleration level. Only the median predicted hazard curve obtained from the logic tree of SHARE-PSHA is used. A Monte Carlo sampling is used to obtain the distribution of predicted exceedances over the observation lifetime of the stations (see section 2.2 of second chapter). Ten thousand accelerometric catalogs are simulated to obtain stable results. The hazard model is evaluated considering different lifetimes of stations; 1) the original/uncorrected lifetime (T_{OBS}), 2) the corrected lifetime ($T_{OBS\text{-}GAP1}$) deducing the gaps identified using inter-event times (see section 3.5.1), and 3) the corrected lifetimes ($T_{OBS\text{-}GAP2}$) deducing the gaps identified using missing data (see section 3.5.2).

Table 3: 56 observations with $PGA_{750} \geq 50$ cm/s^2 observed at the accelerometric stations listed in Table 1 .

Record ID (yyyymmddhhmmss)	M_W	EQ Lat (°)	EQ Lat (°)	EQ Depth (km)	Style of Faulting	Station ID	R_{EPI} (km)	PGA_{750} (cm/s^2)	PGA_{SITE} (cm/s^2)	Main shock
19771209155338	5.1	38.35	27.23	26.9	Strike-Slip	3506	13.4	115.5	114.2	0
19771216073729	5.6	38.39	27.19	4.0	Normal	3506	9.0	223.7	221.1	1
19810630075909	4.7	36.17	35.89	63.0	Normal	3102	25.0	111.4	130.4	1
19851206223530	5.1	36.97	28.85	8.9	Strike-Slip	4804	14.7	86.8	108.3	1
19860601064310	4.2	37.96	27.39	10.0	Strike-Slip	905	15.5	50.4	64.7	1
19921106190809	6.0	38.09	27.05	15.0	Strike-Slip	905	41.0	59.3	75.7	1
19941113065601	5.3	36.91	29.05	10.0	Normal	4804	33.0	64.0	81.2	1
19950314000651	4.1	37.88	29.07	5.0	Normal	2002	8.7	136.5	165.4	1
19950926145809	4.9	38.03	30.17	18.8	Strike-Slip	302	3.3	119.8	138.0	0
19950927141554	5.0	38.07	30.20	11.3	Strike-Slip	302	4.1	102.5	122.0	0
19951001155713	6.5	38.12	30.11	10.0	Normal	302	8.0	318.5	295.4	1
19951001180256	5.3	38.05	30.16	28.4	Strike-Slip	302	1.7	137.2	153.6	0
19951001211442	4.4	38.00	30.08	16.8	Strike-Slip	302	8.9	102.7	122.2	0
19951003073811	4.9	37.97	30.08	11.0	Strike-Slip	302	11.9	79.8	99.7	0
19951005161521	5.0	38.00	30.14	11.8	Strike-Slip	302	6.7	93.8	113.7	0
19951006161558	4.8	38.03	30.14	34.5	Strike-Slip	302	3.6	106.6	125.8	0
19970122175720	5.7	36.21	35.97	20.0	Normal	3102	20.0	122.9	143.1	1
19980404161747	5.2	38.1	30.1	19.3	Normal	302	4.0	112.9	131.7	1
19990817000139	7.6	40.76	29.96	17.0	Strike-Slip	1612	40.0	88.3	106.4	1
19990817000139	7.6	40.76	29.96	17.0	Strike-Slip	4106	43.0	182.6	183.4	1
19990817000139	7.6	40.76	29.96	17.0	Strike-Slip	8101	101.0	322.2	337.4	1
19990913115529	5.8	40.76	30.05	15.0	Strike-Slip	4107	5.0	444.1	448.7	1
19991111144127	5.6	40.79	30.22	14.3	Strike-Slip	5401	11.0	228.5	261.8	0
19991112165721	7.1	40.82	31.20	11.2	Strike-Slip	8101	5.0	466.1	455.6	1
20000402185742	4.5	40.86	30.29	8.8	Strike-Slip	5401	16.0	62.1	76.8	0
20000823134129	5.5	40.68	30.72	15.0	Strike-Slip	5402	8.0	67.2	87.4	1
20020203071129	6.5	38.58	31.16	10.0	Normal	301	68.0	80.9	103.4	1
20021214010248	4.8	37.52	36.20	10.0	Normal	4604	15.0	57.3	62.0	1
20030501002708	6.3	38.95	40.40	15.0	Strike-Slip	1201	14.0	358.6	388.3	1
20030501093555	4.1	38.87	40.54	9.1	Strike-Slip	1201	5.0	83.0	94.3	0
20030723045609	5.3	38.05	28.89	28.3	Normal	2007	13.0	82.7	105.7	0
20030726083654	5.4	38.06	28.91	21.3	Normal	2007	14.0	90.9	114.5	1
20060208040743	4.5	40.71	30.41	6.8	Normal	5401	4.0	109.6	132.2	1
20060208052427	4.1	40.71	30.38	4.1	Strike-Slip	5401	3.3	63.1	78.0	0
20061024140025	5.2	40.42	28.99	7.9	Normal	1609	15.0	59.9	78.9	1
20061024140026	5.2	40.42	28.99	7.9	Normal	1608	16.0	66.4	83.0	1
20061024140038	5.2	40.42	28.99	7.9	Normal	1606	13.0	139.6	169.1	1
20061024140041	5.2	40.42	28.99	7.9	Normal	1607	9.0	190.9	190.1	1
20070825220536	5.3	39.29	41.03	15.8	Strike-Slip	1206	2.0	119.4	143.9	1
20090217052819	5.2	39.13	29.05	15.5	Normal	4504	37.0	63.9	82.9	1

20101111200800	5.0	37.86	27.37	14.0	Normal	905	10.0	79.3	99.6	1
20101208215052	3.4	37.83	27.36	13.5	Strike-Slip	905	26.0	91.5	113.9	0
20110120020936	4.2	40.73	29.77	12.5	Strike-Slip	4113	6.0	76.8	97.9	1
20110519201522	5.9	39.14	29.08	12.0	Normal	4304	32.0	76.9	98.1	1
20110519201522	5.9	39.14	29.08	12.0	Normal	4306	26.0	56.4	73.7	1
20110519201522	5.9	39.14	29.08	12.0	Normal	4504	39.0	261.2	288.2	1
20110524025528	3.7	39.10	28.96	5.0	Strike-Slip	4305	2.0	63.5	84.7	0
20110528054717	5.1	39.12	29.05	9.2	Normal	4305	7.0	75.0	98.0	0
20110627211358	5.0	39.11	29.03	10.4	Normal	4305	5.0	80.1	103.7	0
20110711160912	4.5	40.25	29.95	5.0	Normal	1101	12.0	96.2	87.4	1
20111023104120	7.1	38.75	43.46	16.0	Reverse	6503	38.0	144.6	174.0	1
20111109192333	5.6	38.43	43.23	8.0	Strike-Slip	6501	17.0	159.6	187.0	0
20120503152025	5.3	39.18	29.09	3.1	Normal	4305	13.0	170.5	196.2	1
20120610124415	6.1	36.34	28.67	40.0	Strike-Slip	4803	52.0	154.9	177.0	1
20120707070745	4.2	40.82	30.41	6.6	Strike-Slip	5401	9.6	53.3	66.3	1
20120722092602	4.8	37.55	36.38	7.6	Normal	4604	4.0	253.9	265.2	1

EQ Lat & EQ Lon : Latitude and longitude of earthquake in degrees.
EQ Depth: Depth of the earthquake in kilometers.
PGA_{SITE}: Observed PGA given by TR-NSMN
PGA_{750}: PGA at V_{S30}=750m/s calculated dividing the PGA_{SITE} by the amplification calculated (see text for further information)
Main shock is 1 if the earthquake is a main shock; Main shock is 0 is the earthquake is a dependent event.

In SHARE-PSHA it is assumed that the occurrence of exceedances follows a Poisson process. Therefore the accelerometric data used for testing should be declustered to remove dependent events. In this chapter, we test the influence of dependent events in the dataset. We compare the results by 1) considering only the observations from mainshocks (see the last column of Table 3) and also 2) considering all observations without declustering.

The results are displayed in two different ways in Figure 3.14; 1) the comparison of predicted and observed number of exceedances (left column of Figure 3.14) and 2) the comparison of the predicted and observed number of sites with exceedances (right column of Figure 3.14). For acceleration levels higher than or equal to 103 cm/s^2, observations are consistent with the prediction of SHARE-PSHA (within the 2.5 and 97.5 percentiles of predicted distribution, see section 2.2 of second chapter). There are no observed exceedances at accelerations higher than 556 cm/s^2. For the smallest acceleration levels considered (between 52.7 and 103 cm/s^2), the coherency between the PSHA model and the observations varies depending on whether the gaps are considered and how they are calculated. When gaps are identified using inter-event times and deduced from original lifetimes (lifetimes corrected using the first method), the model predicts more than observed exceedances between 52.7 cm/s^2 and 73.8 cm/s^2. When gaps are identified using missing data (lifetimes corrected using

the second method), the predicted number of exceedance is lower and the model is consistent with the observations for all levels of accelerations except at 52.7 cm/s^2, where the observed number of exceedances is smaller than predicted. The results obtained using original lifetimes are shown in Figure 3.13 to illustrate the influence of lifetime corrections. We think that the original observation lifetimes contain many gaps and that the actual observation lifetimes are somewhere between the corrected lifetimes from the first and the second method.

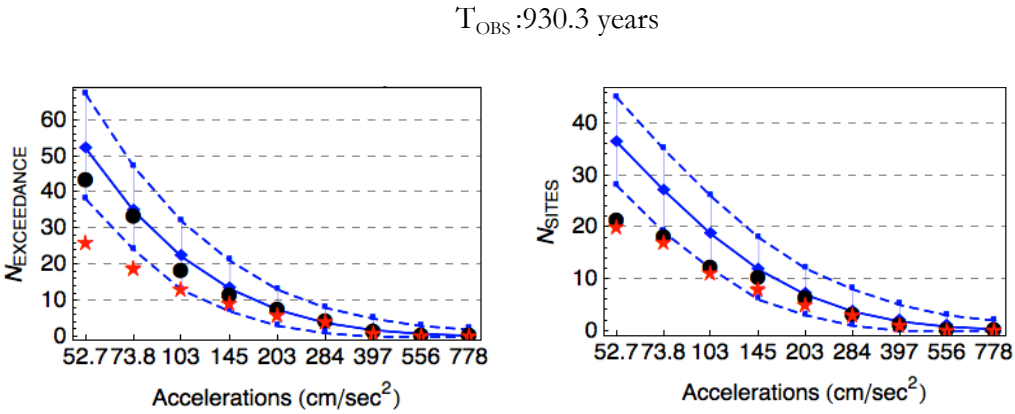

Figure 3.13: Comparison of the observed and predicted number of exceedances at different acceleration levels considering original observation lifetimes at 137 stations with minimum inter-site distance of 10 km. Left: the comparison based on the number of exceedances at sites considered, Right: the comparison based on the number of sites with exceedance. Blue curves: median and percentiles 2.5 and 97.5 of the predicted distributions (see section 2.2 of second chapter), black circles: observed exceedances considering all records (including foreshocks/aftershocks), red stars: observed exceedances considering only records of mainshocks.

As can be seen in Figure 3.14, the total number of exceedance N_{EXC} is sensitive to the clustering in the dataset used for testing, whereas the results based on the total number of sites with exceedance N_{SITES} is not modified. Considering the number of exceedances gives significantly different results when foreshocks and aftershocks are included. Considering the number of sites with exceedance N_{SITES}, only the maximum acceleration observed at a site matters, and this acceleration is usually produced by a mainshock. The results based on N_{SITES} are consistent with the results obtained using N_{EXC} when only independent observations (mainshocks) are considered. Therefore, further in this study, we will display only the results based on the number of sites with exceedance (N_{SITES}).

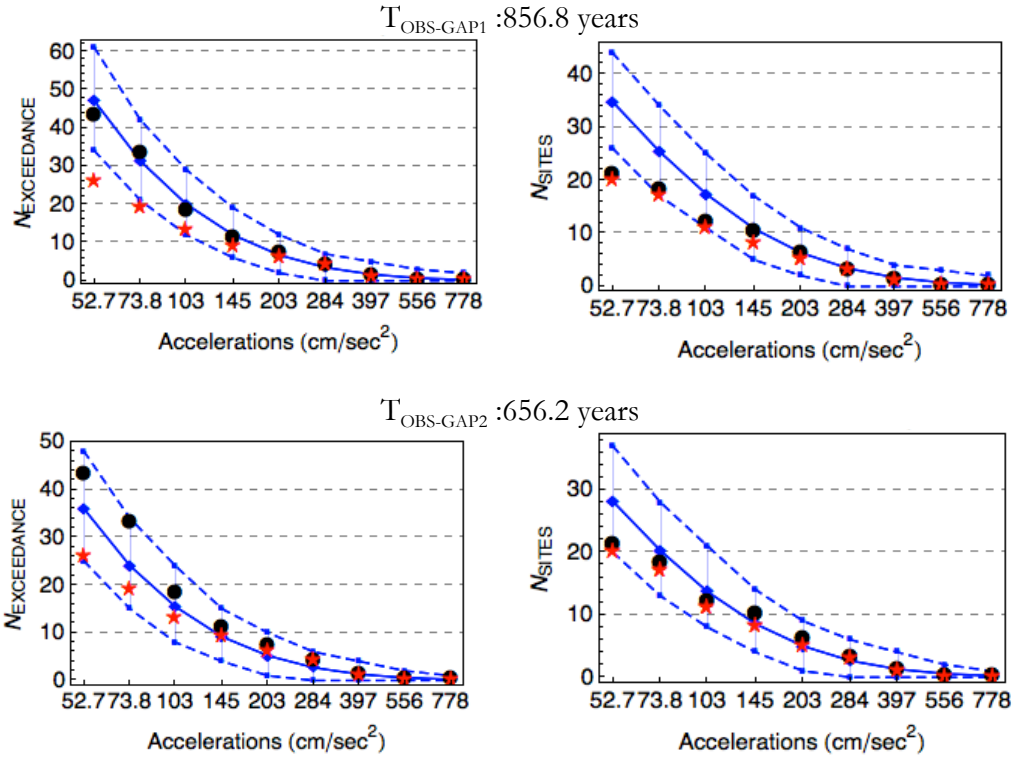

Figure 3.14: Comparison of the observed and predicted number of exceedances at different acceleration levels using 137 stations with a minimum inter-site distance of 10 km. Left column: the comparison based on the number of exceedances at sites considered, Right column: the comparison based on the number of sites with exceedance. The results are obtained considering corrected lifetimes, with gaps obtained using inter-event times (top, $T_{OBS-GAP1}$) and using missing records (bottom, $T_{OBS-GAP2}$). Blue curves: median and percentiles 2.5 and 97.5 of the predicted distributions (see section 2.2 of second chapter), black circles: observed exceedances considering all records (including foreshocks/aftershocks), red stars: observed exceedances considering records of mainshocks only.

The testing methodology assumes independent events. Therefore, the list of earthquakes responsible for exceedances has been systematically checked in order to remove multiple records of the same earthquake at different stations. Figure 3.15 shows the magnitudes and source-to-site distances of all earthquakes (mainshocks) causing exceedances at selected sites. When two records at two stations are produced by the same earthquake, we simply discard the site with the lowest acceleration.

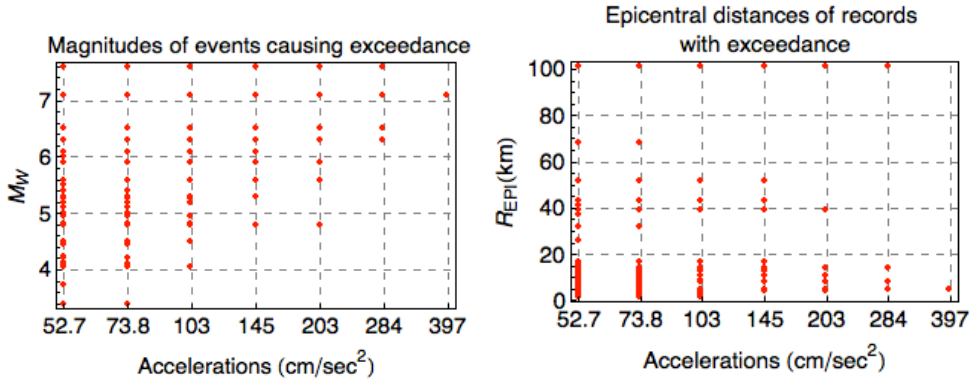

Figure 3.15: (a) Magnitudes of all earthquakes causing ground motions stronger than the accelerations (from mainshocks only) selected for testing. (b) Epicentral distances.

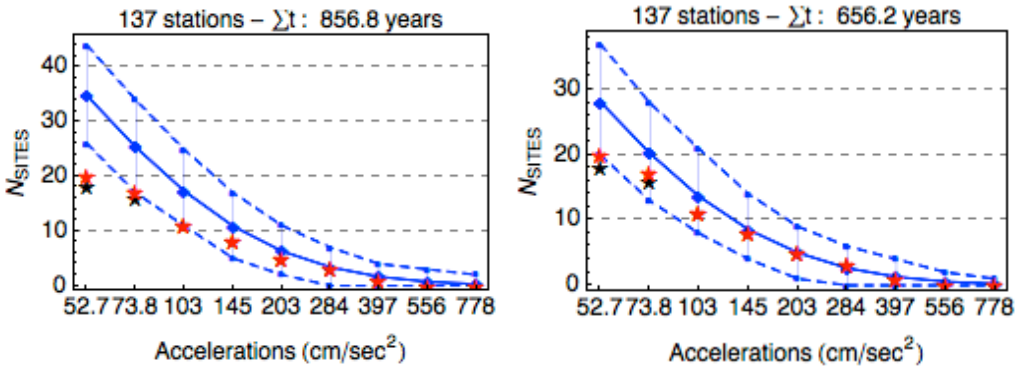

Figure 3.16: Comparison of the observed and predicted number of exceedances at different acceleration levels using 137 stations with a minimum inter-site distance of 10 km and using corrected lifetimes. Gaps are identified using inter-event times (Left, $T_{OBS\text{-}GAP1}$) and missing records (Right, $T_{OBS\text{-}GAP2}$). Blue curves: median and percentiles 2.5 and 97.5 of the predicted distributions (see section 2.2 of second chapter). Red stars: observed exceedances considering records of mainshocks only. Black stars indicate the reduced number of sites in the case of double-counting.

The results considering the double-counting are shown in Figure 3.16. Discarding sites to ensure independence of sites brings minor changes to the results and does not change the conclusions.

3.6.1.1 Considering the uncertainty of site amplification equation

We used a nonlinear site amplification equation to convert the ground shakings observed at the stations into a ground motion observed at a site with V_{S30}=750 m/s. In the previous sections, we used the median amplification values given by Sandikkaya *et al.* (2013) to

calculate PGA_{750} (Table 3). Sandikkaya *et al.* (2013) also provided the standard deviation σ=0.8142 of the natural logarithm of amplification, Ln(Amp), for V_{REF}=750 m/s

This high value of standard deviation provided by Sandikkaya *et al.* (2013) causes a big difference in calculated PGA_{ROCK} values. In some cases the calculated values may be unrealistic. For example, if we consider that the observed acceleration (PGA_{SITE}) is 110 cm/s^2 at a site with V_{S30}=450 m/s, the amplification for this case is 1.1. The PGA_{750} is equal to 100 cm/s^2 (see Equation 3.3). If σ=0.8142, the amplification ranges between 2.45 and 0.5 at median-σ and at median+σ respectively. Thus PGA_{750} varies between 45 (median-σ) and 220 cm/s^2 (median+σ) if we sample the Ln(Amp) between $\pm1\sigma$. However if the site conditions were stiffer, the ground motion should be smaller. In this case, the PGA_{750} is expected to be smaller than 110 cm/s^2, which is the observed PGA at V_{S30} of 450 m/s.

The site amplification equation of Sandikkaya *et al.* (2013) relies on a large amount of data from many regions of the world (5530 records from Greece, Italy, Turkey, Taiwan, Japan and California). The standard deviation σ represents the variability of the amplification considering all data including different V_{S30} values, different source-to-site distances, different magnitudes and different regions, etc… Therefore, the value σ=0.8142 given by Sandikkaya *et al.* (2013) is very high to cover the uncertainty of all cases (personal communication with A. Sandikkaya). The value σ=0.8142 is very high compared with other values given by Papaspiliou *et al.* (2012). This study analyzed the sensitivity of σ for different cases; depending on the analyses used to establish a nonlinear site amplification function, 2) depending on the site conditions, and 3) depending on the spectral periods. Papaspiliou *et al.* (2012) found that σ did not exceed 0.3 for any of the considered case. In this section, we test different values of the standard deviation of Ln(Amp) for evaluating the SHARE-PSHA, considering both σ =0.8142 and σ =0.3 (Figure 3.17).

To check the influence of the variability of Ln(Amp), we sampled the distribution of Ln(Amp) following these steps:

1) We assume that possible values of Ln(Amp) follow a normal distribution with a mean value Ln(Amp) and a standard deviation σ =0.8142 or σ =0.3.
2) A random value of Ln(Amp) is taken following a log-normal probability distribution sampled between $\pm1\sigma$.

3) The PGA_{750} value is calculated dividing PGA_{SITE} by the random value of Ln(Amp) obtained from step 2.
4) The previous steps are repeated for all observations given in Table 3.
5) We evaluate the coherency between the SHARE-PSHA and the dataset of calculated PGA_{750} values.
6) 10000 cases are simulated to capture the variability of PGA_{ROCK} due to uncertainty of Ln(Amp).

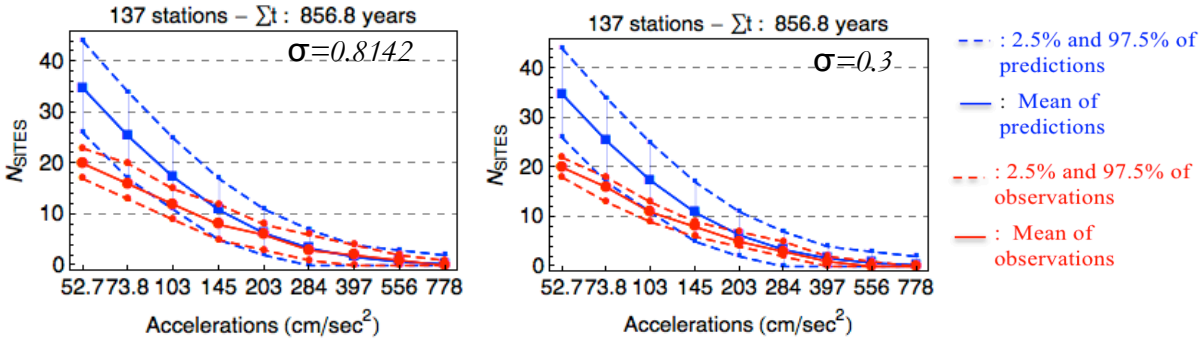

Figure 3.17: Comparison of the observed and predicted number of sites with exceedance at different acceleration levels, considering 137 stations with minimum inter-site distance of 10 km. The uncertainties in PGA_{ROCK} introduced using a site-amplification equation are represented as a probability distribution. The standard deviation is taken as (left) σ=0.8142 as given in Sandikkaya *et al.* (2013), (right) σ=0.3 as given in Papaspiliou *et al.* (2012). Only the results obtained considering corrected lifetimes deducing the gaps identified in first method are shown as an example.

The results considering the uncertainty of Ln(Amp) are displayed in Figure 3.17 (only for the lifetimes corrected using 1st method). As expected, the distribution of observed exceedances is wider when σ=0.8142 than for σ=0.3. Note that N_{SITES} does not have the same standard deviation as Ln(Amp) because the standard deviation of N_{SITES} is not directly proportional to σ. The mean of N_{SITES} is the same as when neglecting the uncertainty on Amp (σ = 0) (Figure 3.14, 2nd raw, right). The effect of σ on the testing results are also checked using the corrected lifetimes of stations ($T_{OBS\text{-}GAP1}$ and $T_{OBS\text{-}GAP2}$). For all cases, the conclusions on the coherency between predictions and observations do not change when the uncertainty of amplification is considered (for σ between 0 and 0.8142). The mean of the observed number of exceedances fall within the bounds of the predicted distribution at accelerations higher than 103 cm/s^2. For the accelerations between 52.7 and 73.8 cm/s^2, the results obtained using T_{OBS}

and $T_{OBS\text{-}GAP1}$ indicate that the model over-predicts the observed hazard, whereas when using $T_{OBS\text{-}GAP2}$ the model is consistent with the observations.

3.6.1.2 Effect of minimum inter-site distance selection on testing results

The testing method assumes independent observations. Therefore we imposed a minimum inter-site distance to weaken the correlation between sites. In the previous sections, we used a minimum inter-site distance R_{MIN}=10 km. In this section, we will test the influence of this parameter by testing other values, R_{MIN}=0 and R_{MIN}=60 km. There are 137 stations with R_{MIN}=10 km, 189 stations with R_{MIN}=0 and 49 stations with R_{MIN}=60 km.

The results for R_{MIN}=10 km are shown in Figure 3.14 and the results for R_{MIN}=0 and R_{MIN}=60 km in Figure 3.18 (see Figure 3.19 for the location of sites). In all cases, the observations fall within the bounds of the predictions for accelerations equal to or higher than 103 cm/s^2 when using corrected lifetimes. For acceleration smaller than 103 cm/s^2, the coherency between the observations and the predictions increases when increasing R_{MIN} (decreasing the number of stations). At 52.7 cm/s^2, the model predicts more than observed N_{SITES} for both estimates of corrected lifetimes ($T_{OBS\text{-}GAP1}$ and $T_{OBS\text{-}GAP2}$) for R_{MIN}=0, whereas the model is consistent with the observations for R_{MIN}=60km and when using $T_{OBS\text{-}GAP2}$. At 73.8 cm/s^2, the model is consistent with the observations for R_{MIN}=60 km and for both estimates of the corrected lifetimes. At and above 103 cm/s^2, the model is consistent with the observations for all values of R_{MIN}=60 km and for all estimates of corrected lifetimes. At and above 397 cm/s^2, the results rely on no observed exceedance but the model cannot be rejected. We have to keep in mind that increasing the inter-site distance to ensure the independency of sites results in using fewer stations for evaluating PSHA models. When fewer stations are used, we exploit shorter observations periods for testing and thus the model is more difficult to reject (larger uncertainty on the predicted rate of exceedances). On the other hand, selecting large inter-site distances ensures the independency of sites.

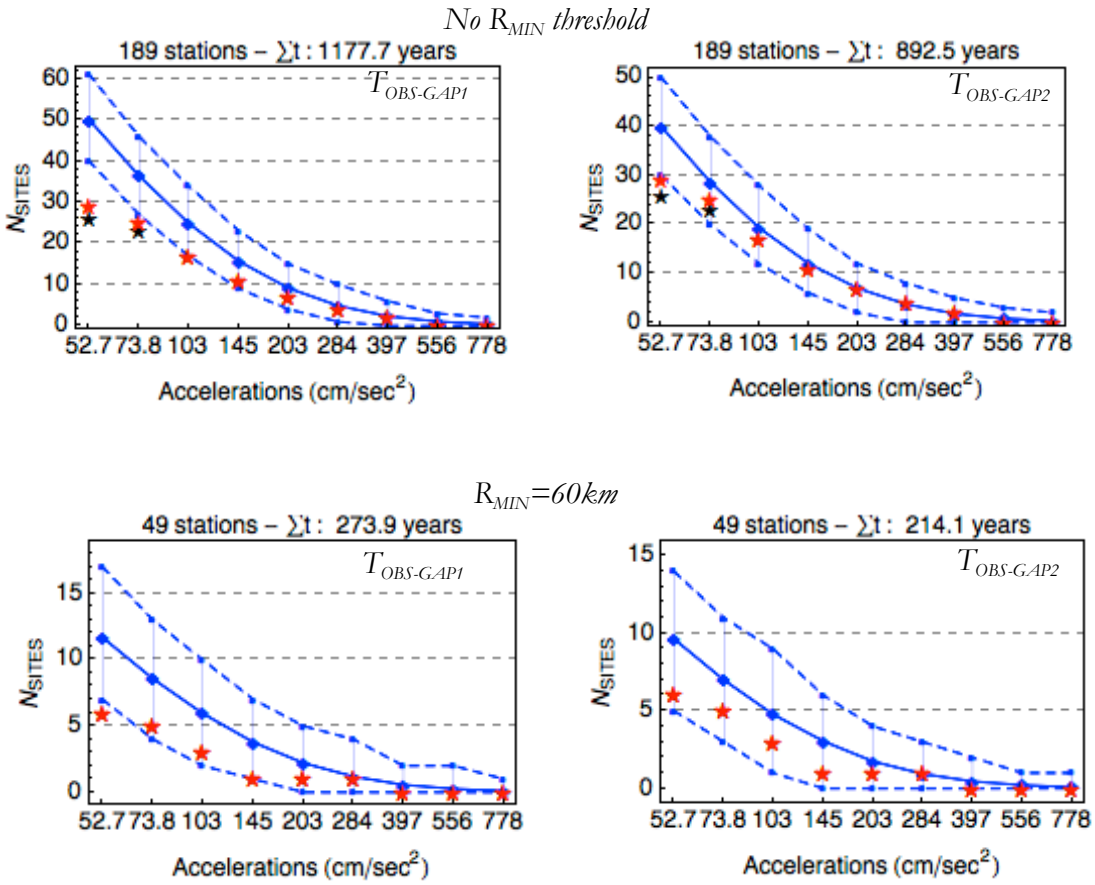

Figure 3.18: Comparison of the observed and predicted number of sites with exceedances at different acceleration levels and considering different selections of sites. (1st raw) All 189 stations (No minimum inter-site distance threshold), (2nd raw) 49 stations out of 189 with a minimum inter-site distance R_{MIN}=60 km. The results are obtained considering the lifetimes obtained deducing the gaps identified using inter-event times (right) and using missing records (right). Blue curves: median and percentiles 2.5 and 97.5 of the predicted distributions (see section 2.2 of second chapter), black stars: reduced number of sites in the case of double-counting, red stars: observed exceedances considering only records of mainshocks.

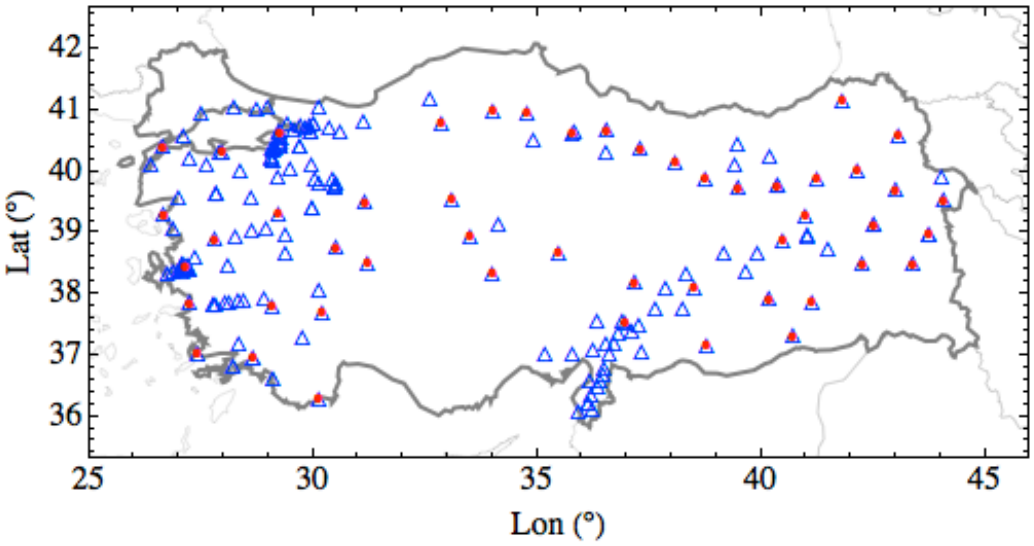

Figure 3.19: Blue triangles: all 189 selected stations, Red points: 49 sites selected with an inter-site distance ≥ 60km.

3.7 Conclusion and Discussions

We evaluated the predictions of the SHARE-PSHA model for the Turkish territory using the accelerometric database of the Turkish National Strong Motion Observation Network. We checked the reliability of the data and selected as many sites as possible to increase the observation length.

We first applied the test considering 137 stations with a minimum inter-site distance of 10 km to avoid multiple observations from the same earthquake at different sites. The observation lifetimes of stations are calculated in two different ways; 1) the interruption in operation are determined using a statistical method based on inter-event times of observations at each station, and 2) the interruptions in operation are detected looking at the missing records in the dataset and they are deduced from the observation lifetimes of stations. The total observation lifetime calculated using the second method is shorter than the lifetimes obtained using first method. The actual observation lifetimes of stations are likely between the lifetimes identified considering the gaps from the first method and the second method.

The results show that the observation and the predictions for accelerations between 103 and 397 cm/s^2 are consistent at 137 sites for all observation lengths considered (R_{MIN}=10 km). For accelerations between 52.7 and 73.8 cm/s^2, the model predicts more than observed

exceedances when the corrected-lifetimes are estimated based on inter-event times. When gaps are identified from missing observations, the model is consistent with the observations at all acceleration levels except at 52.7 cm/s^2, where the model predicts too many exceedances. The results at accelerations higher than 556 cm/s^2 rely on no observed exceedance.

Table 4: Summary of the testing results for different selections of sites and different estimated observation duration based on the comparison of N_{SITES}

PGA	49 sites (R_{MIN}=60)			137 sites (R_{MIN}=10 km)			189 sites (R_{MIN}=0)		
cm/s^2	T_{OBS}	$T_{OBS-GAP1}$	$T_{OBS-GAP2}$	T_{OBS}	$T_{OBS-GAP1}$	$T_{OBS-GAP2}$	T_{OBS}	$T_{OBS-GAP1}$	$T_{OBS-GAP2}$
52.7	O	O	□	O	O	□	O	O	O
73.8	□	□	□	O	□	□	O	O	□
103	□	□	□	O	□	□	O	□	□
145	□	□	□	□	□	□	□	□	□
203	□	□	□	□	□	□	□	□	□
284	□	□	□	□	□	□	□	□	□
397	□*	□*	□*	□	□	□	□	□	□
556	□*	□*	□*	□*	□*	□*	□*	□*	□*
778	□*	□*	□*	□*	□*	□*	□*	□*	□*

* : The test relies on no observed exceedances
O: model predicts more than observed hazard

The hazard model is also tested for different choices of station selections, corresponding to different values of the minimum inter-site distance R_{MIN}=0, R_{MIN}=10 km and R_{MIN}=60 km. We considered 189 and 49 sites with a minimum inter-site distance R_{MIN}=0 and R_{MIN}=60 km respectively in order to check the stability of the results. For accelerations higher than 103 cm/s^2 the model is consistent with the observations for all values of R_{MIN}. At smaller accelerations the results obtained using R_{MIN}=0 are almost the same as those obtained using 137 sites (R_{MIN}=10). The only difference is the overestimation at 73.8 cm/s^2 when $T_{OBS-GAP1}$ is used considering 189 sites with R_{MIN}=0. When 49 sites are considered (R_{MIN}=60km), the model appears to be more consistent with the observations than when using 137 sites (R_{MIN}=10km) and 189 sites (R_{MIN}=0) at acceleration smaller than 103 cm/s^2. However, due to the small number of stations considered, we should keep in mind that the results obtained using 49 sites (R_{MIN}=60km) exploit shorter total observation lengths.

The results depend on the site amplification model used for calculating the ground motion at V_{S30}=750 cm/s. The generating database of the equation used in this study (Sandikkaya *et al.* 2013) covers a wide region (Greece, Italy and Turkey, Taiwan, Japan and California). An elaborated study on the adaptability of this site amplification equation should

be done. Also, another technique for estimating the amplification factor could be used, e.g. using the GMPE developed mainly from Turkish accelerometric data by Derras *et al.* (2013).

We should always consider these results with great caution considering that they are limited by the available data. The longest observation period at the accelerometric stations considered is 29 years in Turkey. Secondly, the results are dependent on the site amplification equation used to obtained the PGA values at V_{S30}=750 m/s.

3.8 Supplement

3.8.1 The earthquake catalog used to generate synthetic data

We use two earthquake catalogs, 1) the SHARE European Earthquake Catalog (SHEEC) for the time window before 2006 and 2) the catalog of B.Ü. KOERI National Earthquake Monitoring Center (www.koeri.boun.edu.tr) for the time after 2006. The SHEEC catalog, compiled within the SHARE project, is provided for two time windows separately. Before 1900, the catalog is compiled within SHARE project and relies on the work of the "Network of Research Infrastructures for European Seismology" (NERIES, Stucchi *et al.* 2013). After 1900, The catalog is gathered by GFZ Potsdam as a part of "The European-Mediterranean Earthquake Catalogue" (EMEC) project (Grünthal & Wahlström, 2012 and Grünthal *et al.* 2013). However, the SHEEC catalog does not cover central and eastern part of Turkey (it extends up to longitude 32°). For Central and Eastern Turkey (longitude between 32° and 45°), we use the SHARE-CET earthquake catalog (Sesetyan *et al.* www.emidius.eu/SHEEC/docs/SHARE_CET.pdf). These catalogs are available on the web (www.emidius.eu/SHEEC, last retrieved on 09/01/2014). Finally, since both catalogs extend until 2006, we use the catalog of B.Ü. KOERI National Earthquake Monitoring Center (www.koeri.boun.edu.tr) for the period starting from 01/01/2007 in the whole Turkish territory. We checked that there are no common earthquakes, and no overlap in time and space between these catalogs. (see Figure 3.S20 for the combined catalog).

The magnitudes of earthquakes in EMEC and SHARE-CET catalogs are moment magnitudes (some were converted from local magnitudes or intensities when necessary). KOERI provides the magnitudes of earthquakes mainly in local magnitude (M_L) and in moment magnitude for a few earthquakes. To use a homogenous magnitude scale for all earthquakes, we converted M_L to M_W using Akkar *et al.* (2010) conversion equation for Turkey.

The minimum magnitude of the EMEC and SHARE-CET catalogs are M_W4 for Turkey. We considered the earthquakes with $M_W \geq 4$ from the catalog of KOERI to keep the same minimum magnitude threshold. As shown in Figure 3.S21, the earthquake catalog is complete for magnitudes $M_W > 4$ since around 1968. The number of earthquakes that occurred within the spatial window extending from 34° to 43° in latitude and from 24° to 45° in longitude is 7138. These events are used in this study to generate the synthetic dataset after 1968.

We generate the synthetic dataset at 204 accelerometric stations using the GMPE Akkar & Çagnan 2010 (AC2010). The magnitude validity range of AC2010 is 3.5-7.6 (MW). The upper limit of the VS30 validity range is 760 m/s. In order to calculate the generic response spectra predicted by the ground-motion model AC2010 for the earthquakes at the considered sites, we need some parameters about both the sites and the sources. One of the main missing parameter related to the earthquakes is the exact nodal plane solution. The knowledge of the correct nodal plane is necessary for calculating the Joyner-Boore distance (RJB) and for deciding the style of faulting required by the ground-motion model. A random selection of correct nodal plane may causes some bias in these values.

Since the rupture length of earthquakes with moment magnitude smaller than 5.5 are generally smaller than 5 km, the effect of nodal plane solution on distance calculations is limited. When generating the synthetic history at stations, we assume that the epicentral distance (R_{EPI}) is equal to the Joyner-Boore distance (R_{JB}) for events with moment magnitude smaller than 5.5. Most events (99.5%) which occurred between 1968 and 2013 have a moment magnitude smaller than 5.5.

For the 138 events with magnitudes higher than 5.5, it is necessary to take into account the extension of the rupture surface and the geometry of the rupture plane, especially if they are observed at sites close to the source. In order to calculate R_{JB} for records with magnitude higher than 5.5, it is also necessary to know the location of the hypocenter on this surface. In this study, the hypocenter is assumed to be located in the center of the rupture plane. Furthermore, the rupture length and rupture widths are calculated from the magnitudes using the equation given by Leonard (2010). Twenty-one events are found more than 100 km far from the accelerometric stations considered (204 stations). For these events we assumed $R_{JB}=R_{EPI}$.

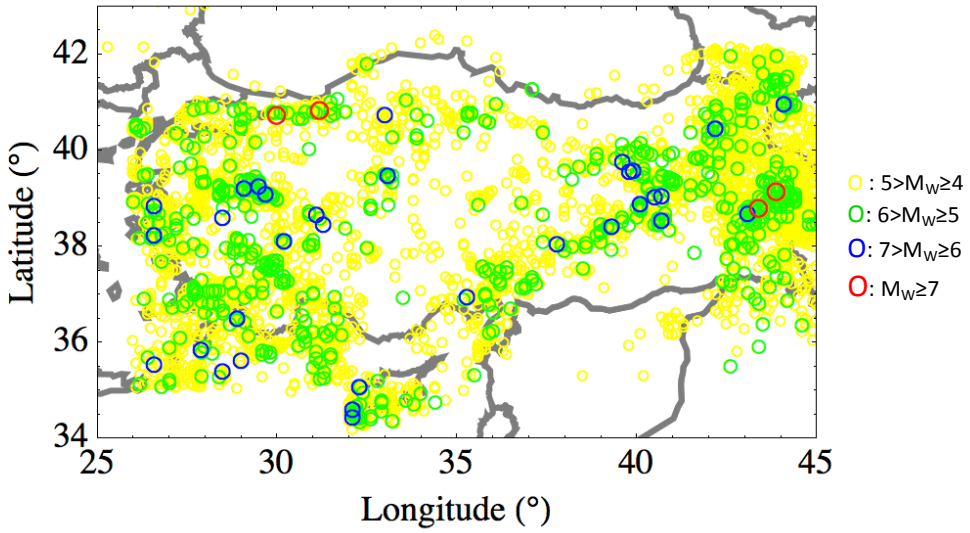

Figure 3.S20: Maps of earthquakes in the combined earthquake catalog used in this study (EMEC, SHARE-CET and KOERI catalogs). See text for further information about the catalogs.

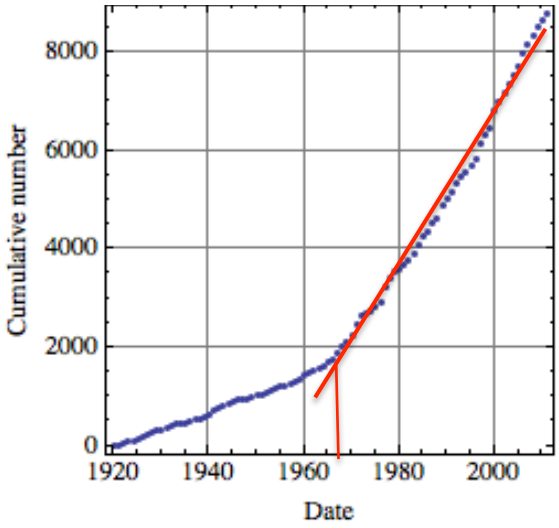

Figure 3.S21: Cumulative number of earthquakes with magnitude $M_W \geq 4$ in the earthquake catalog. The catalog is assumed to be complete for $M_W \geq 4$ since around 1968.

We looked for the exact nodal plane solutions in the databases provided by different agencies (GMT, ISC and RESORCE) and papers (Tibi *et al.* 2001, Tan *et al.* 2008, Pilidou *et al.* 2004, Cisternas *et al.* 1989, Çevikbilen & Taymaz 2012, Alptekin *et al.* 1986, Eyidogan & Jackson 1985, Irmak *et al.* 2012, Irmak 2013, Pınar & Kalafat, 1999, Papazachos, 1990). We could find the correct nodal plane solution for 79 events with $M_W \geq 5.5$. For all events with $M_W \geq 6.5$, the correct nodal plane solutions are used to calculate R_{JB}. We could obtain the

double-couple fault plane solutions (2 possible nodal planes) of 20 earthquakes. For these earthquakes, the correct nodal plane is estimated plotting the fault mechanism solution on the fault map of Turkey (Bozkurt *et al.* 2001). In order to estimate the correct nodal planes, we looked at the strike or dip angles of the faults and/or compared the fault mechanism of the event with other events that occurred on the same fault (Figure 3.S22). For 7 events without a fault plane solution, we used the nodal plane of events that occurred on the same fault and very close to these events. For 11 events of magnitude between 5.5 and 6, we could not estimate the correct nodal plane solution looking at the fault maps and at neighboring events therefore we assumed $R_{JB}=R_{EPI}$.

In the database of Akkar *et al.* (2010), the faulting styles of the earthquakes with magnitude ≥5.5 were determined using Frohlich & Apperson (1992) approach. If the faulting style of an earthquake is classified as odd mechanism using the Frohlich & Apperson (1992) approach, the authors used the rake and dip angles to decide the mechanism of the events following one of the three approaches: Boore *et al.* (1997), Campbell (1997) or Sadigh *et al.* (1997) (see Table 3 of Akkar *et al.* 2014). In this study we follow the same procedure to determine the faulting styles. For events classified as odd mechanism using the approach of Frohlich & Apperson (1992), we followed the method of Campbell (1997, Equation 3.S4), which is one of the methods followed also by Akkar *et al.* (2010) when Frohlich & Apperson (1992) gave odd mechanism. For the events with magnitude smaller than 5.5 or with unknown fault solution, we assumed a strike slip mechanism. The generating dataset of AC2010 GMPE was dominated by strike slip earthquakes (70%), 28% of the data correspond to normal faulting earthquakes and only 2% of the data correspond to reverse faulting earthquakes. Bommer *et al.* (2003) indicate that the effect of style of faulting on ground-motion seems to be larger at distances close to the rupture but the differences in mean residuals are found to be less significant than 5%. The method of Campbell (1997) to determine the faulting styles of earthquakes using the rake and slip is given in Equation 3.S4. This approach is used if an earthquake is classified as odd mechanism using the approach of Frohlich & Apperson (1992). λ is rake angle and δ is dip angle.

$$\begin{aligned} &\text{If } |\lambda| < 22.5 \; or \; |\lambda| < 157.5 \;\; => \; Strike\ Slip \\ &\text{If } 157.5 \geq |\lambda| \geq 22.5 \text{ and } |\delta| \geq 45 \;\; => \; Reverse \\ &\text{If } 157.5 \geq |\lambda| \geq 22.5 \text{ and } |\delta| < 45 \;\; => \; Thrust \end{aligned} \qquad \textbf{(3.S4)}$$

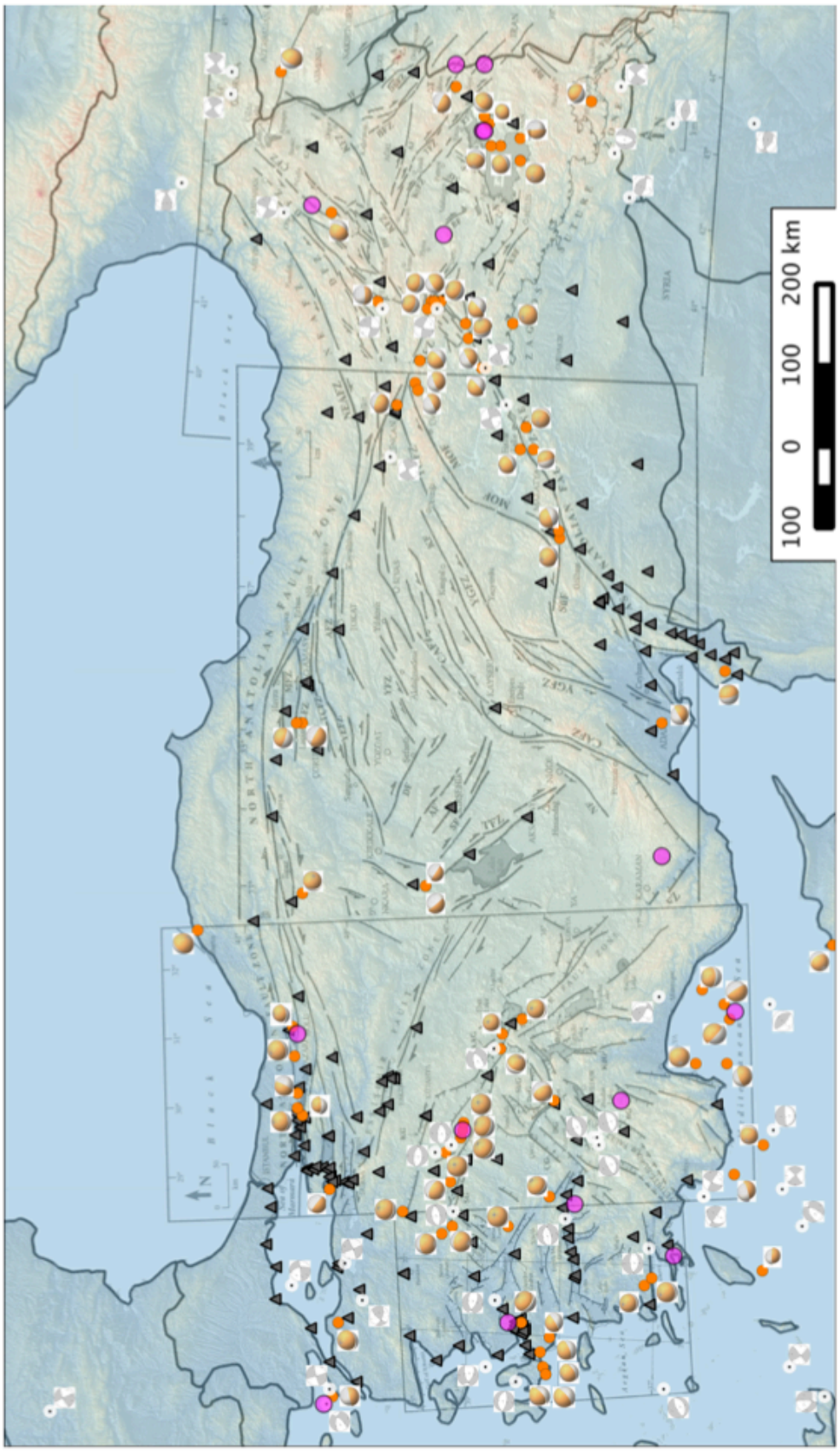

Figure 3.S22: Locations and fault mechanisms of earthquakes with $M_W \geq 5.5$ found in the earthquake catalog. Fault maps are extracted from Bozkurt (2001) and superimposed on the map. Small circles are locations of events with exact nodal plane solutions. Circles with point in the center are the locations of events with two nodal plane solutions. Big circles are events without fault mechanism.

3.9 Acknowledgements

Many thanks to Abdullah Sandikkaya from Middle East Technical University for his great help especially on the dataset used in this chapter. Thanks also to Aida Azari Sisi from Middle East Technical University for her contribution in processing the accelerometric data.

3.10 Data and resources

1) SHARE hazard model, www.efehr.org
2) Accelerometric data, http://kyh.deprem.gov.tr/ftpe.htm
3) The earthquake catalog of SHEEC, http://www.emidius.eu/SHEEC/
4) Code cluster 2000 (Reasenberg, 1985),
   http://earthquake.usgs.gov/research/software/index.php
5) GCMT earthquake catalog, http://www.globalcmt.org/CMTsearch.html
6) ISC earthquake catalog, http://www.isc.ac.uk/iscbulletin/search/bulletin/
7) NEIC earthquake catalog, http://earthquake.usgs.gov/earthquakes/eqarchives/epic/

Chapter 4

Evaluating the probabilistic seismic hazard models using macroseismic intensities in France

Contents

4.1 Introduction

France and its neighboring countries are low to moderate seismicity countries where destructive earthquakes rarely occur. However, some moderate earthquakes caused damage in France during the last few centuries: 1356 Basel (Swiss) earthquake with the maximum epicentral intensity is equal or greater than IX (Mayer Rosa & Cadiot, 1979), 1580 Strait of Dover earthquake with the maximum epicentral intensity higher than IX (Melville *et al.* 1996, Neilson *et al.* 1984), 1682 Vosges earthquake with the maximum epicentral intensity of VIII (Quenet 2005, Lambert 1997, Urry 1913), 1909 Lambesc (Provence) earthquake with magnitude around 6.2 (Stich *et al.* 2005, Lambert 1997) and etc. Geological evidences suggest the occurrences of stronger earthquakes in earlier ages. For example, Sebrier *et al.* (1997) analyzed the occurrences of destructive earthquakes with magnitude around 7 (M_W) in the Nimes Fault and they predicted occurrence intervals between 10 ka and 100 ka for these earthquakes based on paleoseismic data.

Although macroseismic intensity databases bear higher uncertainties than the instrumental databases, they are of great importance in evaluating PSHA models due to their wider coverage in time and space. The macroseismic intensity database of France is indeed considerable in terms of its time coverage. It extends roughly a thousand years backward in time and statistical evaluations show that the completeness periods for observed intensities higher than V go back as early as 1800s at some sites. Secondly, macroseismic intensity data are also appealing because of the quantity of observations. Macroseismic databases contain more data than accelerometric databases at higher return periods (>475 years), which are of interest for earthquake engineering.

In the literature, there are some studies on the evaluation of PSHA models using macroseismic intensities Dowrick and Cousins (2003) used up to 158 years of macroseismic observations at 47 selected sites in New Zealand. The isoseismals were obtained using an attenuation relationship. Authors selected the earthquakes with magnitude higher than 5.25 and with focal depths less than 100 km. Stirling & Petersen (2006) compared the intensities observed at 26 sites in New Zealand and 52 sites in the United States with the respective national hazard maps. The authors used empirical conversion equations for converting the observed intensities into peak ground accelerations. Mezcua *et al.* (2013) study follows a method similar to the one followed by Stirling & Petersen (2006) using the historical data from

Spain. Mucciarelli *et al.* (2008) compared the ranking of sites based on the exceedance rates given by different models rather than evaluating the values of predicted rates.

We use the historical records of felt intensities at a group of sites (cities and towns) in France to obtain the historical number of sites with exceedances as done in Stirling & Petersen (2006). The observed number of sites with exceedances is compared with the predicted number of sites with exceedances given by the PSHA models. The method used to obtain the distribution of the predicted number of sites with exceedances at selected acceleration values (or return period values) is illustrated in Figure 2.1 of the second chapter. Two of the PSHA models, MEDD2002 and AFPS2006, which were evaluated using the accelerometric data from France, will be evaluated also using historical data (see section 2.2 of second chapter for further information about the PSHA models).

Several difficulties have to be dealt with before using the macroseismic intensity catalog. In order to use intensity data for evaluating hazard estimations, we should evaluate the completeness periods of the historical observations to be able to calculate the observed rates of exceedances. Secondly, a conversion between intensities and accelerations is required since the probabilistic estimations are given in terms of exceedance rates of accelerations not in terms of intensities.

This chapter attempts to use macroseismic intensity data for testing hazard estimations. After providing general information about macroseismic intensity data of France, the first step consists in analyzing the completeness of the database in time, and to select locations and time windows where the history is complete. We will introduce the empirical conversion relations used to convert the acceleration thresholds selected for testing into intensities. The uncertainties and limits of the conversion equations used will be discussed and the results obtained using different equations will be compared.

4.2 Sisfrance Data

In the beginning of 1980s, safety precautions for natural risks in France have been introduced. This created the need to better understand the seismic activity in France. A database of historical earthquakes for France was compiled in 1974, which gave rise to the "Sismicité de la France" database (SisFrance, www.sisfrance.net, Scotti *et al.* 2004). The revision of historical catalogs was initiated in 1974 with the aim of building a homogenous

database, SisFrance. Since 1974, the quality and completeness of the SisFrance database have improved, with the collaboration of three institutions; IRSN (the **I**nstitut de **R**adioprotection et de **S**ûreté **N**ucléaire, the French Institute for Radiological Protection and Nuclear Safety), EDF (**E**lectricité **d**e **F**rance, Electricity of France) and BRGM (**B**ureau de **R**echerches **G**éologiques et **M**inières, the Geological and Mining Research Bureau). Within the framework of SisFrance, the existing catalogs, archives of journals, administrative documents etc. of France and neighboring countries have been gathered and analyzed. This work was done with the contribution of geologist, seismologist, historians etc. The database is still updated annually. We use the database provided by EDF that is not publicly available on SisFrancewebsite. This database consists of 105862 observations from 6214 events recorded at 27107 sites (last retrieved on 18/11/2013). The available database covers the time period until 2007.

In France, the documents providing information on earthquakes before 17th century are mainly annals and chronicles, resolution of the city council, records of community or administration, familial records, memorials, etc. (Lambert 1997). In the 17th century, journals were a very important tool for the distribution of information and reported details about earthquakes (Lambert 1997). In the 18th century, people started to investigate the earthquakes rather than accepting them as a misfortune. During the 18th century, memories, books and disquisition, additionally to the administrative documents, have been written especially after the 1755 Lisbon earthquake (e.g. Goudar 1756, Bertrand 1757, Dolomieu 1784). In the 19th century, in many countries in Europe, many documents (memories, felt reports, annals, chronicles) about the seismicity in different regions have been published. The macroseismic intensity surveys also started during this period. In the beginning of the 20th century, two seismological institutions were founded in France, the "Institut de Physique du Globe de Strasbourg" was founded in 1919 and the "Bureau Central Sismologique Français" (BCSF) was founded in 1921. These institutions performed earthquake studies using questionnaires. Detailed information on earthquakes felt each year in France has been published (Annales and Annuaires de l' Institut de Physique du Globe de Strasbourg). Rothé (1977) compiled previous works on historical earthquakes. The experts of SisFranceworking group have been working on the database since 1975 and updated it frequently. In this study we use the most recent version provided by EDF.

The SisFrance database is based on the previous dataset of Rothé (1977) as a starting point (Scotti *et al.* 2004). The SisFrance working group evaluated the reliability and nature of the events listed in Rothé's catalog. They suggested that some events were fake earthquakes (misinterpretation of the documentary sources) and some observations were not reporting earthquakes (they belong to different natural phenomena like landslides, storms and etc). According to SisFrance policy, these observations were not excluded from the SisFrance dataset but are kept with a label indicating their characteristics. In the database, there are 855 observations related to tsunamis, site effects or landslides and 350 observations related to fake earthquakes. These observations are not taken into account further in this study.

The interpretation of observed intensities relies on the effects of earthquakes on buildings, objects, people and the environment. The strength of the SisFrance database lies in assigning a reliability coefficient for describing the uncertainty of the earthquake characteristics and the interpretation of the documentary sources. In the database, the reliabilities of the parameters were evaluated at different steps of interpretation. The reliability coefficients were attributed to the date and time of earthquakes, location of earthquake epicenters, the epicentral intensities, the documentary sources and observed intensity values at sites. The reliabilities of observed intensity values are given in 3 classes. A (sure, 36312 observations), B (sure enough, 63360 observation) and C (uncertain, 4985 observation).

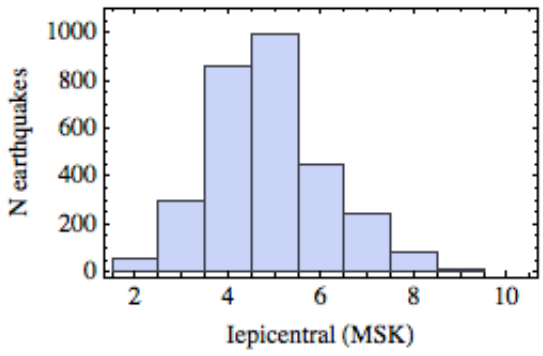

Figure 4.1: Distribution of the epicentral intensity (I_{EPC}) values of all events with known I_{EPC} observed in metropolitan France.

We focus on observations reported at sites in metropolitan France, which is the region of interest covered by PSHA models. The sites are mainly administrative communes, except some sites known by their local/historical names (no political identity). The data observed in

metropolitan France consist of 91089 observations from 5061 events. The distribution of the epicentral intensities (I_{EPC}) of the earthquakes with known I_{EPC} is shown in Figure 4.1.

The SisFrance database is homogenous in term of the observed intensities. The severity of the ground shakings is classified only according to the Medvedev–Sponheuer–Karnik scale (MSK-64, Medvedev *et al.* 1967). The MSK-64 scale has 12 discrete intensity degrees based on the descriptions of the ground shaking levels (see Table III of Medvedev *et al.* 1967). Higher intensity levels indicate higher damage. Although the intensities are given in terms of Roman numerals in the paper of Medvedev *et al.* (1967), we use the corresponding Arabic numerals in this study. The minimum intensity threshold of the SisFrance database is set to 2 (MSK-64). As described in Table III of Medvedev *et al.* 1967, the intensities smaller than 2 are imperceptible to people.

In MSK-64 scale, the intensity degrees are expressed only by integers (decimals are not used). In the SisFrance data, half degrees between two integers are used in some cases. The intensities given in half degrees in SisFrance database represent different cases depending on the reliability coefficient of the observation. For example, an intensity level of 4.5 indicates that the ground shaking level is half way between two closest integer value if it has a reliability coefficient of A (ground shaking is exactly half degree higher than 4 and half degree less than 5). If it has a reliability coefficient of B or C, it means that it is not clear whether the level of ground shaking is 4 or 5.

Another parameter provided by the SisFrance data is the parameter about the determination of mainshocks and aftershocks. If an earthquake belongs to a cluster of seismic activity, it is mentioned in the database. Thus the observations of main shocks, aftershocks and the swarms can be selected separately. This allows us to apply the test using the observations from mainshocks to satisfy the independency of the observations in time required for the Poisson assumption (see section 2.2 of second chapter).

4.3 Conversion equations between intensities and PGA

In order to allow the direct comparison of observed intensities and predicted ground motions, one of these two parameters should be converted to the other one using empirical conversion relationships. There are many conversion equations in the literature established for active crustal regions (e.g., Faenza & Michelini, 2010; Wald *et al.,* 1999; Tselentis & Danciu,

2008). The independent variables included in the functional form of these relations vary between different studies. Some equations enable a direct conversion between intensities and ground motions, whereas some others require also earthquakes parameters such as magnitude, focal depth etc. The earthquake parameters of historical earthquakes may be inaccurate, especially if they occurred before the instrumental period or if they rely on few observations. Thus we will consider only the correlation equations that enable direct conversion between ground motion and intensities.

In the literature, there are many equations correlating intensities and PGAs (PGA-I correlation) enabling direct conversion from one parameter to the other. Several PGA-I correlation equations were established using databases of different countries. e.g. Wald *et al.* (1999) for California, Faenza & Michelini (2010) for Italy, Atkinson & Kaka (2006, 2007) for Central United States, Davenport (2003) for New Zealand, Bigault & Guéguen (2011) for France.

In this study we will use more than one PGA-I correlation equation for comparing the results for different equations. Due to the lack of correlation equations derived using data from France, we will also use PGA-I correlations established using datasets from other regions. We refer to the previous studies for selecting the PGA-I correlation equations. Delavaud *et al.* (2012) coupled a set of GMPEs with a set of PGA-I correlation equations to predict intensities at different sites for France. The predictions obtained are compared with the observations from SisFrance data. Delavaud *et al.* (2012) found that Faenza & Michelini (2010) equation provides the best fit to the data. Bigault & Guéguen (2011) evaluated different equations established for active crustal regions using data from the RAP and the BCSF (Cara *et al.* 2006 and Cara *et al.* 2007). They indicate that the correlation equations that best fit the French dataset are the equations of Atkinson & Kaka (2006) and Bigault & Guéguen (2011).

Following these previous studies, we decided to use three equations in this study; 1) Faenza & Michelini (2010, FM2010), 2) Atkinson & Kaka (2006, AK2006) and 3) Bigault & Guéguen (2011, BG2011). Table 4.1 gives the characteristics of the selected ground motion to intensity conversion equations. The functional forms of the equations are given in equations 1, 2 and 3 respectively for FM2010, AK2006 and BG2011.

Table 4.1: Characteristics of the PGA-I correlation equations used in this study

Reference	Magnitude range	Variables (PGA)	Functional form	Intensity scale	Region
Faenza & Michelini (2010)	4 - 6.9 (M_W)	$G_{MEAN}H$	Linear	MCS	Central US California
Atkinson & Kaka (2006)	2-7 (M_W)	$G_{MEAN}H$	Quadratic	MMI	Italy
Bigault & Guéguen (2011)	3.3-5.4 ($M_{L,RENASS}$)	$G_{MEAN}H$	Quadratic	EMS98	France

*$G_{MEAN}H$ is the geometrical mean of two horizontal components

The comparison of the intensities predicted by three selected PGA-I correlation equations is shown in Figure 4.2. The mean predicted intensities from FM2010 are larger than the other equations, except for small PGAs (<5 cm/s^2) and very high PGAs (>500 cm/s^2). The mean predictions of AK2006 and BG2011 are very close to each other. The predictions of these two equations are slightly different at one standard deviation away from the mean due to the difference in standard deviation (σ=0.93 for AK2006 and 1.06 for BG2011). The FM2010 model has the smallest standard deviation (0.35) between these three models.

Several intensity scales are available to evaluate the severity of intensities. MCS (Mercalli-Cancani-Sieberg, Sieberg 1932), MMI (Modified Mercalli Intensity, Stover & Coffman 1993, Wood & Neumann 1931), EMS (European Macroseismic Scale, Grünthal 1998), MSK (Medvedev, Sponheuer and Karnik scale, Medvedev *et al.* 1964), JMA (Japan Meteorological Agency, JMA 1996) scales are the more commonly used. The scales of the intensity term in the PGA-I correlation equations vary depending on the dataset used. The three PGA-I correlation equations used in our study, FM2010, AK2006 and BG2011, use the MCS, MMI and EMS98 scales respectively.

$$I_{MCS} = 1.68 \pm 0.22 + 2.58 \pm 0.14 \log PGA \quad (\sigma = 0.35) \tag{1}$$

$$I_{MMI} = 0.372 (\log PGA)^2 + 1.319 \log PGA + 2.315 \quad (\sigma = 0.93) \tag{2}$$

$$I_{EMS98} = 0.37 (\log PGA)^2 + 1.3 \log PGA + 2.3 \quad (\sigma = 1.06) \tag{3}$$

Since intensity is not a scalar value, it is not straightforward to convert one intensity scale to another one. Some subjective parameters are involved in the assigned intensity values, such as the interpretation of experts who analyzed the historical documents. Following the study of Musson *et al.* 2010, who compared different intensity scales, we assume that these intensity scales are equivalent up to the intensity 10 (see Table 2 of Musson *et al.* 2010). All the intensities observed for sites in metropolitan France in the SisFrance database are smaller than 10.

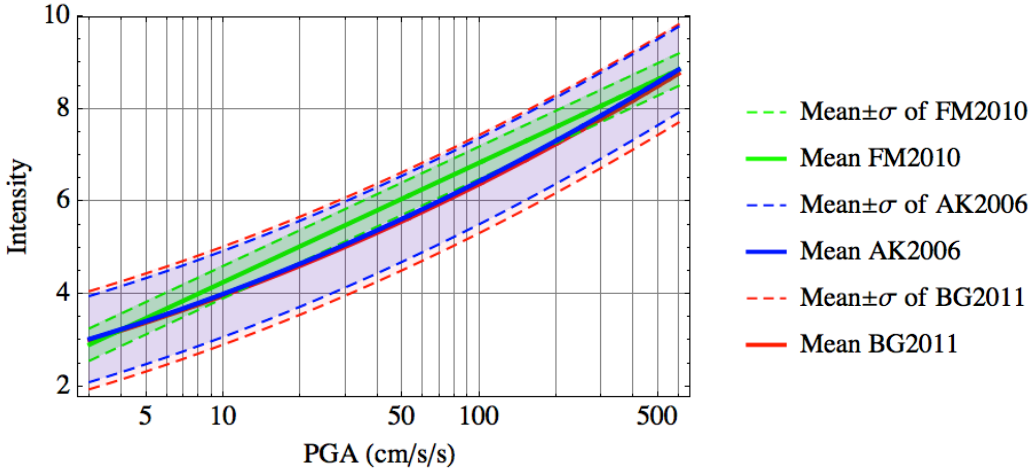

Figure 4.2: Comparison of 3 conversion equations; Faenza & Michelini (2010, FM2010) for Italy, Atkinson & Kaka (2006, AK2006) for Central US and California and Bigault & Guéguen (2011, BG2011) for France. Solid lines represent the mean and dashed lines represent the predictions at ±σ (standard deviation).

4.4 Method for testing a PSHA model using a PGA-I correlation equation

The method applied here on intensity data is identical to the method introduced in the Chapter 2, and applied in Chapter 2 and 3 (testing PSHA against accelerometric data). To enable the comparison of the predicted accelerations with the observed intensities, we apply a conversion between the observed intensities and PGAs. Figure 4.3 illustrates the method used to test a PSHA model (AFPS2006 as an example) using the mean predictions from a PGA-I correlation equation (AK2006), considering only 5 cities as an example. The PSHA model is tested at four acceleration levels corresponding to intensities 5, 6, 7 and 8 given by the AK2006 correlation equation.

Sites	Median $\lambda_{\geq 156cm/s^2}$	Observation Time Length (years)	Maximum observed intensity at the site (max I_{OBS})	Mean PGA equivalent to max I_{OBS} (cm/s^2)	27 cm/s^2 (I=5)			
					27 cm/s^2 (I=5)	69 cm/s^2 (I=6)	156 cm/s^2 (I=7)	330 cm/s^2 (I=8)
Tarbes	0.000591	190	6	69	1	1	0	0
Pau	0. 001854	207	6	69	1	1	0	0
Nice	0. 000373	207	6	69	1	1	0	0
Briancon	0. 001281	116	7	156	1	1	1	0
Strasbourg	0. 000581	150	6.5	105	1	1	0	0
					↓	↓	↓	↓
					5	5	1	0

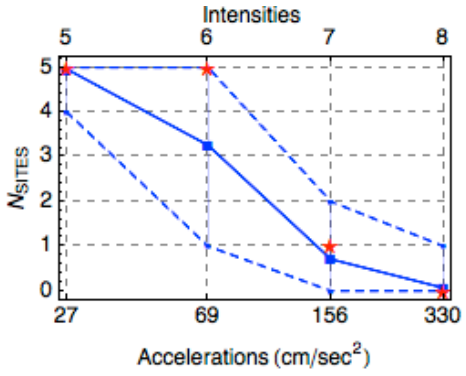

Figure 4.3: Example considering 5 sites: steps for testing AFPS2006 model at a range of acceleration levels. Mean predictions of the PGA-I correlation equation are used (AK2006). Observed numbers of sites with exceedance are superimposed to predicted numbers. The blue curves (predicted distribution) are obtained following the steps explained in Figure 2.1 of second chapter.

4.4.1 Considering the uncertainties of PGA-I correlation equations

In general, PGA-I correlation equations are generated to predict intensities from accelerations. If the least square regression method is used for building the PGA-I equation, it cannot be reverted. This means that if PGA is the independent variable and intensity is obtained by regression against PGA, the equation cannot be used to predict PGA from intensity. In practice, the equations are used in both directions regardless of the regression methods used in many studies. For example, Stirling & Petersen (2006) converted the observed intensities to PGA using Wald *et al.* (1999) correlation equation, although Wald *et al.* (1999) equation should be used only to predict intensities from accelerations.

Among the three correlation equations selected in this study, AK2006 and BG2011 should be used only to estimate the intensity values corresponding to a given PGA. The relationship of Faenza & Michelini (2010) is an exception. The advantage of this relation is that

it is generated using an orthogonal distance regression, which enables the use of this equation to predict PGA from intensity as well as to predict intensity from PGA. Thus this equation can be used to predict the acceleration equivalent to intensities. However, the standard deviation of the equation represents the distribution of the intensities equivalent to a fixed PGA. In this study, we use the three PGA-I correlation equations to convert the acceleration threshold selected for testing into intensities.

The PGA-I correlation equations predict a range of possible intensity values corresponding to a given acceleration level (see Figure 4.4). The distribution is defined with a mean value and a standard deviation. The uncertainty of the PGA-I correlation equation should be considered when testing PSHA models.

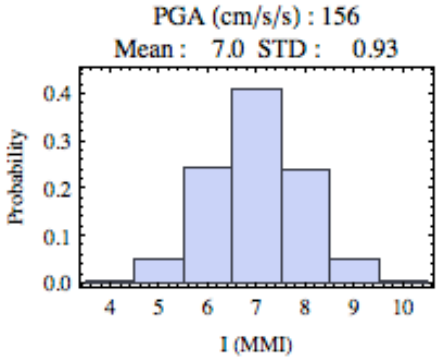

Figure 4.4: Example for the distribution of intensities corresponding to PGA=156 cm/s^2 given by AK2006 correlation equation (Equation 2). The standard deviation of the distribution is 0.93. The mean intensity value corresponding to PGA=156 cm/s^2 is 7 (MMI). The probability distribution of macroseismic intensities is sampled within the range ±σ, corresponding to intensities between 6 and 8.

In this study, the probability distribution for the observed number of sites with exceedances is obtained by sampling the intensity distribution given by PGA-I correlation equation within the range ±σ. The steps followed to obtain the distribution of observed exceedances accounting for uncertainties in the PGA-I correlation equation are illustrated in Figure 4.5 for the acceleration threshold 156 cm/s^2 (mean I=7 according to AK2006) as an example. We apply a Monte Carlo sampling with 10000 runs. In each run, we select a random intensity I_R following the distribution of intensity for a fixed PGA given by the selected PGA-I relation, sampled within the range ±σ. Then we count the number of sites, among the sites considered, with at least one observation higher than or equal to I_R to obtain the observed number of sites with exceedances.

Sites	Maximum observed intensity at the site (I_{MSK})		Monte Carlo Sampling (10000 runs)				
			Run 1 I_R=6	Run 2 I_R=7	Run 3 I_R=8	……	Run 10^4 I_R=7
Tarbes	6	→	1	0	0	……	0
Pau	6	→	1	0	0	……	0
Nice	6	→	1	0	0	……	0
Briancon	7	→	1	1	0	……	1
Strasbourg	6.5	→	1	0	0	……	0
			↓	↓	↓	……	↓
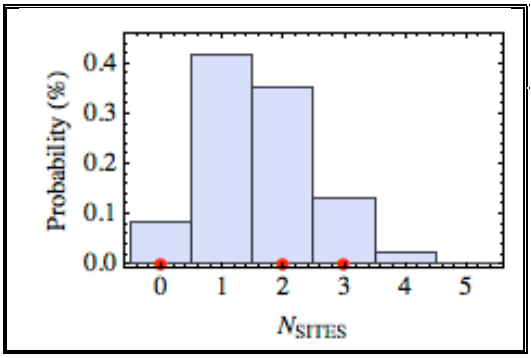		←	5	1	0	……	1

Figure 4.5: Steps followed to obtain the distribution of the observed number of sites that experienced a PGA≥156 cm/s^2 at least once during their observation lifetime, example considering 5 sites. In the Monte Carlo sampling section, 1 indicates the exceedances of I_R, 0 indicates the non-exceedance of I_R. Red points show the probability distribution of N_{SITES} corresponding to the 2.5 percentile, mean and 97.5 percentile of the distribution.

The steps illustrated in Figure 4.5 are repeated for all acceleration levels selected for testing. To test the PSHA models, we evaluate the consistency of the predicted and observed rate of exceedances, accounting for uncertainties on the observed number of exceedances (Figure 4.6).

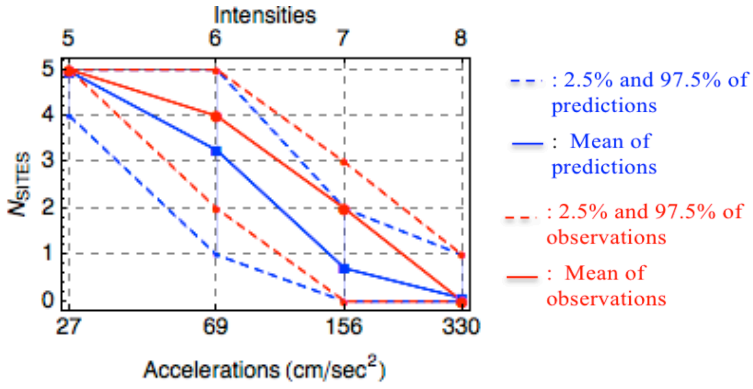

Figure 4.6: Testing AFPS2006 model at different acceleration levels for the same 5 sites as in Figure 4.5 (example).

4.5 Determining completeness periods

The completeness of the macroseismic intensities observed at a site is related to many parameters such as the population density, documentation, social and political conditions, and the temporal evolution of all these parameters. As can be seen in Figure 4.7, higher intensity levels cover longer observations time periods compared to smaller intensities. As explained in Table III of Medvedev *et al.* 1967, intensities less than 5 do not have significant effects on objects and buildings. The documentaries about the earthquakes with intensity less than 5 rely only on the descriptions of the population and everybody does not feel them. Therefore they are less likely to be complete for longer time periods compared to higher intensity levels that generate more memorable effects. In our study, the minimum intensity level selected for testing is set to 5.

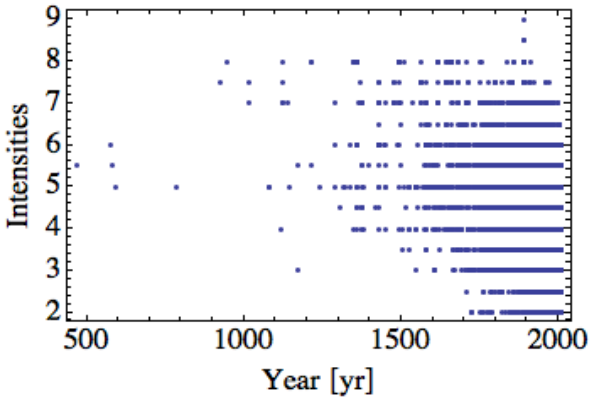

Figure 4.7: Intensities observed at sites in metropolitan France as a function of time. The highest epicentral intensity of earthquakes observed at the French sites is MSK9 (The Ligurian earthquake of 23 February 1887).

Previous studies on testing PSHA models followed different methods to estimate the completeness of observations. Stirling & Petersen (2006) selected a fixed completeness period identical for all sites based on an opinion of an expert (e.g. for I>6 since 1931 for USGS database). Mezcua *et al.* (2013) calculated the completeness time periods using the statistical approach of Albarello *et al.* (2001) for the Spanish historical dataset as a whole. However, a completeness period that is representative for a region may not be representative at individual sites found in this region. Site-specific conditions, like the site history, may cause differences in completeness period. For example, in mountainous regions, the completeness period is generally shorter than for sites in valleys due to the sparse settlement and the lack of historical

documents (J. Lambert, BRGM, personal communications). Therefore we study the completeness of intensities higher than 5 (minimum intensity threshold selected) at each site individually.

The completeness of the database for intensities higher than the selected threshold at selected sites can be studied in two different ways; 1) assessing the completeness and quality of the historical documents at the site (e.g. Stucchi *et al.* 2004) and 2) using the statistical approach based on the observed data at a site (e.g. Albarello *et al.* 2001). The method based on the evaluation of historical documents is a valuable effort to estimate the completeness of observations at sites by seeking for more documents, going back to the archives, analyzing them under political, economical, social perspectives and etc. This method is independent from the number of observed data at the site. However, there have not been enough studies on the historical assessment of completeness of observations at sites in France. The second approach relies on statistical evaluation of the existing observations. These methods compare the variation of the observed number of exceedances above selected intensity thresholds over time to determine the starting date of completeness for the intensity level of interest. They assume that a part of the dataset at a site is complete and that the occurrence of accelerations at the site is stationary in time.

In this study, we evaluate the completeness at each site individually using the statistical method of Albarello *et al.* (2001). This method gives a probability distribution of the completeness start date for an intensity threshold. The mean value of this distribution is chosen as the start time of completeness for the selected intensity level at the site. The completeness time period extends from the completeness starting date until 2007 (SisFrance database is providing data up to 2007). Figure 4.8 presents the results for Briançon as an example (see supplement section 4.11.3 for more examples). At this site, the completeness periods for intensities higher than or equal to 4 are complete since 1916, where as intensities higher or equal to 5 are complete since 1891. Therefore if we use observed data with $I_{OBS} \geq 5$, only the time window since 1891 should be considered for testing.

When few data are available, the application of the Albarello method is difficult and the result might not be reliable. Therefore we also checked visually the cumulative number of observations $I_{OBS} \geq 5$ over time. This analysis suggests that it is safer to impose 1800 as the minimum starting date of completeness periods for $I_{OBS} \geq 5$.

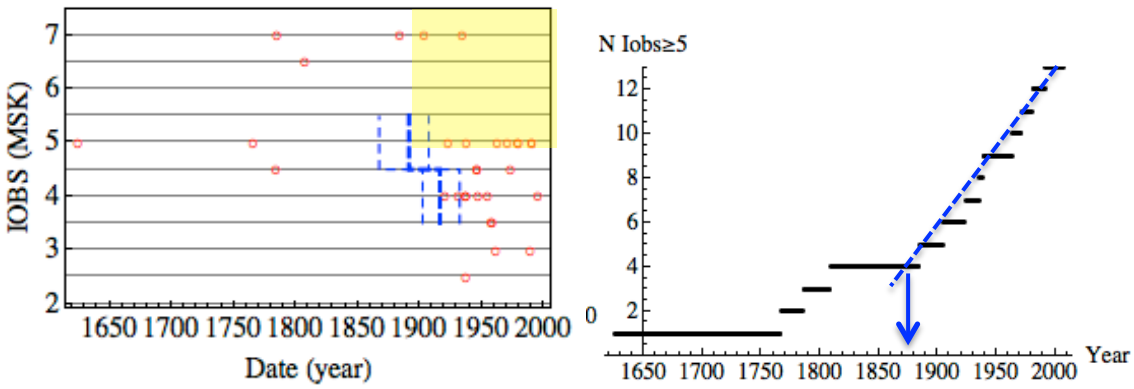

Figure 4.8: Example of the completeness analysis for Briançon (Provence), using Albarello *et al.* (2001) statistical method (left). The vertical dashed lines indicate the completeness starting date for intensities higher than 4 and 5. Thick lines indicate the mean value for the completeness period and thin blue lines indicate the 25 and 75 percentiles. The yellow shaded area represents the complete part of the dataset for I≥5. (right) Cumulative number of observations with I_{OBS}≥5 as a function of time for Briançon site.

4.6 Selecting the minimum acceleration level for testing PSHA models

To account for uncertainties introduced when PGA-I correlation equations are used, we sample the intensity distribution corresponding to the acceleration thresholds within the range ±σ. At each site, we use intensities higher than or equal to 5 observed during the completeness period to test the PSHA models at acceleration levels corresponding to intensities I≥5. As shown in Figure 4.9, all three correlation equations considered in this study (FM2010, AK2006, BG2011) predict intensities higher than 5 for accelerations higher than 77 cm/s^2. Therefore, we can test the PSHA models at accelerations higher than 77 cm/s^2 using observed intensities higher than 5 without under-estimating the number of observed exceedances.

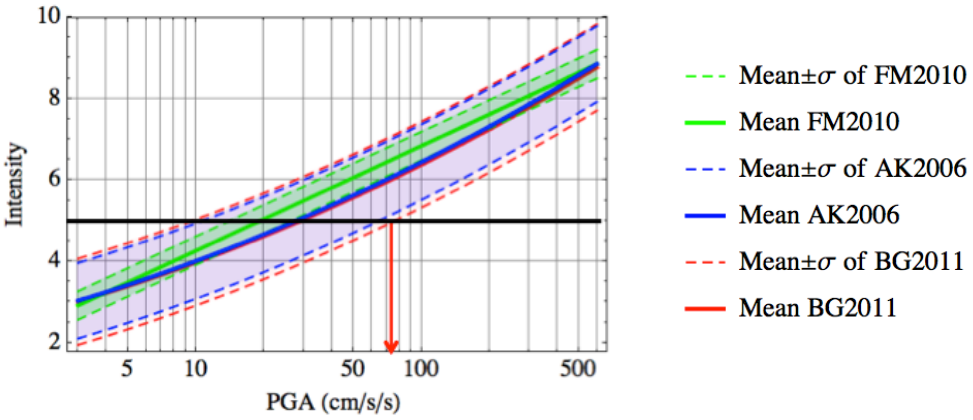

Figure 4.9: Distribution of intensities corresponding to a range of accelerations predicted by three PGA-I correlation equations. All three correlation equations considered in this study (FM2010, AK2006, BG201) predict an intensity higher than 5 for accelerations higher than 77 cm/s^2 (when sampled within ±1σ.)

4.7 Selecting the sites

The testing methodology and the intensity database imposes some constraints on the selection of stations. Here we list the criteria for selecting the sites used for testing the PSHA models.

1) The statistical technique used to determine the completeness periods (Albarello 2001) relies on the available data at each site. A minimum number of observations $I_{OBS} \geq 5$ is required in order to apply the technique. Therefore we selected sites that have at least 8 observations with $I_{OBS} \geq 5$.

2) We test the PSHA models for accelerations higher than 77 cm/s^2 considering observed intensities higher or equal to 5 (see Section 4.6). The PSHA studies of MEDD2002 and AFPS2006 provide results in terms of accelerations corresponding to fixed return periods. The minimum return period used for testing should correspond to accelerations higher than 77 cm/s^2 at the selected sites. Therefore we selected sites that have a predicted PGA corresponding to return periods 100 years given by MEDD2002 and 475 years given by AFPS2006 higher than 77 cm/s^2. Therefore MEDD2002 and AFPS2006 models will be tested for return periods higher than or equal to 100 and 475 years respectively.

3) In SisFrance database, a site corresponds to a municipality (geographical administrative subdivision). Municipalities can be close to each other. We decided to keep a

minimum distance of 20 km between the sites considered in the testing. Among the sites found closer than 20 km far from each other, we chose the site with the longest completeness period.

We generated a synthetic intensity dataset using the earthquake catalog of Geoter (Drouet 2012, see supplement section 4.11.1 for further information about the earthquake catalog) and the intensity attenuation equations developed for several region in France by Bakun & Scotti (2006). There are many uncertainties when estimating synthetic intensity data using an intensity attenuation equation combined with an historical earthquake catalog: e.g. highly dispersed data used to generate the attenuation relation, uncertainties in the estimation of the homogeneous magnitude M_W, depth and location of historical events and etc. Therefore, we used the synthetic data only to have a general idea about the completeness of observations with intensities higher or equal to 5 at the selected sites. Bakun & Scotti (2006) equations rely on calibrating events with magnitudes 3.6 to 5.4 (M_w). For all earthquakes in the catalog with Mw≥4, predicted intensities are generated. We check how many I≥5 are missing at the selected sites in the intensity database. Among the sites selected using the first three criteria explained above, 4 sites appeared to have some missing observations. They are replaced with other sites that are found in the same region and that do not have any missing observations (see Figure 4.10 for an example). These new sites also satisfy the three criteria explained above. The list of the selected sites that are finally used for testing is given in Table 4.2. (see supplement section 4.11.3 for completeness evaluation at 25 sites).

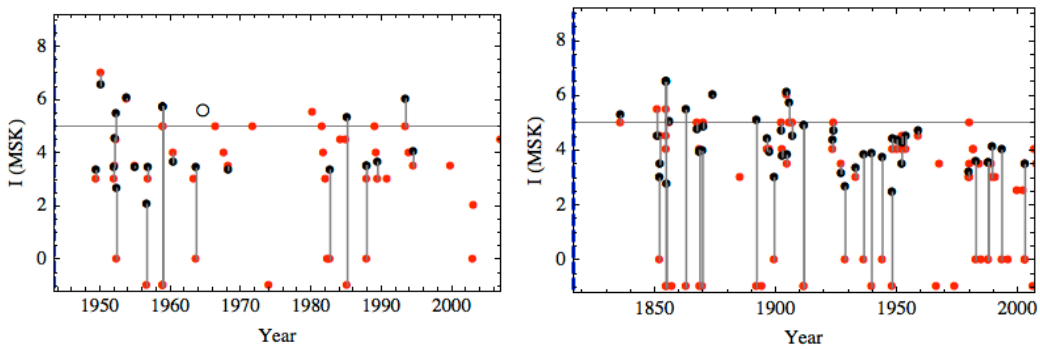

Figure 4.10: Example: Observation history at two sites. (Left) the city of Campan that has one missing records with intensity higher than 5. (Right) the city of Tarbes replacing Campan. Tarbes has no missing records and it satisfies the three selection criteria (see the text). The distance between Tarbes and Campan is 28 km. •: Observed intensities in SisFrance database, •: predicted intensities corresponding to existing observed intensities, o: Predicted intensities with I_{OBS}≥5 that are missing in the SisFrance data. Vertical dashed line is the completeness period for intensities higher than 5 at the given site. Observations with I=-1 given in the SisFrance data represent the

observations for which an intensity values could not be assigned. Observations with I=0 given in the SisFrance data represent the observations that are not felt at the site (I<2).

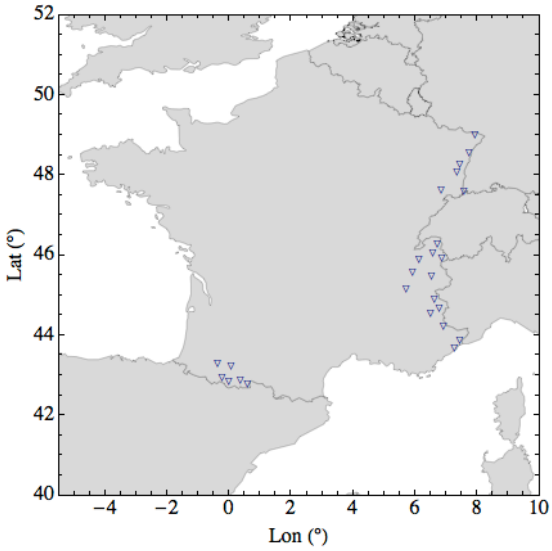

Figure 4.11: Locations of 25 sites selected for testing PSHA models. At these sites, both the acceleration at 100 years return period for MEDD2002 model, and the acceleration at 475 years return period for AFPS2006 model are ≥ 77 cm/s^2 (minimum acceleration threshold that can be tested considering I≥5).

Finally, 25 sites are selected for testing the PSHA models. As a consequence of the selection criteria explained above, the selected sites are found only in the active regions of France (Figure 4.11). Therefore the results of this study will be valid only for this set of sites (belonging to the Pyrenees, the Alps and the Upper Rhine Graben). The distribution of intensities observed at the selected sites is shown in Figure 4.12. The SIGMA hazard model (Carbon *et al.* 2012, Drouet 2012), covering south-east France, considered for testing in Chapter 2, is not considered for testing here as only 8 sites out of the 25 are found in the south-east of France.

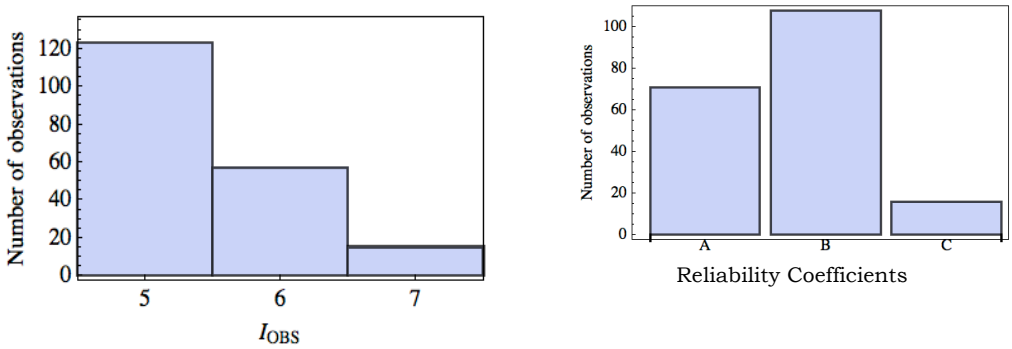

Figure 4.12: (left) Distribution of intensities observed during the completeness periods at 25 sites. (right) Distribution of reliability factors attributed to the intensities observed at 25 sites.

Table 4.2: List of the 25 selected sites

Site	Lon (°)	Lat (°)	Maximum observed intensity during completeness period	Length of completeness period for intensities higher than 5 (years)	Number of observations higher than 5 (MSK)
Abondance	6.72	46.28	6.	114	8
Annecy	6.13	45.9	7.	207	9
Arreau	0.37	42.9	5.5	75	11
Arrens-Marsous	-0.22	42.95	6.5	70	11
Bagnères-De-Luchon	0.6	42.8	7.	105	15
Belfort	6.85	47.65	6.	207	11
Briançon	6.63	44.9	7.	116	13
Ceillac	6.78	44.67	6.5	66	9
Chambery	5.92	45.57	6.5	167	10
Chamonix-Mont-Blanc	6.87	45.92	5.	93	8
Cluses	6.58	46.07	5.5	66	8
Colmar	7.35	48.08	6.	207	10
Embrun	6.5	44.57	7.	76	9
Grenoble	5.72	45.18	6.5	174	16
Huningue	7.58	47.6	5.5	125	8
Luz-Saint-Sauveur	0.	42.87	6.	90	16
Moutiers	6.53	45.48	6.	130	9
Nice	7.27	43.7	6.	207	14
Pau	-0.37	43.3	6.	207	12
Saint-Etienne-De-Tinée	6.92	44.25	5.5	68	9
Sélestat	7.45	48.27	5.5	136	9
Sospel	7.45	43.88	5.	75	8
Strasbourg	7.75	48.58	6.	150	19
Tarbes	0.07	43.23	6.	191	18
Wissembourg	7.93	49.03	7.	207	13

4.8 Testing the PSHA models against observations

The comparison between the historical observations and the predicted hazard obtained from MEDD2002 model considering 25 sites are shown in Figure 4.13. The comparison is displayed separately for the three different PGA-I correlation equations (FM2010, AK2006, BG2011). Whatever the PGA-I equation used, the number of sites predicted by the MEDD2002 model is consistent with the observed number of sites, at return periods 475, 975 and 1975 years. The observed mean number is within the percentiles 5 and 95 of the model distribution. The observed distribution is quite close to the predicted distribution (see section 2.2 of second chapter), both in terms of mean and percentiles, when applying AK2006 and

BG2011 equations. As expected, results for AK2006 and BG2011 equations are very similar. Whatever the PGA-I equation used, the MEDD2002 model seems to estimate more than observed exceedances at 100 years of return period (mean observed number of sites lower than the predicted 2.5% percentile).

The AFPS2006 model is tested at return periods higher than or equal to 475 years and at accelerations higher than or equal to 77 cm/s^2. For all return periods higher than or equal to 475 years, the model is consistent with observations (observed mean within the bounds of the predicted distribution, see section 2.2 of second chapter). For all acceleration levels tested (between 77 and 243 cm/s^2, see Figure 4.15) the model is consistent with observations for all three PGA-I correlation equations. The mean of observed exceedances fall on the 97.5 percentile of the predicted distribution given by AFPS2006 at acceleration 150 and 200 cm/s^2 when BG2011 equation is used. Results for testing AFPS2006 at selected acceleration levels sampling the PGA-I correlation equation within $\pm 2\sigma$ are given in supplement section 4.11.2 for comparison.

As shown by the results, the selection of the PGA-I correlation equation has a strong impact on the PSHA testing results. At 77 cm/s^2 (see Figure 4.15), the mean number of observed sites with exceedance is 9 when FM2010 equation is used whereas it is 15 when BG2011 equation is used. Still, both values are within the bounds of the predicted distribution. For a fixed acceleration, FM2010 predicts mean intensity values which are higher than BG2011, but with an associated uncertainty which is much lower (0.35 for FM2010 and 1.06 for BG2011, see Figure 4.2).

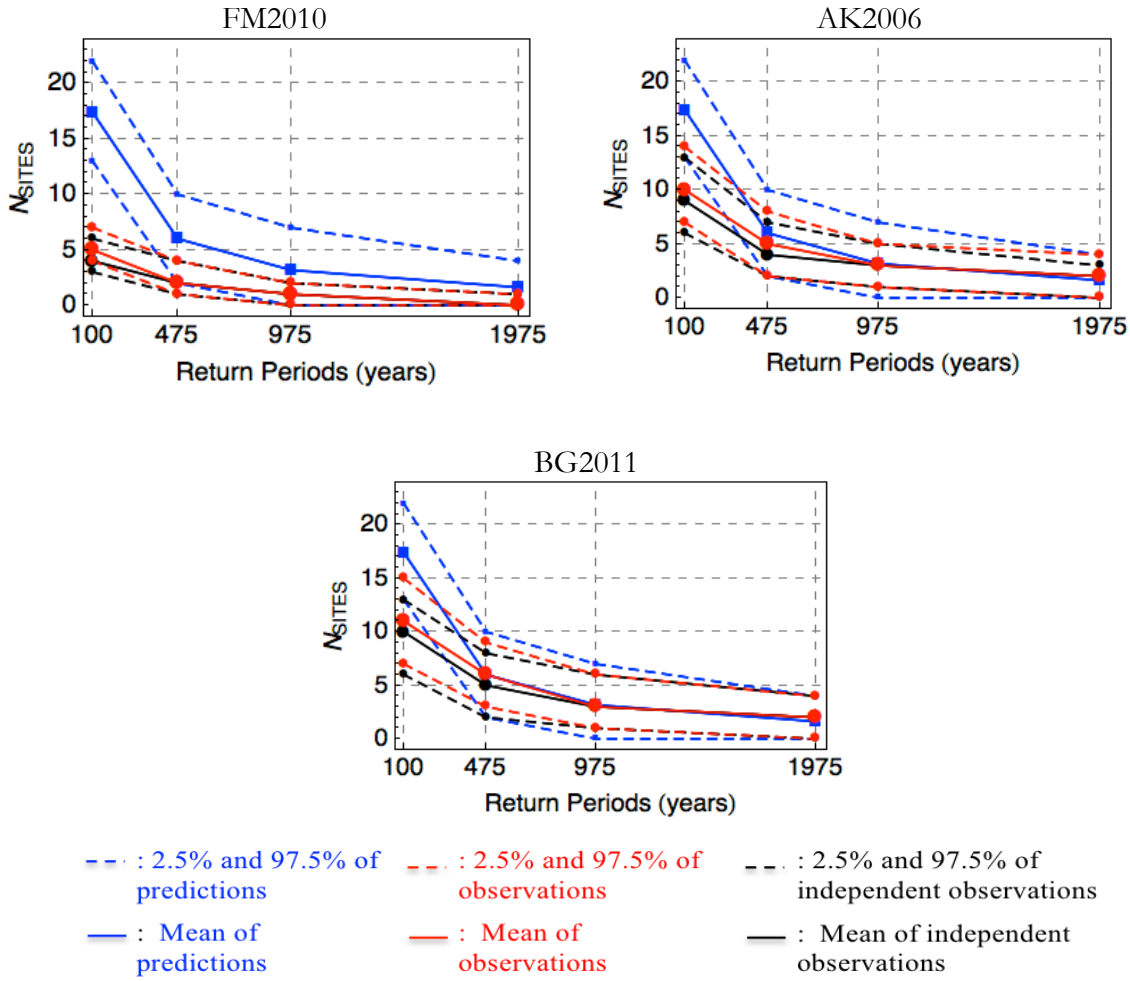

Figure 4.13: Testing the MEDD2002 probabilistic seismic hazard model against macroseismic intensity data observed at 25 sites, for accelerations corresponding to return periods 100 years and larger. Total observation length at 25 sites is 3329 years. The results are displayed separately for the three PGA-I correlation equations. The PGA-I correlation equations are sampled within ±1sigma. N_{SITES} is the number of sites where the acceleration threshold is exceeded. Blue curves: median and percentiles 2.5 and 97.5 of the predicted distributions (see section 2.2 of second chapter), red curves: observed exceedances considering only records of mainshocks, black curves: reduced number of sites in the case of double-counting (PGA-I correlation equations are sampled within ±1sigma).

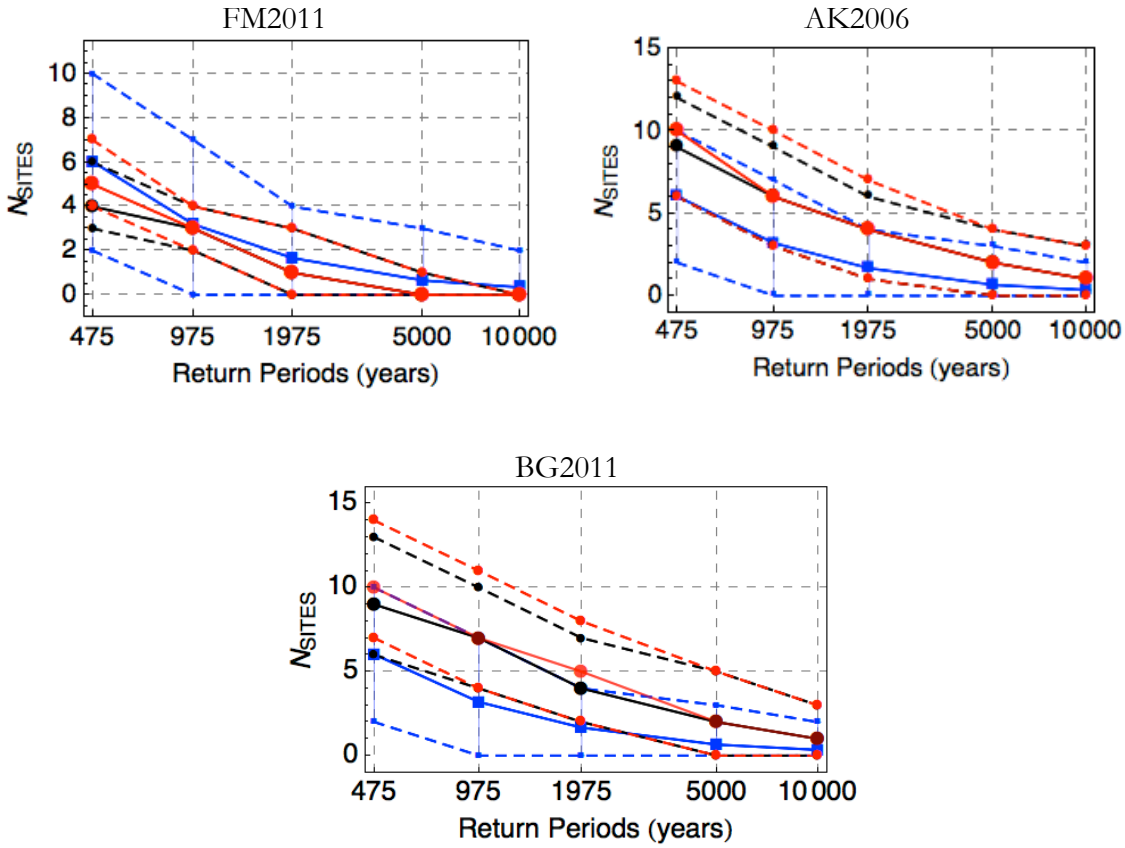

Figure 4.14: Testing the AFPS2006 probabilistic seismic hazard model against macroseismic intensity data observed at 25 sites, for accelerations corresponding to return periods 475 years and larger. Total observation length at 25 sites is 3329 years. (See Figure 4.13 for legend.) The results are displayed separately for three PGA-I correlation equations. Blue curves: median and percentiles 2.5 and 97.5 of the predicted distributions (see section 2.2 of second chapter), red curves: observed exceedances considering only records of mainshocks, black curves: reduced number of sites in the case of double-counting (PGA-I correlation equations are sampled within ±1sigma).

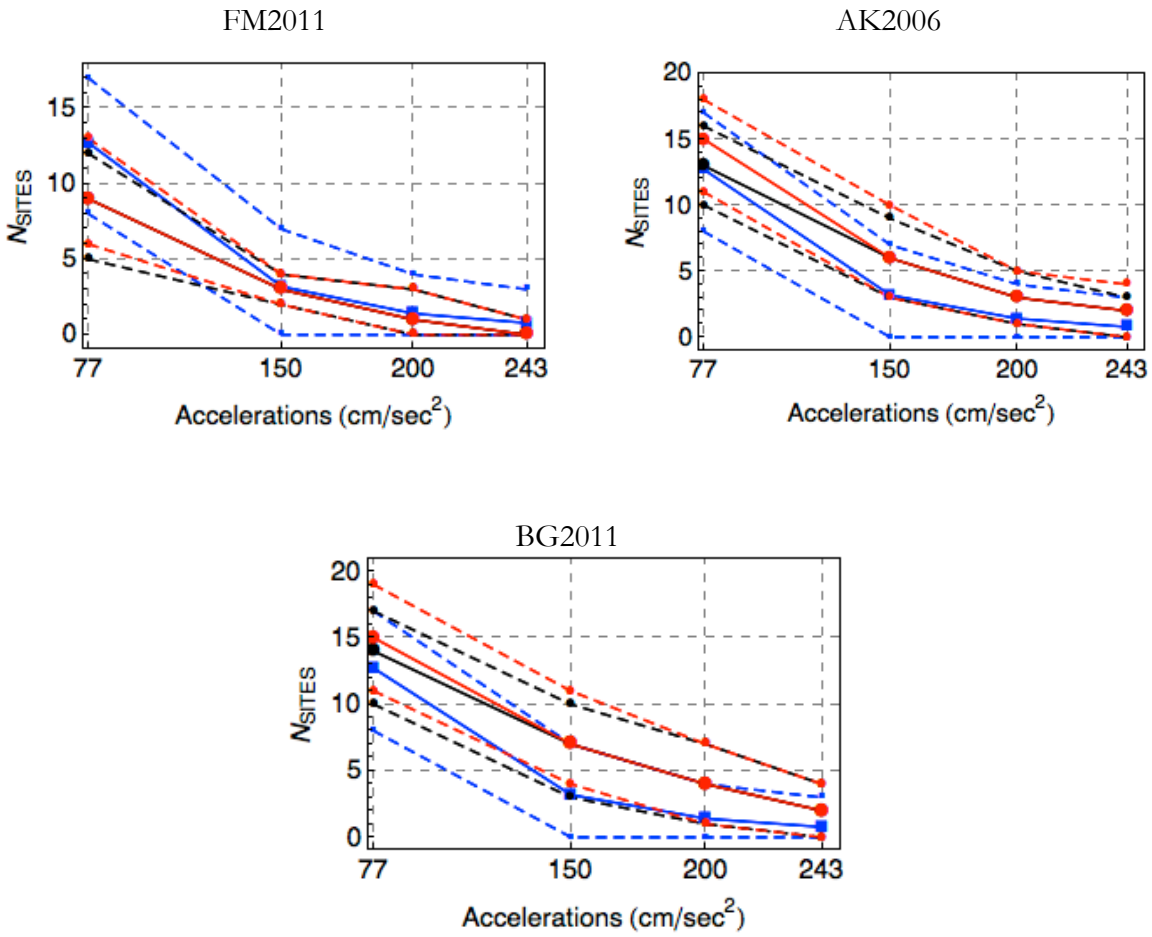

Figure 4.15: Testing the AFPS2006 probabilistic seismic hazard model at selected acceleration levels against macroseismic intensity data observed at 25 sites. Total observation length at 25 sites is 3329 years. (See Figure 4.13 for legend.) The results are displayed separately for three PGA-I correlation equations. Blue curves: median and percentiles 2.5 and 97.5 of the predicted distributions (see section 2.2 of second chapter), red curves: observed exceedances considering only records of mainshocks, black curves: reduced number of sites in the case of double-counting (PGA-I correlation equations are sampled within ±1sigma). See Figure 4.S18 for the results obtained sampling the correlation equations within ±2sigma.

4.9 Conclusion and Discussions

In this study, we have used a database of intensities to test PHSA models. Using observed intensities rather than measured accelerations (as in Chapter 2) allows investigating a longer time window.

Intensity data are only partly included in the PSHA models. Therefore the intensity database contains valuable information that can be used to test the PSHA models. When building the earthquake catalog necessary for the probabilistic seismic hazard assessment, the spatial distribution of intensities for each earthquake are analyzed to derive the epicentral location and an estimate of the magnitude of the earthquake. The earthquake catalog is further used to establish the frequency-magnitude distributions for each source zone. The intensity information at individual sites is never again used in the process of PSHA, and thus is lost. Testing PSHA against intensities enable to use this site information (history at the site). Here we have examined the differences between the predicted number of sites with exceedance with the observed number of sites using the historical intensity database. Testing is led for intensities higher or equal to 5. The completeness periods of sites are estimated using the statistical method of Albarello *et al.* (2001). Since this statistical method relies on the observed data, sites with a minimum number of observations $I \geq 5$ must be selected. Furthermore, only accelerations higher or equal to 77 cm/s^2 can be tested. As a result, the sites used for testing are found in the most active regions of France..

Three PGA-I correlation equations are selected to test the hazard estimations (hazard curves in terms of accelerations) using the historical data (macroseismic intensities), based on the studies by Delavaud *et al.* (2012) and Bigault & Guéguen (2011). Although it is more common to convert intensities to accelerations when testing PSHA models (e.g. Stirling & Petersen 2006, Mezcua *et al.* (2013), Stirling & Gerstenberger 2009), here we prefer to convert the acceleration levels selected for testing into intensities. Two reasons for this choice: 1) two of the 3 PGA-I correlation equations used (AK2006 and BG2011) are designed to estimate intensities from accelerations (only in this direction), 2) the standard deviations of these PGA-I correlation equations represent the uncertainty of the calculated intensities corresponding to a given acceleration level.

For the three correlation equations used, the predictions of MEDD2002 model are consistent with the observations for return periods 475, 975 and 1975 years. However the observations are below the 95% confidence interval at 100 years of return period, which suggest that the model over predicts the hazard at 100 years of return period. The AFPS2006 model could be tested only at return periods higher than 475 years and accelerations between 77 and 243 cm/s^2. AFPS2006 model is consistent with the observations at all return periods and accelerations selected. Not much can be concluded at 10000 years of return period as the results rely on no observed exceedances (FM2010 correlation equation). Both of the PSHA models tested appears to be consistent with observations at these return periods. The results do not allow us to discriminate between these PSHA models at the return periods of interest in earthquake engineering.

These results are valid for the sites considered, and we do not believe that they can be extrapolated to the regions sampled (Pyrenees, Alps, Alsace). Only sites where the acceleration at 475 years (for AFPS2006) and at 100 years (for MEDD2002) are higher than 77cm/s^2 could be considered. As a consequence, the testing is led for a set of sites in the most active regions of France. Furthermore, in order to be able to estimate completeness time periods for I≥5, applying the Albarello (2001) method, sites with a minimum number of observations I≥5 in their history have been selected. It is possible that by doing so, a bias is introduced and that the analysis is concentrating too many sites with exceedances than sampling the regions under study randomly (regions selected in this study are restricted to the 77 cm/s^2 contour). This is why until more tests are performed, the conclusions of the present study should not be extrapolated. Ideally, the completeness time window should be evaluated independently from the observations (e.g. on historical knowledge at the sites), and the sites should be selected based on the predicted exceedance rates only (criteria independent form the observations).

Moreover, only a small part of the SisFrance database can be used, due to completeness reasons. In SisFrance database, if an earthquake is felt but the intensity level felt at the site could not be interpreted, it is reported in the database. At the 25 selected sites for testing, intensity values are reported as undetermined in SisFrance database for 8% of observations. None of these observations can be considered in this study due to their unknown intensity values. One option would be to re-construct the history at the sites by using an atlas of isoseismals (like done in Rey *et al.* 2008, BRGM report). For all earthquakes in

SisFrance, the isoseismals should be drawn. The observed intensity history at sites could be completed with intensities inferred from isoseismals maps.

Besides, one must not forget that the amplitude and the duration of ground shakings at a site depend on the local site conditions. Site effects may enhance the severity of earthquake observed at the site. Site effects at the sites considered for testing the PSHA models should be taken into account. Unlike the accelerometric stations, the historical sites are municipalities that cover a region. Therefore to evidence site effects in the SisFrance database might be a difficult task. At last, the PSHA testing analyses would bear less uncertainty if an equation intensity-acceleration adapted for France could be identified (for intensity levels of interest in the testing). Such a study will not be possible in France until more strong motion recordings correlated with estimate of intensities are available.

4.10 Data and resources

1- SISFRANCE: Files ("*OBSIRENE.xlsx*", "*LOCALITES.xlsx*", "*EVTSIRENE.xlsx*" and "*EPCSIRENE.x*lsx") given on 04/09/2013 by EDF (CEIDRE / TEGG / SGG). The SisFrance database (also available at http://www.sisfrance.net/) belongs to BRGM, EDF and IRSN.
2- Earthquake catalog of Geoter: sent by EDF (P. Traversa) on 10/04/2014 (file name "*Catalogue_sismicite_FRANCE_2013.txt*").

4.11 Supplement

4.11.1 Evaluating the completeness of data using earthquake catalog

To evaluate the completeness of the observations at the selected sites, we generated synthetic data inferred from an earthquake catalog. The catalog of Geoter (Drouet 2012) is a homogenized catalog in terms of magnitude (M_W) covering roughly the last 1000 years. Few moment magnitudes have been estimated directly from waveforms, most magnitudes are obtained by converting different magnitude types into Mw. Equivalent moment magnitudes have been derived for historical earthquakes (magnitudes between 1.9 to 7.2). Locations of earthquakes are plotted on the map (Figure 4.S16).

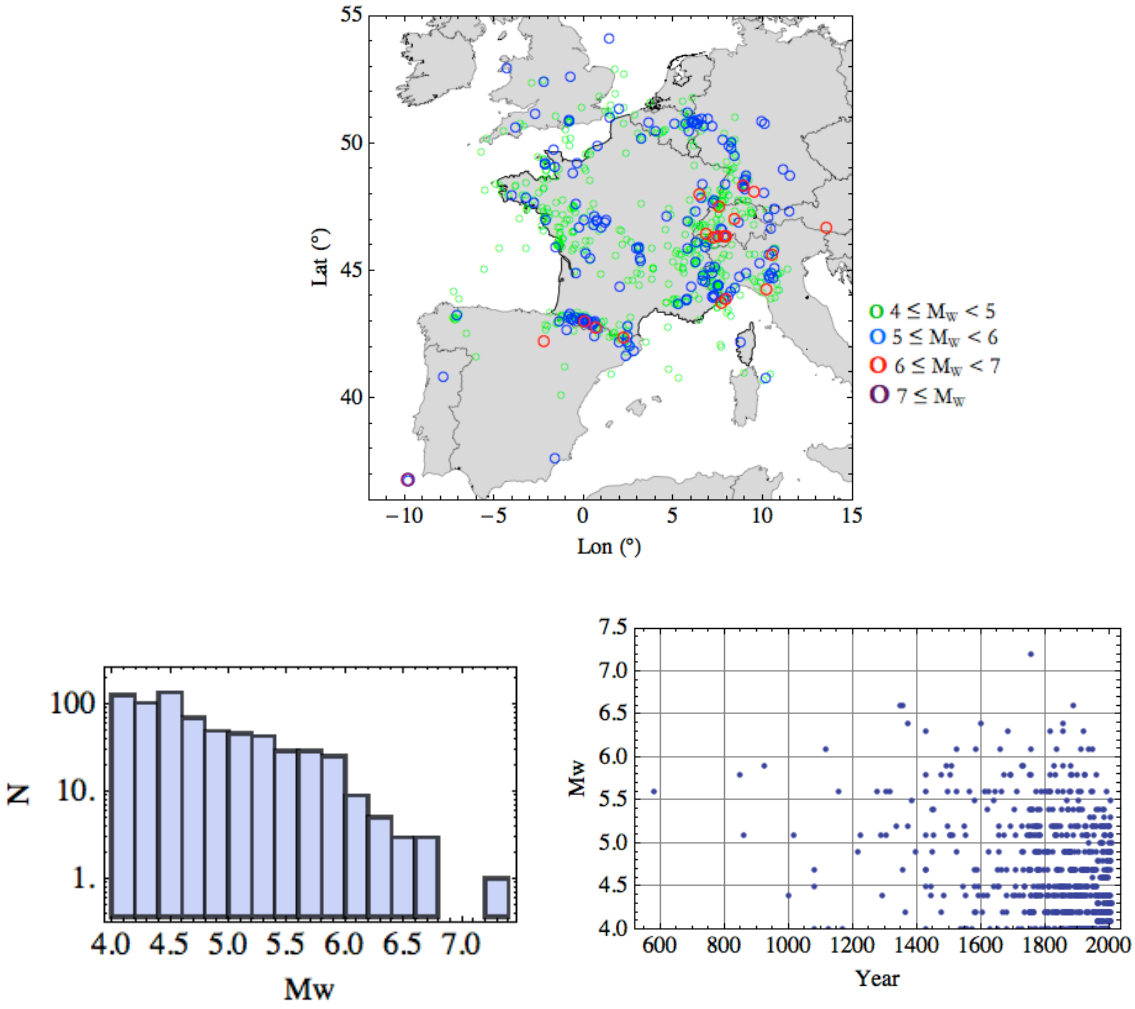

Figure 4.S16: (top) Map of all earthquakes in Geoter Earthquake Catalog with magnitudes higher than or equal to 4(M_W). (bottom, left) magnitude distribution. (bottom, right) time series of earthquake magnitudes

The attenuation relationship of Bakun & Scotti (2006), based on intensities from the SisFrance data, is used to estimate intensities at each selected site. The synthetic intensity data is calculated using the magnitudes, focal depths, dates and the locations of the events in the earthquake catalog. We considered only the magnitudes higher than 4 (M_W) due to the magnitude validity threshold limit of the attenuation relationship. The attenuation relationship of Bakun & Scotti (2006) predicts real numbers for intensities. We rounded the predicted intensities to the closest integer to compare them with observed intensities.

4.11.2 Sampling the PGA-I correlation equations within ±2sigma range

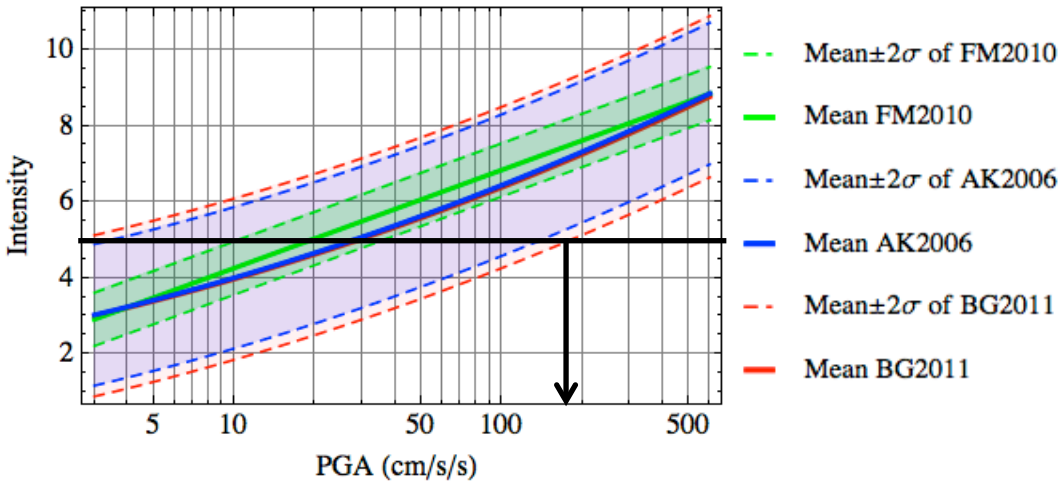

Figure 4.S17: Determining the minimum acceleration level that can be used for testing the PSHA models when the three PGA-I correlation equations selected are sampled within ±2σ. All three correlation equations considered in this study (FM2010, AK2006, BG201) predict an intensity higher than 5 for accelerations higher than 180 cm/s^2 when they are sampled within ±2σ.

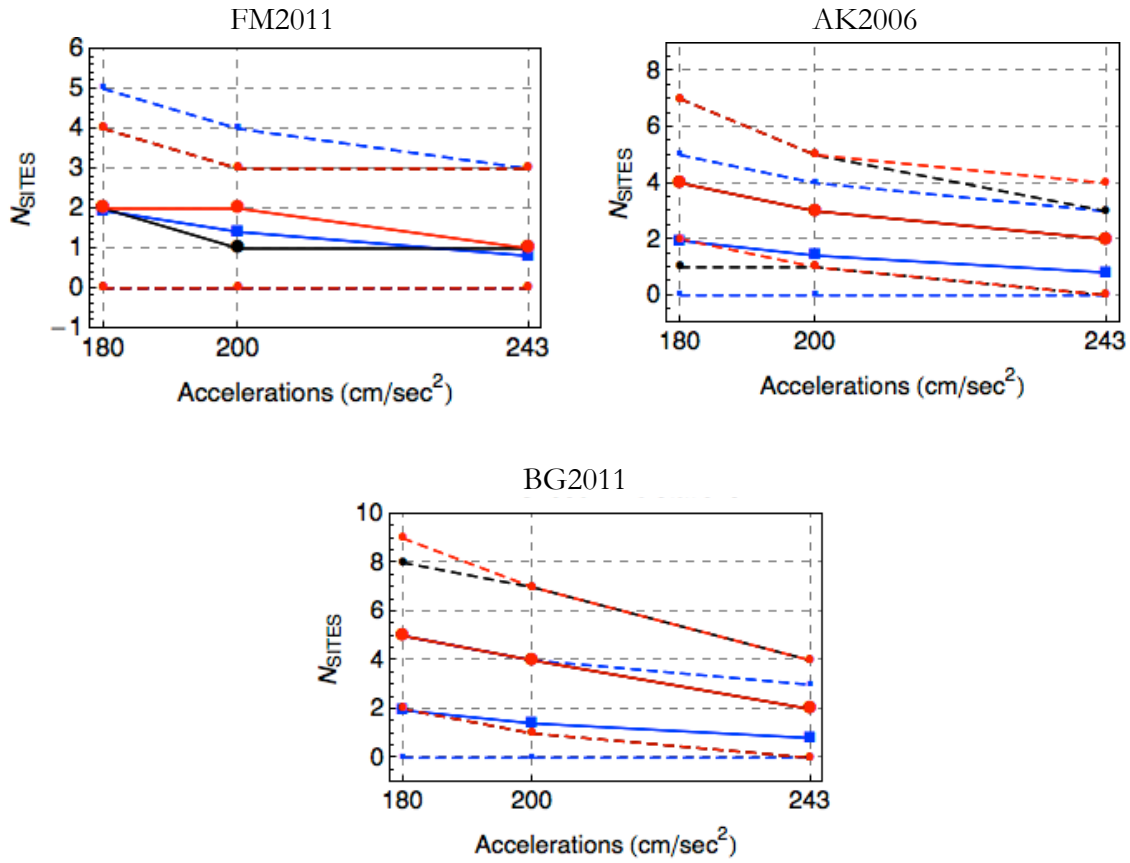

Figure 4.S18: Testing the AFPS2006 probabilistic seismic hazard model against macroseismic intensity data observed at 25 sites. Total observation length at 25 sites is 3329 years. (See Figure 4.13 for legend.) The results are displayed separately for three PGA-I correlation equations. Blue curves: median and percentiles 2.5 and 97.5 of the predicted distributions (see section 2.2 of second chapter), red curves: observed exceedances considering only records of mainshocks (PGA-I correlation equations are sampled within ±**2**sigma), black curves: reduced number of sites in the case of double-counting. The minimum acceleration level selected for testing is determined based on the accelerations corresponding to intensities higher than 5 at mean-2sigma of the distribution predicted by the three PGA-I correlation equations used (see Figure 4.S17).

4.11.3 Determining the completeness periods at selected sites

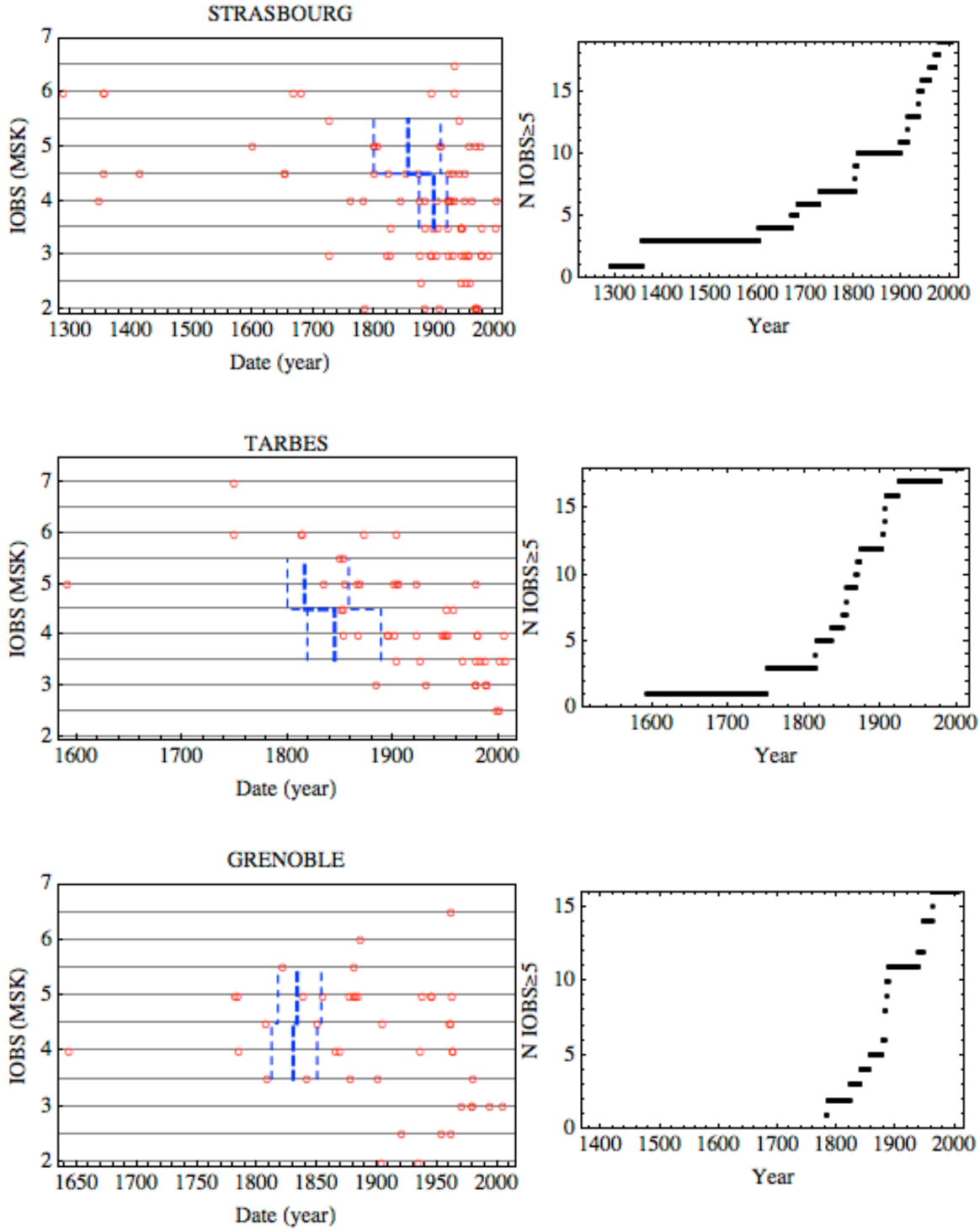

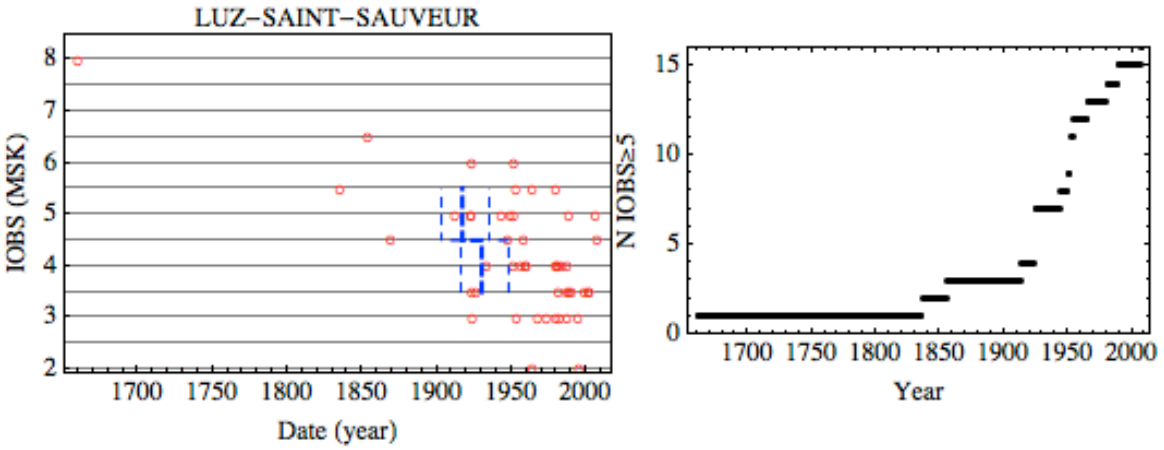
LUZ–SAINT–SAUVEUR
IOBS (MSK)
Date (year)
N IOBS≥5
Year

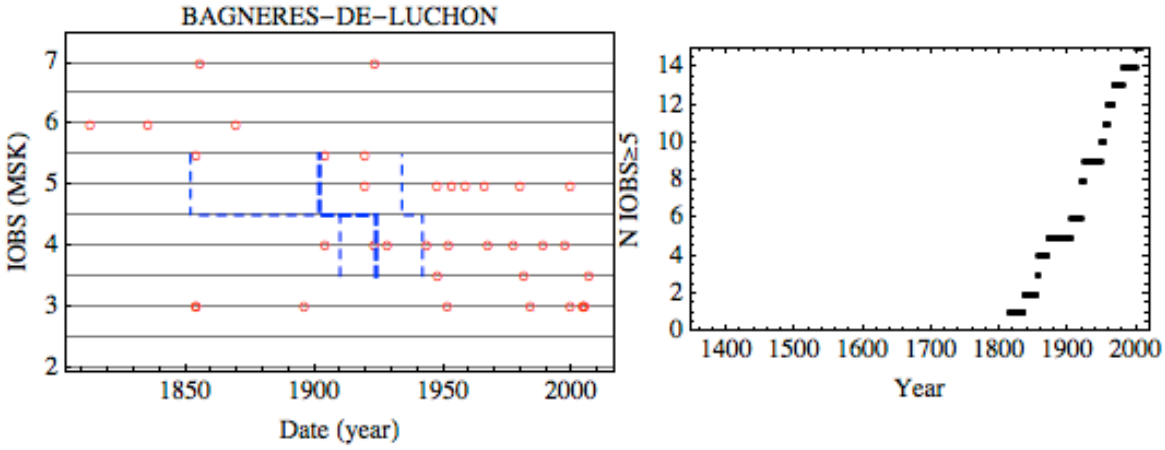
BAGNERES–DE–LUCHON
IOBS (MSK)
Date (year)
N IOBS≥5
Year

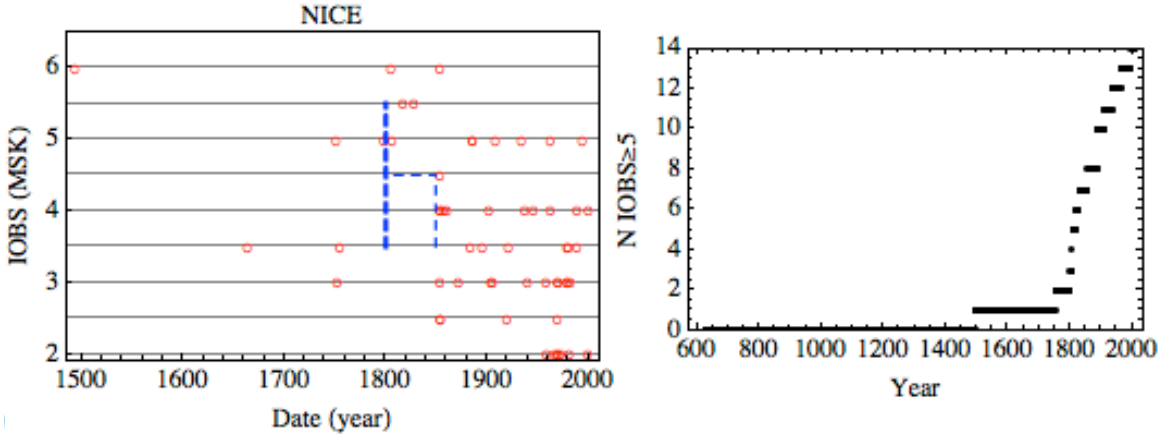
NICE
IOBS (MSK)
Date (year)
N IOBS≥5
Year

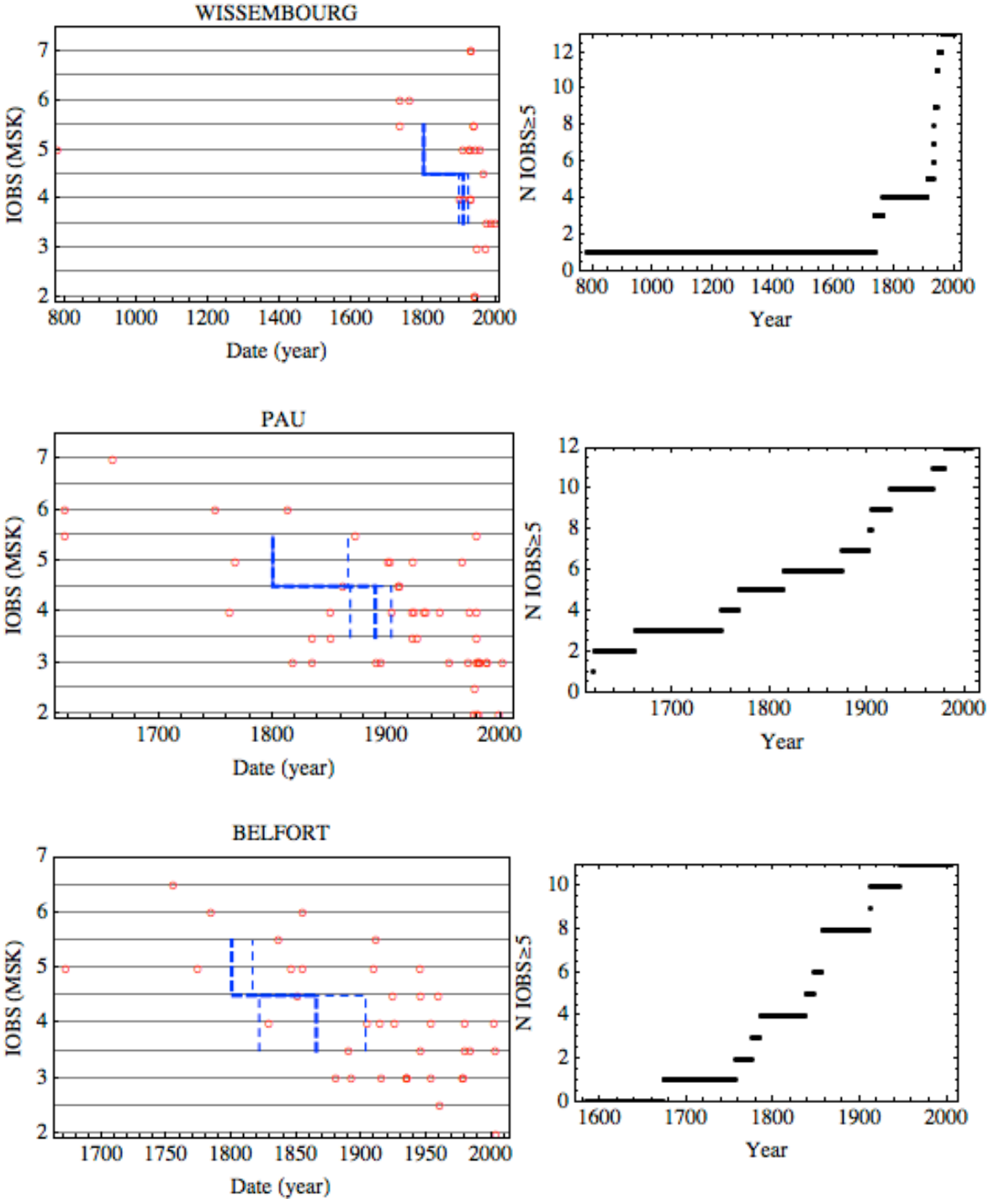
WISSEMBOURG
IOBS (MSK)
Date (year)
N IOBS≥5
Year
PAU
IOBS (MSK)
Date (year)
N IOBS≥5
Year
BELFORT
IOBS (MSK)
Date (year)
N IOBS≥5
Year

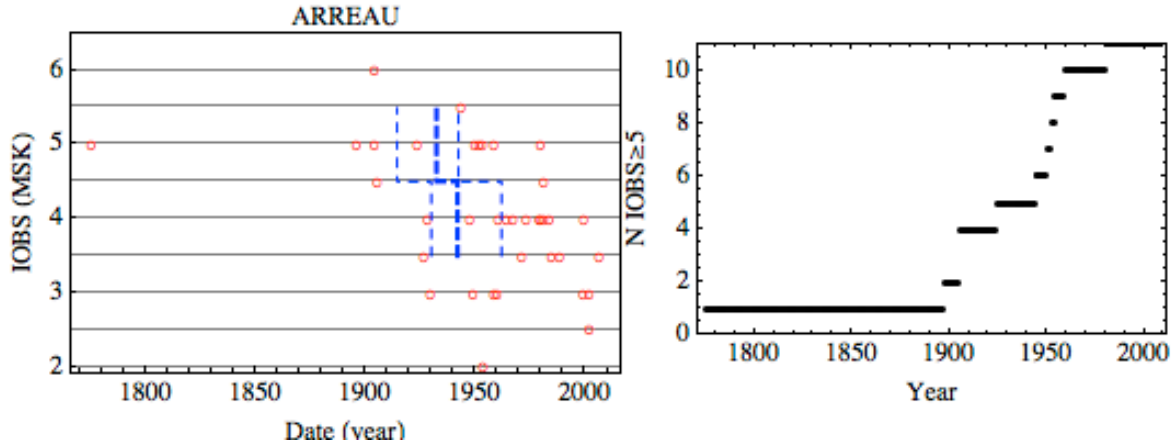
ARREAU
IOBS (MSK)
Date (year)
N IOBS≥5
Year

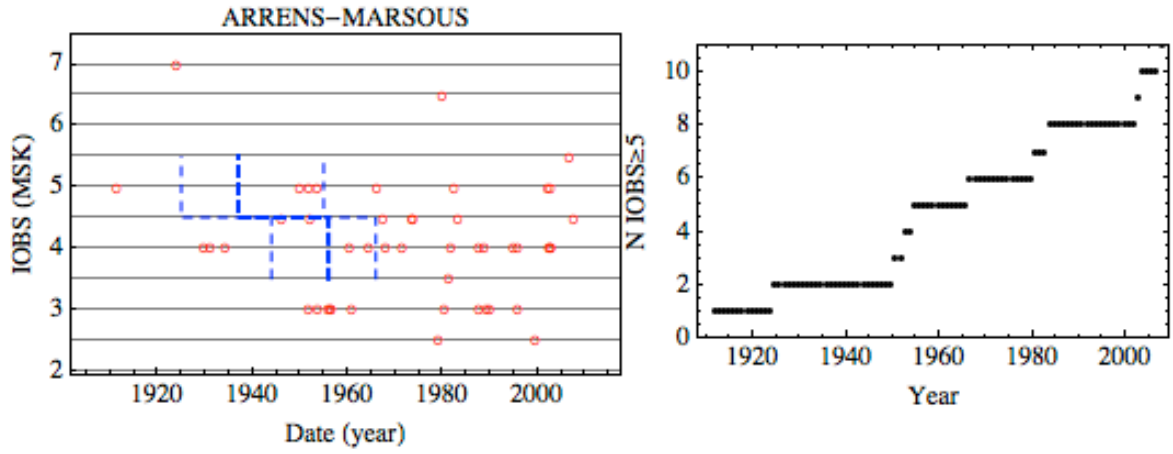
ARRENS−MARSOUS
IOBS (MSK)
Date (year)
N IOBS≥5
Year

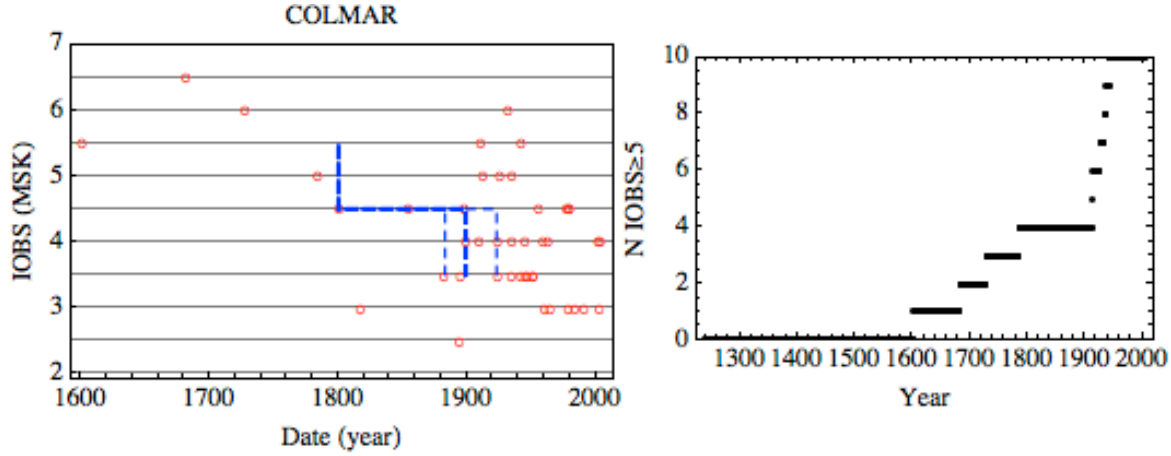
COLMAR
IOBS (MSK)
Date (year)
N IOBS≥5
Year

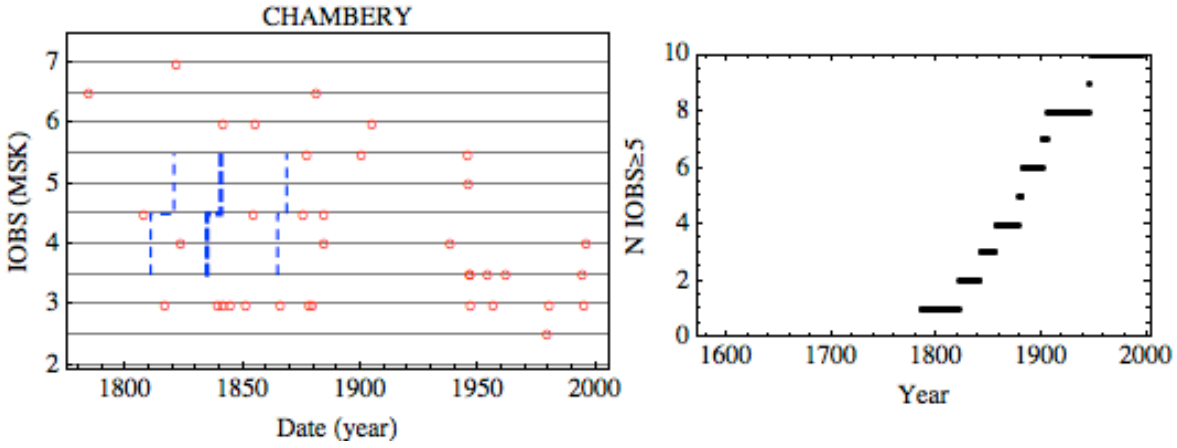
CHAMBERY
IOBS (MSK)
Date (year)
N IOBS≥5
Year

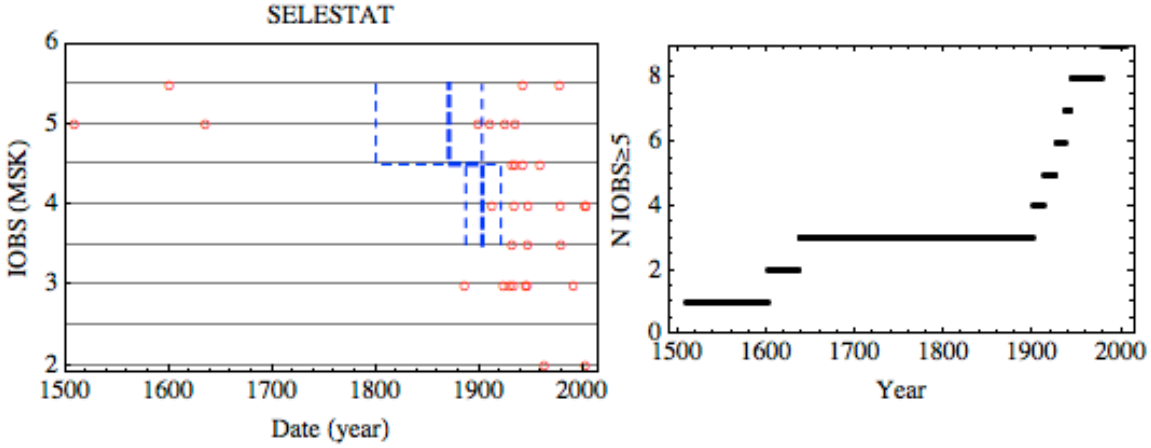
SELESTAT
IOBS (MSK)
Date (year)
N IOBS≥5
Year

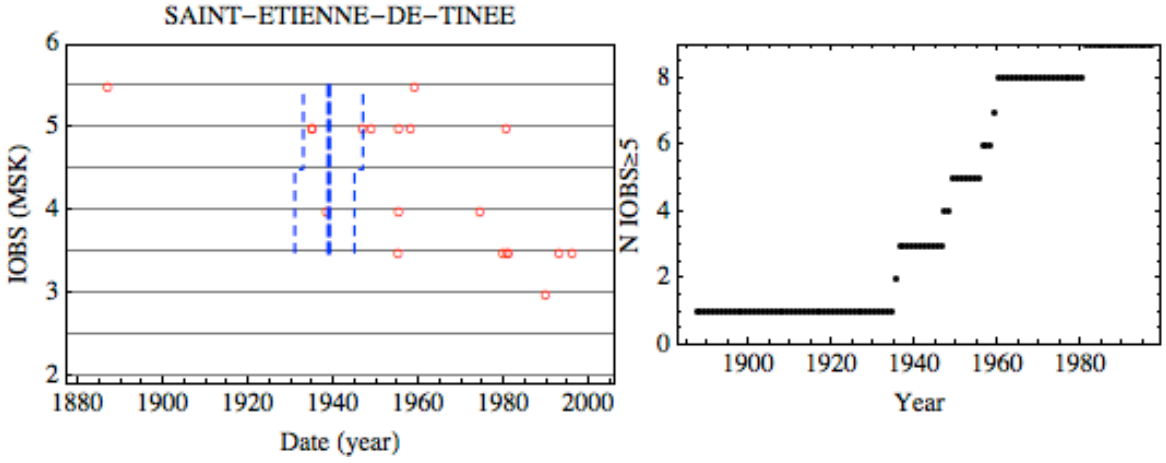
SAINT−ETIENNE−DE−TINEE
IOBS (MSK)
Date (year)
N IOBS≥5
Year

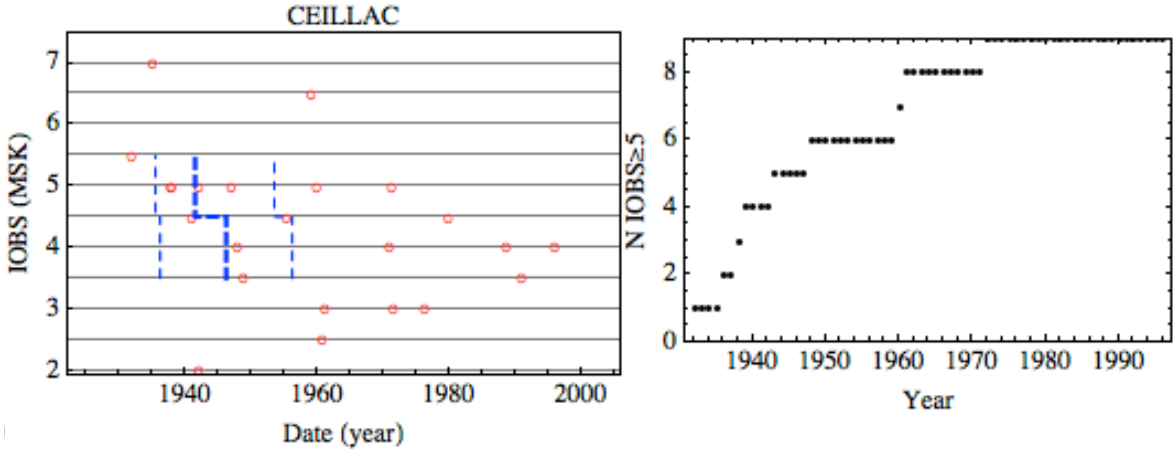
CEILLAC
IOBS (MSK)
Date (year)
N IOBS≥5
Year

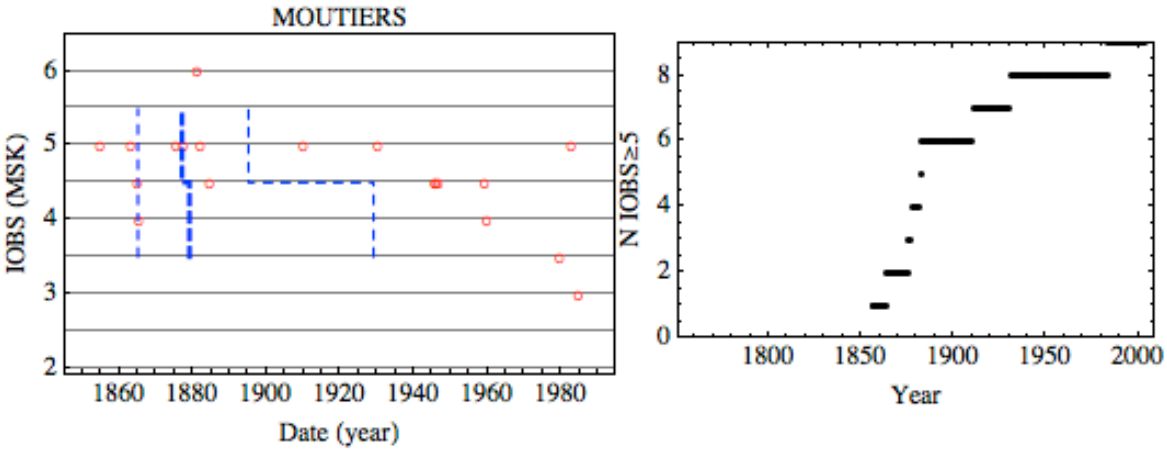
MOUTIERS
IOBS (MSK)
Date (year)
N IOBS≥5
Year

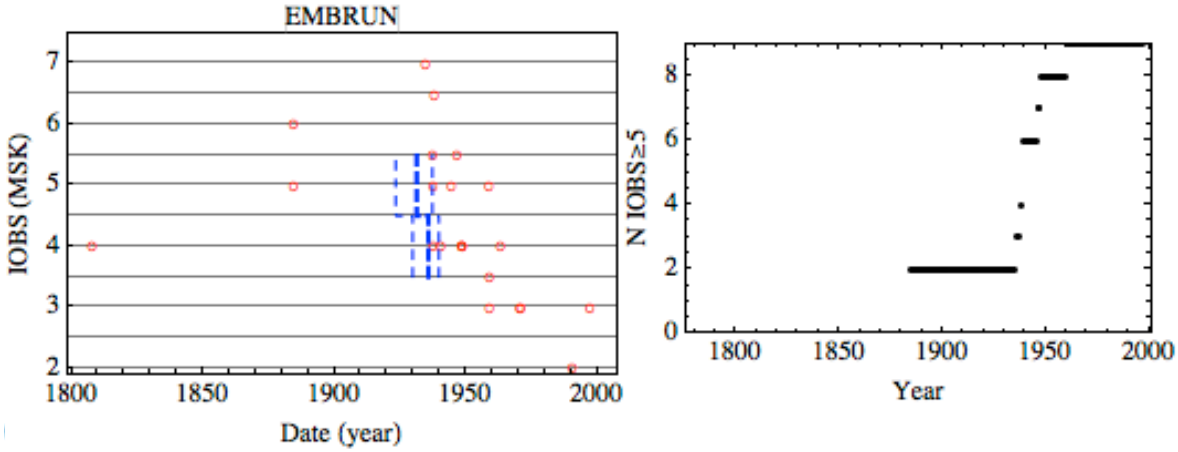
EMBRUN
IOBS (MSK)
Date (year)
N IOBS≥5
Year

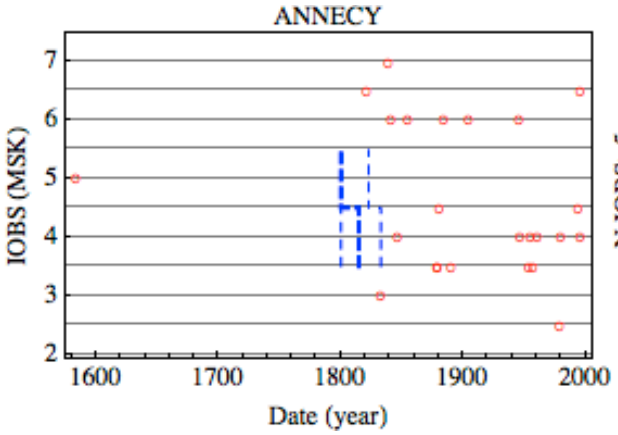
ANNECY
IOBS (MSK)
Date (year)
1600
1700
1800
1900
2000
2
3
4
5
6
7

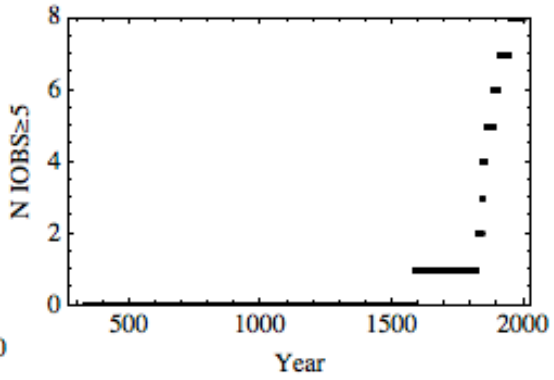
N IOBS≥5
Year
500
1000
1500
2000
0
2
4
6
8

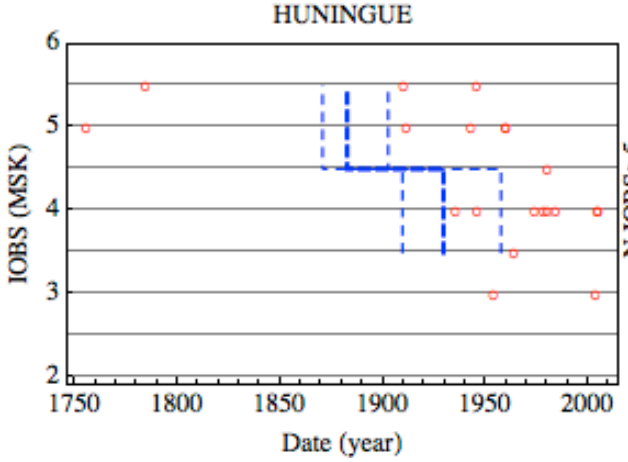
HUNINGUE
IOBS (MSK)
Date (year)
1750
1800
1850
1900
1950
2000
2
3
4
5
6

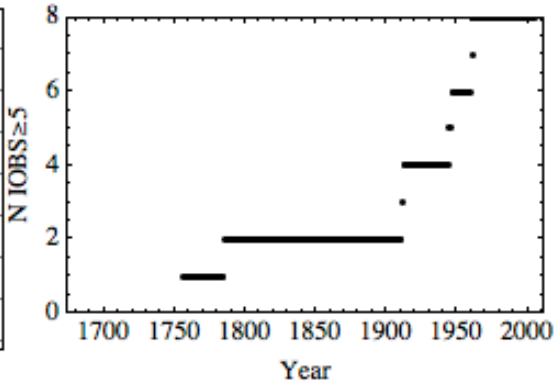
N IOBS≥5
Year
1700
1750
1800
1850
1900
1950
2000
0
2
4
6
8

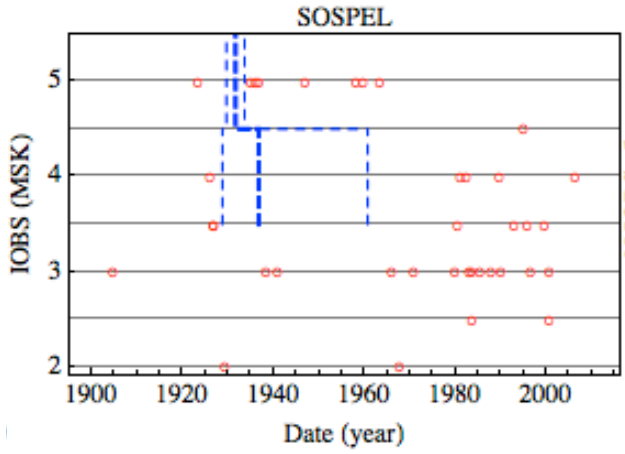
SOSPEL
IOBS (MSK)
Date (year)
1900
1920
1940
1960
1980
2000
2
3
4
5

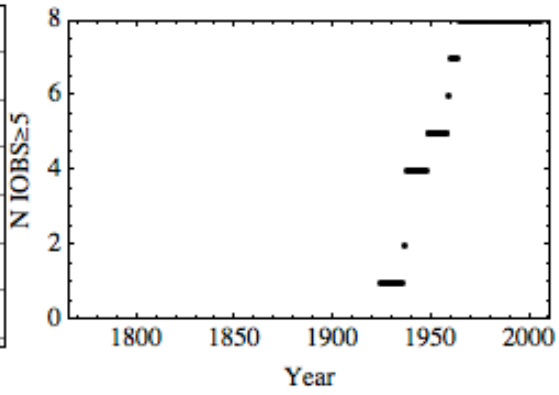
N IOBS≥5
Year
1800
1850
1900
1950
2000
0
2
4
6
8

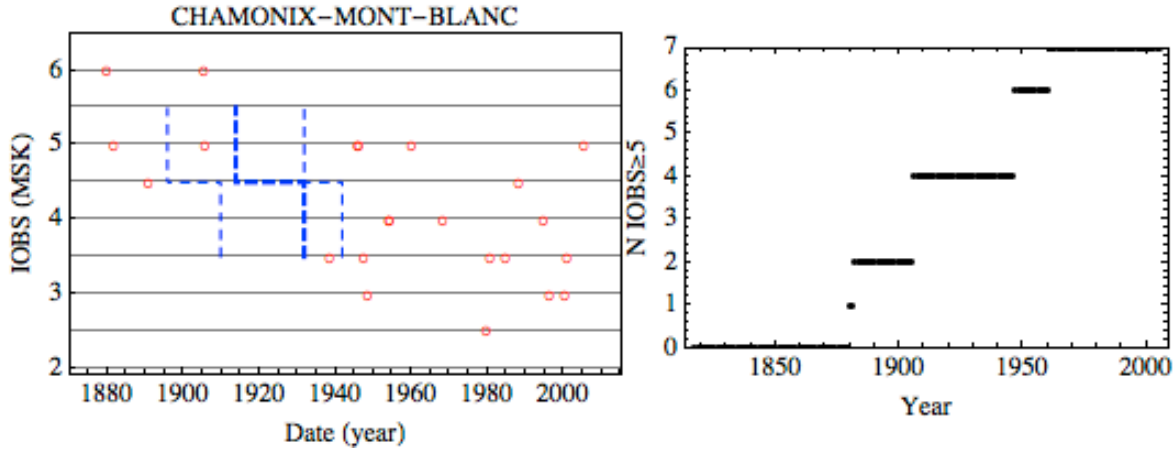
CHAMONIX–MONT–BLANC
IOBS (MSK)
Date (year)
N IOBS≥5
Year

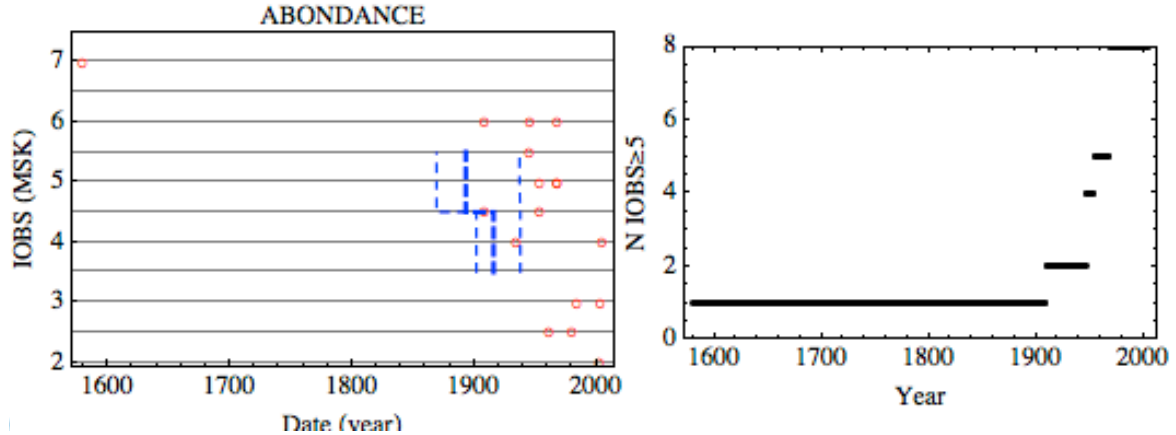
ABONDANCE
IOBS (MSK)
Date (year)
N IOBS≥5
Year

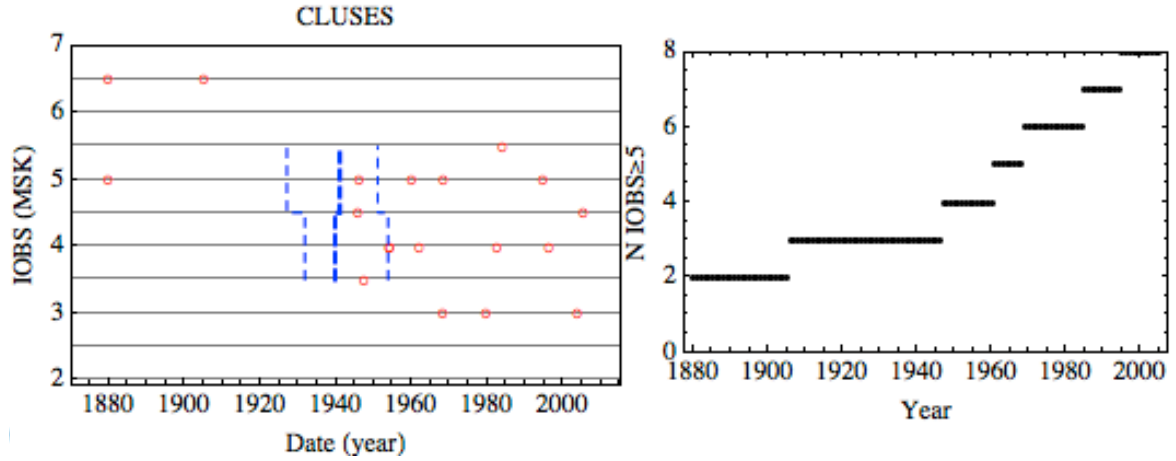
CLUSES
IOBS (MSK)
Date (year)
N IOBS≥5
Year

Chapter 5

Conclusions and perspectives

In this study, we propose to compare the predicted hazard given by PSHA models with observations. The methodology is a variant of the techniques introduced in Albarello & D'Amico (2008) and Gerstenberger & Stirling (2010). To compensate for short observation time windows at individual sites, a sampling in space is implemented. The observed number of sites with exceedance over the total time window available is compared to the predicted number of sites given by the PSHA model. We study the limits and the sensitivities of the testing method to understand if the results are stable and meaningful. We analyse the dependence of the results on:

- The number of sites sampled, the spatial region sampled, and the length of the observation time windows used

- The inter-distance between sites to ensure that sites can be considered independent (assumption required by the testing method),

- Using the observed number of sites with (one or more) exceedance or the total number of exceedances

- Suppressing or not double-counting (same earthquake recorded at more than 1 site)

- Including or not aftershocks

Besides, thorough studies to identify potential gaps in the recorded data have ben led, showing that this aspect should not be neglected. Also, testing has been led on synthetic data with simulations carried out based on an earthquake catalog coupled to a ground-motion prediction equation, in order to extend the observation time windows.

The method is first applied to France using accelerometric data or synthetic data (obtained from an earthquake catalog) and testing three PSH models (MEDD2002, AFPS2006

and SIGMA2012). The results show that all models over-estimate the number of sites with exceedance for low acceleration levels (below 30 to 70 cm/s^2 depending on the model and the dataset) or short return periods (smaller than 50 yrs for AFPS2006 and 475 yrs for MEDD2002). For higher ground motion levels/return periods, the models are consistent with the observations. However, there are very few observations above 70 cm/s^2 so that it is difficult to reject a model at these ground-motion levels.

In the second chapter, we use accelerometric data from the Turkish network, which contain higher ground motions (PGA up to around 500 cm/s^2). We evaluate the consistency between the hazard results from SHARE ("Seismic Hazard Harmonization in Europe", Woessner et al. 2012) and accelerometric data in Turkey. The model is tested using different sets of stations with different inter-site distances and observation lifetimes. Results show that the SHARE PSHA model is consistent with the observations for accelerations larger than 103 cm/s^2 and for all sets of sites and observation lengths considered. For accelerations between 52.7 and 103 cm/s^2, the fit is sensitive to the observation time windows used.

Previous studies testing PSHA against observations provide results for 1 or 2 acceleration levels (Albarello & D'Amico 2008, Gerstenberger & Stirling 2010). By leading the tests systematically for a wide range of accelerations, we show that the results obtained for one acceleration level should not be extrapolated to other levels.

Using accelerometric data both in France and in Turkey allow us to reject PSHA models at small acceleration levels (smaller than ~100 cm/s^2), where the predicted rate was higher than observed. However, the tests did not allow us to reject models or distinguish between different models at the return periods (acceleration levels) of interest in earthquake engineering (> 475 years), due to the small number of observations at moderate-to-high acceleration levels. Indeed, the observation lifetime of accelerometric stations that could be exploited are limited.

The French historical intensity database allows us to investigate longer return periods and stronger acceleration levels. It is shown that the intensity levels and the time coverage of macroseismic intensity data enable to test PSHA for return periods of interest in earthquake engineering in France unlike the accelerometric data. However, considering the uncertainties in the macroseismic intensities and the hypothesis required to apply to method, the results based on macroseismic intensities should be examined with great caution. Further studies are required to validate the results obtained using macroseismic intensities. At present, the two limiting key

points are: the selection of an equation intensity-PGA adapted to the French data, and the estimation of completeness time periods for intensity levels. Rather than estimating the completeness based on the data themselves, completeness periods could be evaluated based on historical grounds (e.g. Stucchi *et al.* 2004 in Italy). In such case, sites with few or no data could be included in the analysis. Furthermore, to increase the number of sites and be more confident about completeness, an atlas of isoseismals like the one currently under development at the BRGM (first version in Rey *et al.* 2008) could be used to re-construct the observation history at the sites. The testing could thus be led on a selection of sites independent from the number of observed intensities, and uniformly distributed in space. A lot remains to be done for testing PSHA against intensity data.

Bibliography

Akkar, S. & Bommer, J.J. (2010). Empirical Equations for the Prediction of PGA, PGV, and Spectral Accelerations in Europe, the Mediterranean Region, and the Middle East. *Seismological Research Letters*, 81, 195–206.

Akkar, S. & Çagnan, Z. (2010). A Local Ground-Motion Predictive Model for Turkey, and Its Comparison with Other Regional and Global Ground-Motion Models. *Bulletin of the Seismological Society of America, 100* (6), 2978–2995.

Akkar, S., Çagnan, Z., Yenier, E., Erdogan, Ö., Sandıkkaya, M. A., & Gülkan, P. (2010). The recently compiled Turkish strong motion database: preliminary investigation for seismological parameters. *Journal of Seismology,* 14(3), 457–479.

Akkar, S., Sandıkkaya, M. A., Senyurt, M., Azari Sisi, A., Ay, B. Ö., Traversa, P., Douglas, J., et al. (2014). Reference database for seismic ground-motion in Europe (RESORCE). *Bulletin of Earthquake Engineering,* 12(1), 311–339.

Albarello, D., Camassi, R. & Rebez, A. (2001). Detection of space and time heterogeneity in the completeness of a seismic catalog by a statistical approach: an application to the Italian area. *Bulletin of the Seismological Society of America*, 91(6), 1694-1703.

Albarello, D. & D'Amico, V. (2008). Testing probabilistic seismic hazard estimates by comparison with observations: an example in Italy. *Geophysical Journal International*, 175, 1088–1094.

Alptekin, Ö., Nábelek, J. L. & Toksöz, M. N. (1986). Source mechanism of the Bartin earthquake of September 3, 1968 in northwestern Turkey: Evidence for active thrust faulting at the southern Black Sea margin. *Tectonophysics*, 122(1–2), 73–88.

Anderson, J. G. & Brune, J. N. (1999). Probabilistic seismic hazard analysis without the ergodic assumption. *Seismological Research Letters*, 70(1), 19-28.

Anderson, J. G., Brune, J. N., Biasi, G., Anooshehpoor, A. & Purvance, M. (2011). Workshop Report: Applications of Precarious Rocks and Related Fragile Geological Features to US National Hazard Maps. *Seismological Research Letters,* 82(3), 431-441.

Atkinson, G.M. (2008). Ground-Motion Prediction Equations for Eastern North America from a Referenced Empirical Approach: Implications for Epistemic Uncertainty. *Bulletin of the Seismological Society of America,* 98, 1304–1318.

Atkinson, G. M. & Kaka, S. I. (2006). Relationships between felt intensity and instrumental ground motion for New Madrid ShakeMaps. Department of Earth Sciences, Carleton University.

Baker, J.W., Abrahamson, N.A., Whitney, J.W., Board, M.P. & Hanks, T.C. (2013). Use of Fragile Geologic Structures as Indicators of Unexceeded Ground Motions and Direct Constraints on Probabilistic Seismic Hazard Analysis. *Bulletin of the Seismological Society of America,* 103, 1898–1911.

Baker W. J. (2008). An Introduction to Probabilistic Seismic Hazard Analysis (PSHA), http://www.stanford.edu/~bakerjw/Publications/Baker_%282008%29_Intro_to_PSHA_v1_3.pdf, 72 pages, version 1.3, last retrieved 11/04/2014.

Bakun, W. H. & Scotti, O. (2006). Regional intensity attenuation models for France and the estimation of magnitude and location of historical earthquakes. *Geophysical Journal International*, 164 (3), 596–610.

Beauval, C. & Scotti, O. (2004). Quantifying Sensitivities of PSHA for France to Earthquake Catalog Uncertainties, Truncation of Ground-Motion Variability, and Magnitude Limits. *Bulletin of the Seismological Society of America,* 94, 1579–1594.

Beauval, C., Bard, P.-Y., Hainzl, S. & Guéguen, P. (2008). Can Strong-Motion Observations be Used to Constrain Probabilistic Seismic-Hazard Estimates? *Bulletin of the Seismological Society of America,* 98, 509–520.

Beauval, C. (2011). On the use of observations for constraining probabilistic seismic hazard estimates - brief review of existing methods. *International Conference on Applications of Statistics and Probability in Civil Engineering*, August 1-4, Zurich, Switzerland, 5 pages.

Beauval, C., Tasan, H., Laurendeau, A., Delavaud, E., Cotton, F., Guéguen, P. & Kuehn, N. (2012). On the Testing of Ground‐Motion Prediction Equations against Small‐Magnitude Data. *Bulletin of the Seismological Society of America,* 102, 1994–2007.

Bertrand, E. (1757). *Mémoires historiques et physiques sur les tremblemens de terre*. Pierre Gosse.

Bigault G. & Guéguen P. (2011). Evaluation de la vulnérabilité du bâti à partir des caractéristiques générales des structures. Programme ALCOTRA, project Interreg RickNat, groupe sismicité, 53 p.

Bommer, J. J., Douglas, J. & Strasser, F. O. (2003). Style-of-faulting in ground-motion prediction equations. *Bulletin of Earthquake Engineering,* 1(2), 171-203.

Bommer, J.J., Stafford, P.J., Alarcon, J.E. & Akkar, S. (2007). The Influence of Magnitude Range on Empirical Ground-Motion Prediction. *Bulletin of the Seismological Society of America,* 97, 2152–2170.

Boore, D.M. & Atkinson, G.M. (2008). Ground-Motion Prediction Equations for the Average Horizontal Component of PGA, PGV, and 5%-Damped PSA at Spectral Periods between 0.01s and 10.0s. *Earthquake Spectra*, 24, 99.

Boore, D.M., Joyner, W.B. & Fumal, T.E. (1997). Equations for estimating horizontal response spectra and peak acceleration from western North American earthquakes: a summary of recent work. *Seismological Research Letters,* 68: 128–153

Bozkurt, E. (2001). Neotectonics of Turkey–a synthesis. *Geodinamica Acta*, 14(1), 3-30.

Campbell, K.W. (1997). Empirical near-source attenuation relationships for horizontal and vertical components of peak ground acceleration, peak ground velocity, and pseudo-absolute acceleration response spectra. *Seismological Research Letters,* 68:154–179

Cara, M., Schlupp, A. & Sira, C. (2006). Observations Sismologiques : sismicité de la France en 2000, 2001, 2002. Bureau Central Sismologique Français ULP/EOST – CNRS/INSU, Strasbourg.

Cara, M., Schlupp, A. & Sira, C. (2007). Observations Sismologiques : sismicité de la France en 2003, 2004, 2005. Bureau Central Sismologique Français ULP/EOST – CNRS/INSU, Strasbourg.

Carbon, D., Drouet, S., Gomes, C., Leon, A., Martin, Ch. & Secanel, R. (2012). Initial probabilistic seismic hazard model for France's southeast ¼. Geoter Report, SIGMA Project, 2012-D4-41.

Çevikbilen, Y.S., & Taymaz, T. (2012). Earthquake source parameters along the Hellenic subduction zone and numerical simulations of historical tsunamis in the Eastern Mediterranean. *Tectonophysics*, 536–537(0), 61–100.

Chiou, B. S.-J. & Youngs, R. R. (2008). An NGA Model for the Average Horizontal Component of Peak Ground Motion and Response Spectra. *Earthquake Spectra*, 24, 173-215.

Cisternas, A., Philip, H., Bousquet, J. C., Cara, M., Deschamps, A., Dorbath, L., Dorbath, C., et al. (1989). The Spitak (Armenia) earthquake of 7 December 1988: field observations, seismology and tectonics. *Nature*, 339(6227), 675–679.

Cornell, C.A. (1968). Engineering Seismic Risk Analysis. *Bulletin of the Seismological Society of America*, Vol. 58, No. 5, pp. 1583–1606.

Cauzzi, C. & Faccioli, E. (2008). Broadband (0.05 to 20 s) prediction of displacement response spectra based on worldwide digital records. *Journal of Seismology*, 12, 453–475.

D'Amico, V. & Albarello, D. (2008). SASHA: a computer program to assess seismic hazard from intensity data. *Seismological Research Letters*, 79(5), 663-671.

Davenport, P. N. (2003). Instrumental measures of earthquake intensity in New Zealand. *Proceedings of 2003 Pacific Conference on Earthquake Engineering*, Christchurch, February 2003.

Delavaud, E., Cotton, F., Akkar, S., Scherbaum, F., Danciu, L., Beauval, C., ... & Theodoulidis, N. (2012). Toward a ground-motion logic tree for probabilistic seismic hazard assessment in Europe. *Journal of Seismology,* 16(3), 451-473.

Derras, B. ; Bard, P.Y. ; Cotton, F. ; Lemoine, A. ; Douglas, J. ; Traversa, P. (2013). Testing the use of local slope as a proxy to site conditions in GMPEs : The RESORCE case, Joint Assembly Gothenburg, IAHS – IAPSO – IASPEI, Sweden, 22-26 July.

Dolomieu, D. (1784). *Memoire sur les tremblemens de terre de la Calabre pendant l'année 1783*. Antoine Fulgoni.

Dowrick, D. J., & Cousins, W. J. (2003). Historical incidence of Modified Mercalli Intensity in New Zealand and comparisons with hazard models. *Bulletin of the New Zealand Society for Earthquake Engineering*, 36(1), 1-24.

Drouet, S., Cotton, F. & Guéguen, P. (2010). V_{S30}, κ, regional attenuation and Mw from accelerograms: application to magnitude 3-5 French earthquakes. *Geophysical Journal International*, 182, 880–898.

Drouet, S., (2012). PSHA for south-east France using low minimum magnitude. Geoter Report, GTR/ARE/0412-942.

Erdik, M., Biro, Y. A., Onur, T., Sesetyan, K. & Birgoren, G. (1999). Assessment of earthquake hazard in Turkey and neighboring. *Annals of Geophysics*, 42(6).

Eyidogan, H. & Jackson, J. (1985). A seismological study of normal faulting in the Demirci, Alaşehir and Gediz earthquakes of 1969–70 in western Turkey: implications for the nature and geometry of deformation in the continental crust. *Geophysical Journal International*, 81 (3), 569–607.

Faenza L. & Michelini A. (2010). Regression analysis of MCS intensity and ground motion parameters in Italy and its application in ShakeMap. *Geophysical Journal International*, 180 : 1138-1152.

Fonseca, J. F. B. D. & Vilanova, S. P. (2010). The 23 April 23 1909 Benavente (Portugal) M 6.3 Earthquake. *Seismological Research Letters*, 81(3), 534-536.

Frohlich, C. & Apperson, K. D. (1992). Earthquake focal mechanisms, moment tensors, and the consistency of seismic activity near plate boundaries. *Tectonics*, 11(2), 279–296.

Fujiwara, H., Morikawa, N., Ishikawa, Y., Okumura, T., Miyakoshi, J., Nojima, N. & Fukushima, Y. (2009). Statistical Comparison of National Probabilistic Seismic Hazard Maps and Frequency of Recorded JMA Seismic Intensities from the K-NET Strong-motion Observation Network in Japan during 1997–2006. *Seismological Research Letters*, 80, 458–464.

Giardini, D., J. Woessner, L. Danciu, H. Crowley, F. Cotton, G. Grünthal, R. Pinho, G. Valensise, S. Akkar, R. Arvidsson, R. Basili, T. Cameelbeeck, A. Campos-Costa, J. Douglas, M. B. Demircioglu, M. Erdik, J. Fonseca, B. Glavatovic, C. Lindholm, K. Makropoulos, C. Meletti, R. Musson, K. Pitilakis, K. Sesetyan, D. Stromeyer, M. Stucchi, A. Rovida, Seismic Hazard Harmonization in Europe (SHARE): Online Data Resource, doi: 10.12686/SED-00000001-SHARE, 2013.

Goudar, A. (1756). Rélation (sic) historique du tremblement de terre survenu à Lisbonne le premier Novembre 1755... Précédé d'un Discours politique sur les avantages que le Portugal pourroit retirer de son malheur...(par A. Goudar). Chez Philanthrope, à la Vérité.

Grünthal, G. (1998). European Macroseismic Scale 1998 EMS-98. *Cahiers du Centre Européen de Géodynamique et de Séismologie* vol.15, Luxembourg.

Grünthal, G. & Wahlström, R. (2012). The European-Mediterranean Earthquake Catalogue (EMEC) for the last millennium. *Journal of Seismology,* 16(3), 535–570.

Grünthal, G., Wahlström, R. & Stromeyer, D. (2013). The SHARE European Earthquake Catalogue (SHEEC) for the time period 1900–2006 and its comparison to the European-Mediterranean Earthquake Catalogue (EMEC). *Journal of Seismology,* 17(4), 1339–1344.

Humbert, N. & Viallet, E. (2008). A method for comparison of recent PSHA on the French territory with experimental feedback. *The 14th World Conference on Earthquake Engineering, October 12-17*, Beijing, China, 8 pages.

Irmak, T. S. (2013). Focal mechanisms of small-moderate earthquakes in Denizli Graben (SW Turkey). *Earth Planets Space*, 65(9), 943–955.

Irmak, T., Dogan, B. & Karakas, A. (2012). Source mechanism of the 23 October, 2011, Van (Turkey) earthquake (Mw= 7.1) and aftershocks with its tectonic implications. *Earth, Planets and Space*, 64, 991-1003.

Japanese Meteorological Agency (1996). Explanation table of JMA seismic intensity scale. http://www.jma.go.jp/jma/en/Activities/inttable.html

Kalkan, E., Gülkan, P., Yilmaz, N. & Çelebi, M. (2009). Reassessment of probabilistic seismic hazard in the Marmara region. *Bulletin of the Seismological Society of America,* 99(4), 2127-2146.

Kalkan, E., Gülkan, P., Öztürk, N. Y. & Çelebi, M. (2008). Seismic Hazard in the Istanbul Metropolitan Area: A Preliminary Re-Evaluation. *Journal of Earthquake Engineering*, 12(S2), 151-164.

Laboratoire de Détection et de Géophysique (LDG), (2012). Catalog of French seismicity 1962-2011. CEA/Laboratoire de Détection et de Géophysique, Bruyères-le-Châtel, France.

Lambert, J., Bernard, P., Czitrom, G., Dubie, J.Y., Godefroy, P. & Levret-Albaret, A. (1997). Les Tremblements de Terre en France: Hier, Aujourd'hui, Demain (Éditions du BRGM, Orléans), p. 196.

Leonard, M. (2010). Earthquake Fault Scaling: Self-Consistent Relating of Rupture Length, Width, Average Displacement, and Moment Release. *Bulletin of the Seismological Society of America,* 100 (5A), 1971–1988.

Martin, Ch., Combes, P., Secanell, R., Lignon, G., Carbon, D., Fioravanti, A. & Grellet, B., (2002). Révision du zonage sismique de la France: étude probabiliste, under the supervision of the Groupe d'Etude et de Proposition pour la Prévention du risque sismique en France and the Association Française du Génie Parasismique (in French). Geoter Report, GTR/MATE/0701-150.

Martin, Ch. & Secanell, R. (2006). Développement d'un modèle probabiliste d'aléa sismique calé sur le retour d'expérience, Phase 2: Calculs et cartographie suivant l'arbre logique défini par le groupe « zonage », Document GZ7 produit dans le cadre du groupe de travail AFPS « ZONAGE », Geoter Report, GTR/CEA/0306-294, 39 pages (in French).

Mayer Rosa, D. & Cadiot, B. (1979). A review of the 1356 Basel earthquake, *Tectonophysics*, 53, 325-333.

McGuire, R.K., (1976). FORTRAN computer program for seismic risk analysis, U.S. Geological Survey Open-File Report 76-67.

Medvedev, S., Sponheuer, W. & Karník, V. (1964). Neue seismische Skala Intensity scale of earthquakes, 7. Tagung der Europäischen Seismologischen Kommission vom 24.9. bis 30.9.1962. In: Jena, Veröff . Institut für Bodendynamik und Erdbebenforschung in Jena, vol 77. Deutsche Akademie der Wissenschaften zu Berlin, pp 69–76

Medvedev, S.V., Sponheuer, W. & Karnik, V. (1967). Seismic intensity scale version 1964, Punl. Inst. Geody. Jena, 48.

Melville, C.P., Levret, A., Alexandre, P., Lambert, J. & Vogt, J. (1996). Historical seismicity of the Strait of Dover-Pas de Calais, *Terra Nova*, 8, 626-647.

Mezcua, J., Rueda, J. & Blanco, R. G. (2013). Observed and Calculated Intensities as a Test of a Probabilistic Seismic‐Hazard Analysis of Spain. *Seismological Research Letters*, 84(5), 772-780.

Mucciarelli, M., Albarello, D. & D'Amico, V. (2008). Comparison of Probabilistic Seismic Hazard Estimates in Italy. *Bulletin of the Seismological Society of America,* 98, 2652–2664.

Musson, R.M.W, Grünthal, G. & Stucchi, M. (2010). The comparison of macroseismic intensity scales. *Journal of Seismology* 14 (2): 413-428

Musson, R. M. W. & Winter, P. W. (2012). Objective assessment of source models for seismic hazard studies with a worked example from UK data. *Bulletin of Earthquake Engineering*, doi:10.1007/ s10518-011-9299-6.

Neilson, G., Musson, R. M. W. & Burton, P. W. (1984). The "London" earthquake of 1580, April 6. *Engineering geology*, 20(1), 113–141. Elsevier.

Ordaz, M. & Reyes, C. (1999). Earthquake hazard in Mexico City: Observations versus computations. *Bulletin of the Seismological Society of America,* 89, 1379–1383.

Papaspiliou, M., Kontoe, S. & Bommer, J. J. (2012). An exploration of incorporating site response into PSHA-part II: Sensitivity of hazard estimates to site response approaches. *Soil Dynamics and Earthquake Engineering*, 42(0), 316–330.

Papazachos, B. C. (1990). Seismicity of the Aegean and surrounding area. *Tectonophysics*, 178(2–4), 287–308.

Pequegnat, C., Gueguen, P., Hatzfeld, D. & Langlais, M. (2008). The French Accelerometric Network (RAP) and National Data Centre (RAP-NDC). *Seismological Research Letters*, 79, 79–89.

Pilidou, S., Priestley, K., Jackson, J. & Maggi, A. (2004). The 1996 Cyprus earthquake: a large, deep event in the Cyprean Arc. *Geophysical Journal International*, 158 (1), 85–97.

Pınar, A. & Kalafat, D. (1999). Source processes and seismotectonic implications of the 1995 and 1996 Cyprus, Eastern Mediterranean region, earthquakes. *Tectonophysics*, 301(3–4), 217–230.

Prime Ministry Disaster And Emergency Management Presidency Earthquake Department, National Strong Motion Network. Retrieved February 3, (2014), from http://kyh.deprem.gov.tr/tkyhakken.htm

Quenet, G. (2005). Les Tremblements De Terre En France XVIIe-XVIIIe Siècles. *La Naissance D'un Risque, Paris*, Champ Vallon,2005, 592 P.

Reasenberg, P. (1985). Second-order moment of central California seismicity, 1969–1982. *Journal of Geophysical Research: Solid Earth*, 90(B7), 5479–5495.

Régnier, J., Laurendeau, A., Duval, A.-M. & Gueguen, P. (2010). From heterogeneous set of soil data to Vs profile: Application on the French permanent accelerometric network (RAP) sites. Proceedings Fourteenth ECEE—European Conference of Earthquake Engineering, Ohrid, Republic of Macedonia, Paper ID 851.

Rey J., Dewez T. (2008) avec la collaboration de M. Imbault et J. Lambert – Carte de l'aléa sismique par l'approche statistico-historique. Rapport BRGM/RP-54983-FR, 100 pp., 44 fig., 4 tabl.

Rhoades, D., Schorlemmer, D., Gerstenberger, M., Christophersen, A., Zechar, J.D. & Imoto, M. (2011). Efficient testing of earthquake forecasting models. Acta Geophysica, 59, 728–747.

Rhoades, D., Smith, W.D. & Stirling, M.W. (2002). Tests of seismic hazard models, GNS Consultancy Report for Earthquake Commission Research Foundation, Project No. 01/460, 43 pages.

Rothé, J.P. (1977). Listes chronologiques d'épicentres en liaison avec les évènements de SisFrance, Travaux in-édits et Annales et Annuaires de l'Institut de Physique du Globe de Strasbourg.

Sadigh, K., Chang ,C.Y., Egan, J.A., Makdisi, F. & Youngs, R.R. (1997). Attenuation relationships for shallow crustal earthquakes based on California strong motion data. *Seismological Research Letters,* 68:180–189

Sandıkkaya, M. A., Akkar, S. & Bard, P. (2013). A Nonlinear Site‐Amplification Model for the Next Pan‐European Ground‐Motion Prediction Equations. *Bulletin of the Seismological Society of America,* 103 (1), 19–32. doi:10.1785/0120120008

Sandıkkaya, M. A., Yılmaz, M., Bakır, B. S. & Yılmaz, Ö. (2010). Site classification of Turkish national strong-motion stations. *Journal of Seismology,* 14(3), 543–563. doi:10.1007/s10950-009-9182-y

Scherbaum, F., Cotton, F. & Smit, P. (2004). On the Use of Response Spectral-Reference Data for the Selection and Ranking of Ground-Motion Models for Seismic-Hazard Analysis in Regions of Moderate Seismicity: The Case of Rock Motion. *Bulletin of the Seismological Society of America,* 94, 2164–2185.

Scherbaum, F., Delavaud, E. & Riggelsen, C. (2009). Model selection in seismic hazard analysis: An information-theoretic perspective. *Bulletin of the Seismological Society of America,* 99, no. 6, 3234–3247.

Schorlemmer, D. & Gerstenberger, M.C. (2007). RELM Testing Center. *Seismological Research Letters*, 78, 1, 30-36.

Scotti, O., Baumont, D., Quenet, G. & Levret, A. (2004). The French macroseismic database SISFRANCE: objectives, resultsand perspectives. *Annals of Geophysics*, Vol 47, No 2-3 (2004).

Sébrier, M., Ghafiri, A. & Bles, J. L. (1997). Paleoseismicity in France: fault trench studies in a region of moderate seismicity. *Journal of geodynamics*, 24(1), 207-217.

Sesetyan, K., Demircioglu, M., Rovida,A., Albini,P., Stucchi, M., Zare, M., Viganò,D. & Locati, M., SHARE-CET, the SHARE earthquake catalogue for Central and Eastern Turkey complementing the SHARE European Earthquake Catalogue (SHEEC) www.emidius.eu/SHEEC/docs/SHARE_CET.pdf, last retrieved 27 01 2014.

Sieberg, A. (1932). Untersuchungen über Erdbeben und Bruchschollenbau im östlichen Mittelmeergebiet. Gustav Fischer, Jena, 113 pp.

Sollogoub, P., Bard, P.-Y., Hernandez, B., Jalil, W., Labbé, P., Mouroux, P. & Viallet, E. (2007). Rapport du groupe de travail "Zonage", Association Française de génie Parasismique (AFPS), 58 pp. (in French, available on request).

Stein, S., Geller, R. & Liu, M. (2011). Bad Assumptions or Bad Luck: Why Earthquake Hazard Maps Need Objective Testing. *Seismological Research Letters*, 82, 623–626.

Stich, D., Batlló, J., Macià, R., Teves-Costa, P. & Morales, J. (2005). Moment tensor inversion with single-component historical seismograms: The 1909 Benavente (Portugal) and Lambesc (France) earthquakes. *Geophysical Journal International*, 162(3), 850–858.

Stirling, M.W. (2012). Earthquake Hazard Maps and Objective Testing: The Hazard Mapper's Point of View. *Seismological Research Letters*, 83, 231–232.

Stirling, M. & Gerstenberger, M. (2009). Development of tests for long-term earthquake ground motion forecasts in New Zealand, GNS Science Consultancy Report 2009/140. 20p.

Stirling, M. & Gerstenberger, M. (2010). Ground Motion–Based Testing of Seismic Hazard Models in New Zealand. *Bulletin of the Seismological Society of America,* 100, 1407–1414.

Stirling, M. & Petersen, M. (2006). Comparison of the Historical Record of Earthquake Hazard with Seismic- Hazard Models for New Zealand and the Continental United States. *Bulletin of the Seismological Society of America*, 96, 1978–1994.

Stover, C. W. & Coffman, J. L. (1993). Seismicity of the United States, 1568-1989 (revised). US Government Printing Office.

Strasser, F.O., Abrahamson, N.A. & Bommer, J.J. (2009). Sigma: Issues, Insights, and Challenges. *Seismological Research Letters*, 80, 40–56.

Stucchi, M., Albini, P., Mirto, M. & Rebez, A. (2004). Assessing the completeness of Italian historical earthquake data. *Annals of Geophysics*, 47(2-3).

Stucchi, M., Rovida, A., Gomez Capera A.A., Alexandre, P., Camelbeeck, T., Demircioglu, M.B., Kouskouna, V., Gasperini, P., Musson, R.M.W., Radulian, M., Sesetyan, K., Vilanova, S., Baumont, D., Faeh, D., Lenhardt, W., Martinez Solares, J.M., Scotti, O., Zivcic, M., Albini P., Batllo J., Papaioannou, C., Tatevossian, R., Locati, M., Meletti, C., Viganò, D. Giardini, D., The SHARE European Earthquake Catalogue (SHEEC) 1000-1899. *Journal of Seismology*, DOI 10.1007/s10950-012-9335-2, (2012).

Tan, O., Tapırdamaz, M.C. & Yörük, A. (2008). The Earthquake Catalogues for Turkey. *Turkish Journal of Earth Sciences*, 17, No.2, 405-418

Tibi, R., Bock, G., Xia, Y., Baumbach, M., Grosser, H., Milkereit, C., Karakisa, S., et al. (2001). Rupture processes of the 1999 August 17 Izmit and November 12 Düzce (Turkey) earthquakes. *Geophysical Journal International*, 144(2), F1–F7.

Tselentis, G. A. & Danciu, L. (2008). Empirical relationships between modified Mercalli intensity and engineering ground-motion parameters in Greece. *Bulletin of the Seismological Society of America,* 98(4), 1863-1875.

Urry, A. (1913). Le tremblement de terre de Plombières-Remiremont. *Annales de Géographie* (Vol. 22, pp. 300–309). Société de géographie.

Wald, D. J., Quitoriano, V., Heaton, T. H. & Kanamori, H. (1999). Relationships between peak ground acceleration, peak ground velocity, and modified Mercalli intensity in California. *Earthquake spectra*, 15(3), 557-564.

Ward, S.N. (1995). Area-based tests of long-term seismic hazard predictions. *Bulletin of the Seismological Society of America,* 85, 1285–1298.

Woessner J., Giardini, D. & the SHARE consortium (2012). Seismic Hazard Estimates for the Euro-Mediterranean Region:A community-based Probabilistic Seismic Hazard Assessment, Paper Nr. 4337.

Wood, H.O., Neumann, F. (1931). Modified Mercalli intensity scale of 1931. *Bulletin of the Seismological Society of America,* 21:277–283

Yenier, E., Sandıkkaya, M. A. & Akkar, S. (2010). Report on the fundamental features of the extended strong-motion databank prepared for the SHARE Project, Workshop for WP4, Ankara, Turkey.

Zechar, J.D., Gerstenberger, M.C. & Rhoades, D.A. (2010). Likelihood-Based Tests for Evaluating Space–Rate–Magnitude Earthquake Forecasts. *Bulletin of the Seismological Society of America,* 100, 1184–1195.

Zhao, J. X., Zhang, J., Asano, A., Ohno, Y., Oouchi, T., Takahashi, T., Ogawa, H., Irikura, K., Thio, H. K., Somerville, P. G., Fukushima, Y. & Fukushima, Y. (2006). Attenuation relations of strong ground motion in Japan using site classification based on predominant period. *Bulletin of the Seismological Society of America,* 96 (3), 898–913.